THE UNIVERSITY OF CHICAGO

ACTIN DYNAMICS:
FROM SINGLE MOLECULES TO COMPETING CELLULAR NETWORKS

A DISSERTATION SUBMITTED TO

THE FACULTY OF THE DIVISION OF THE BIOLOGICAL SCIENCES

AND THE PRITZKER SCHOOL OF MEDICINE

IN CANDIDACY FOR THE DEGREE OF

DOCTOR OF PHILOSOPHY

DEPARTMENT OF MOLECULAR GENETICS AND CELL BIOLOGY

BY

THOMAS ANDREW BURKE

CHICAGO, ILLINOIS

AUGUST 2016

Table of Contents

LIST OF FIGURES

LIST OF TABLES

ACKNOWLEDGEMENTS

I would like to thank my thesis advisor Dr. David Kovar for his excellent mentorship. His leadership abilities and constant encouragement throughout my time as a student in his lab was second to none. Without his input on scientific questions and mentorship I would not have grown, learned, and enjoyed myself as much as I did. He also cultivated an incredible work environment. Not only were the other Kovar Lab members essential for my scientific development, but also made coming in to lab every day something to look forward to. I truly cherish every aspect of being a part of the Kovar Lab.

I would also like to thank my thesis committee Dr. Benjamin Glick, Dr. Aaron Turkewitz, Dr. Mohan Gupta and Dr. Robert Keenan who all provided insightful and valuable advice on all of my projects that not only improved my research but my personal growth as a scientist as well. On a broader scale I would like to thank the entire cytoskeletal group at the University of Chicago, the departmental administrators and my fellow CMB students for being part of a wonderful scientific environment.

Finally I want to thank my family and friends for their support and positive attitudes. Specifically, I want to thank my wonderful wife Katie who has been my source for inspiration and constant companion throughout my entire time at the University of Chicago. Without her love and unwavering optimism I would not be where I am today.

ABSTRACT

Actin builds an essential part of the cytoskeleton in eukaryotes. Cells utilize the actin cytoskeleton for numerous processes such as endocytosis, motility, and cytokinesis. Multiple actin networks are simultaneously built and maintained in the same crowded cytoplasm. How cells organize and regulate numerous actin networks is an important biological question. Polymerization of the actin cytoskeleton is tightly regulated by activation of assembly factors at specific times and places. Not only is it crucial to understand the molecular mechanisms of how specific actin assembly factors polymerize actin, but it is equally important to understand how actin networks can influence each other on a cell-wide scale. My two projects investigated how actin assembly factors share a common pool of actin monomers in fission yeast and how the actin assembly factors VopL and VopF interact with and polymerize actin filaments.

For my first project I investigated whether diverse actin filament networks are homeostatic, whereby actin assembly factor competition for actin monomers is critical to regulate network size and density. The fission yeast *Schizosaccharomyces pombe* possesses three F-actin networks: Arp2/3 complex-mediated patches, formin For3p-mediated cables, and the formin Cdc12p-mediated contractile ring (Kovar et al. 2011). The amount of actin incorporated into each network is consistent both inter and intra-cellularly, varying less than 50% between structures. The regulation of actin network assembly in cells was thought to be regulated by signaling cascades. If this were true, the systematic depletion of a single actin network should have negligible effects on the other networks. However, in my first project I tested an additional hypothesis that diverse F-actin networks are in competition for actin monomers (G-actin). I discovered that inhibition of the Arp2/3 complex in fission yeast not only eliminates Arp2/3

complex-mediated endocytic actin patches, but due to the newly freed up actin monomer, also induces assembly of ectopic formin-assembled F-actin. Conversely, disruption of the formins increases the density of Arp2/3 complex-mediated actin patches. Disrupting of the flow of monomer by depleting the F-actin severing protein cofilin prevents ectopic actin from forming. Furthermore, modifying actin levels significantly perturbs the fission yeast actin cytoskeleton. Increasing the actin concentration favors Arp2/3 complex-mediated actin assembly, whereas decreasing the actin concentration favors formin-mediated contractile rings. Therefore, competition for G-actin helps regulate the proper amount of F-actin assembly for diverse processes.

My second project focused on the biochemical characterization of two WH2-domain actin assembly factors, VopL and VopF. The WH2 domain is a common actin monomer-binding motif comprising of approximately 17 amino acids and is utilized for multiple different functions within cells like monomer sequestration, assembly factor regulation, as well as a newly identified general class of assembly factors (Dominguez 2016; Paunola et al. 2002). Cells have created multiple assembly factors that utilize the WH2 domain in tandem within the same protein given its high affinity for actin monomers. Multiple organisms have used types of these actin assembly factors for processes such as neural development and cytoplasmic streaming during early embryo development. Conversely, pathogens have mimicked this powerful method of actin assembly for more sinister purposes.

VopF and VopL are WH2-domain containing actin assembly factors utilized by the infectious bacteria that cause cholera, *Vibrio cholerae* and *Vibrio parahaemolyticus* (Tam et al. 2007; Liverman et al. 2007). Unlike other infectious bacteria that secrete proteins to activate host-cell nucleation factors such as Listeria (ActA) and Shigella (IcsA) to hijack the host-cell's

F-actin cytoskeleton for motility, VopF and VopL nucleate the host cell's F-actin directly (Cossart 2000; Tam et al. 2007; Liverman et al. 2007). VopF and VopL are F-actin nucleators and are categorized into the unique group of nucleators such as Spire, Cobl, and Sca2 that rely on tandem G-actin binding WH2 domains for their activity (Chesarone & Goode 2009; Quinlan et al. 2005; Haglund et al. 2010). VopF and VopL are both homodimers, and their domain organization is conserved with 72% protein sequence similarity. From N to C-terminus both have two proline-rich regions, three WH2 domains, followed by a dimerization inducing Vop C-terminal Domain (VCD) that causes a U shaped configuration (Liverman et al. 2007; Tam et al. 2007; Pernier et al. 2013; Namgoong et al. 2011). The F-actin nucleation capabilities of VopF and VopL are undisputed, however recent studies have been in conflict over the exact mechanism employed. Using multi-color TIRF microscopy I have shown that in the presence of actin monomers, VopL and VopF are purely nucleators that associate briefly with the pointed end of actin filaments before dissociating and do not bind to pre-existing filaments. In the absence of monomer VopL and VopF are competent to bind to both the pointed and barbed ends of actin filaments. Additionally VopL and VopF can bind to the barbed end of actin filaments in conditions with saturating profilin with actin monomers. However in the light of the pathogenic nature of *Vibrio* bacteria, we are more prone to believe that the primary function of VopL and VopF are to be highly efficient nucleators that promote the assembly of unproductive F-actin in the host cell thereby disrupting the G- to F-actin homeostasis.

CHAPTER 1: INTRODUCTION

SECTION 1.1 THE ACTIN CYTOSKELETON

Actin is a 42kDa globular protein that is highly conserved in eukaryotes from yeast to humans. Actin exists in two forms simultaneously in cells: either in its monomeric G-actin (globular) form or polymerized into a polar actin filament (F-actin) with a fast growing barbed end and a slow growing pointed end. Actin is the most abundant protein in most eukaryotic cells ranging from 20-500 μM, which is much higher than the critical concentration for monomer addition at both the barbed (0.1 μM) and pointed (0.7 μM) ends (Pollard & Borisy 2003). Spontaneous and erroneous F-actin assembly can be prevented in cells, among other things, by either profilin or the WH2 domain containing protein thymosin beta-4 binding to G-actin. Cells overcome these methods of prevention by activating actin assembly factors through signaling cascades. Assembly factors stimulate the polymerization of G-actin into F-actin. Control of assembly factor activity allows precise regulation over the type and quantity of actin filaments assembled. Cells then utilize these F-actin cytoskeletal networks with various geometrical and biochemical properties for multiple purposes such as cytokinesis, endocytosis, polarity, motility, and adhesion (Campellone & Welch 2010; Pollard & Cooper 2009; Rotty et al. 2013).

SECTION 1.2 ACTIN ASSEMBLY FACTORS

Depending on the cell type, eukaryotes possess up to four identified classes of F-actin assembly factors: the Arp2/3 complex, formins, Ena/VASP, and tandem WH2 domain assembly factors (Chesarone & Goode 2009). Cells employ these F-actin assembly factors to catalyze the

de novo assembly, elongation, or both of actin filaments. Each class has unique biochemical actin assembly properties and is utilized in specific cellular activities.

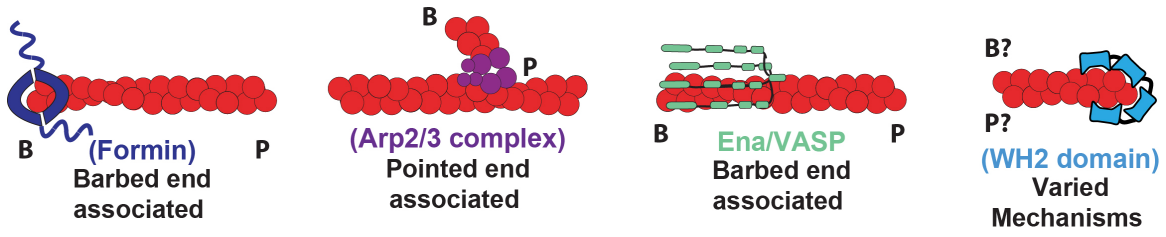

Figure 1-1: Cartoon of the four canonical types of actin assembly factors
Cartoon displaying the localization of Formins, the Arp2/3 complex, Ena/VASP, and the WH2-domain class of actin assembly factors. Generally formins bind to the barbed end of actin filaments and stimulate runs of processive elongation in the presence of profilin, the Arp2/3 complex makes branched filaments from the sides of pre-existing mother filaments and remains bound to the pointed end, Ena/VASP can bundle actin filaments and processively elongate filaments, and the WH2-domain class of assembly factors has a wide variety of actin assembly capabilities ranging from purely nucleation of new actin filaments and binding to the pointed end to riding processively on the barbed end of pre-existing filaments.

The Arp2/3 complex is a seven-unit complex that binds to the side of existing actin filaments to make a densely branched, dendritic network. It does so by nucleating a new filament from the side of the "mother filament" and remaining bound at the pointed end forming an approximately 70° branch (Mullins, Heuser, et al. 1998; Amann & Pollard 2001a; Amann & Pollard 2001b). The Arp2 and Arp3 subunits mimic actin monomers and can promote the nucleation of a new filament (Higgs & Pollard 2001). The Arp2/3 complex is activated by multiple nucleation promoting factors (NPFs) like WASP and WAVE (Higgs & Pollard 2000). NPFs serve two identified purposes. First, NPFs bring the Arp2 and Arp3 subunits close together to mimic an actin dimer, and second to deliver an actin monomer to the Arp2/3 complex to further facilitate nucleation (Goley & Welch 2006; Pollard & Borisy 2003; Marchand et al. 2001). NPFs, in turn, are activated by signaling cascades that involve the GTPase CDC42 (S. H. Lee & Dominguez

2010). Cells utilize these dendritic networks for processes that require coordinated deformation of the plasma membrane or cell wall, like endocytosis or the migration (Rotty et al. 2013; Chhabra & Higgs 2006).

Formins are a family of actin assembly proteins that are classified by their conserved structure encompassing the Formin Homology-1 (FH1) and Formin Homology-2 (FH2) domains. The donut-shaped FH2 domain is sufficient to stimulate F-actin nucleation and bind to the barbed ends of filaments, while the FH1 domains can utilize profilin-actin to stimulate long runs of processive elongation thus polymerizing long, straight filaments (Pring et al. 2003; Paul & Pollard 2008). Most formins possess a diaphanous inhibitory domain (DID) and a diaphanous autoregulatory domain (DAD) at their N and C-termini, respectively (Kovar et al. 2005; Kovar et al. 2006; Goode & Eck 2007). Formins are autoinhibited when the DID is bound to the DAD, but can be activated by the Rho family of GTPases (Campellone & Welch 2010). Cells utilize formins to make long, straight F-actin for processes like cytokinesis, stress fibers, and the protrusive finger-like filopodia (Firat-Karalar & Welch 2011; Mattila & Lappalainen 2008) (C. Yang et al. 2007).

The Ena/VASP family of actin assembly factors are considered to be mainly elongation factors or actin polymerases. Ena/VASP proteins have a conserved domain structure of an EVH1 (localization), proline-rich region (profilin binding), and the EVH2 domain (tetramerization and G/F-actin binding domains) from N to C-terminus (Kwiatkowski et al. 2003). The Ena/VASP tetramer has multiple F-actin binding sites, it can bundle, processively elongate, and uncap actin filaments from the barbed end (Bear & Gertler 2009), (Winkelman et al. 2014; Hansen & Mullins 2010; Breitsprecher et al. 2008). Regulation of the Ena/VASP family of proteins comes in the form of phosphorylation by the cyclic nucleotide-dependent kinases PKA/PKG, although

the underlying mechanism of how tyrosine phosphorylation on the Ena/VASP proteins affects function is still being determined (Krause et al. 2003). Ena/VASP proteins are involved in motility by localizing and polymerizing actin at focal adhesions as well as promoting the formation of the protrusive finger-like filopodia either in cooperation or competiton with formins (Bilancia et al. 2014; Chesarone & Goode 2009).

The most recently discovered types of assembly factors are those that utilize tandem arrays of the Wiskott-Aldrich syndrome protein homology 2 (WH2) domain (Qualmann & Kessels 2009; Paunola et al. 2002). The WH2 domain is an abundant actin monomer-binding motif of approximately 17 amino acids and can be found in the NPFs of the Arp2/3 complex, some formins, the monomer sequestering protein thymosin beta-4, as well as this relatively uncharacterized class of assembly factors (Dominguez 2016; Paunola et al. 2002). Unlike the Arp2/3 complex and formins, there is a wide variety. WH2-domain assembly factors, depending on the isoform, can exist as monomers or dimers and can employ from three to eight of these G-actin binding WH2 domains to stimulate actin assembly (Zuchero et al. 2009; Quinlan 2013). By increasing the local concentration of actin monomers, these factors promote actin filament nucleation and elongation. Given the nascency of the study of WH2 domain assembly factors, little is known about their regulation. Certain isoforms of WH2 domain assembly factors are involved in organismal development, such as the formation of an actin meshwork that promotes cytoplasmic streaming and neural and cardiac development in certain organisms (Quinlan 2013; Xu et al. 2012; Haag et al. 2012). Certain infectious bacteria have co-opted this powerful method of actin filament assembly for nefarious purposes. Some species of *Vibrio* bacteria secrete WH2 domain assembly factors into host cells with the express purpose of polymerizing unproductive

F-actin, depleting the G-actin pool to the detriment of the endogenous networks (Tam et al. 2007; Tam et al. 2010; Liverman et al. 2007).

SECTION 1.3 FINITE POOLS OF MATERIAL LIMIT THE SCALE OF CELLULAR STRUCTURES

Limiting the size and quantity of organelles and cellular structures is critical for proper cellular functions. The cytoplasm is finite and therefore contains a limited quantity of precursors or building blocks for each cellular structure. It is logical that cells would utilize this to their advantage, relying on a relatively passive "limiting pool" mechanism to regulate the size and density of various cellular components (Goehring & Hyman 2012). As a structure is being assembled it is simultaneously depleting the pool of building blocks, thus limiting the rate of assembly and size of the final product. The limiting pool regulatory mechanism is attractive since it may not require any additional active processes that keep track of either the size of the structure being built or the quantity of building block available for assembly. Recently multiple fields of study have focused on this model of organelle and structure scaling that relies on a limiting amount of available components present in the cytoplasm, including how cytoskeletal structure size is regulated by limiting pools of building blocks.

The biflagellate green alga *Chlamydomonas reinhardtii* utilizes flagella for motility. The flagella are built and maintained by a process that links assembly and disassembly through intraflagellar transport particle trains (IFT trains) that deposit microtubule related cytoskeletal elements into growing flagella (Engel et al. 2009). By studying this process endogenously as well as by surgical manipulation of severing one or both flagella on a single *C. reinhardtii* it was shown that the overall length of either one or both flagella influences the assembly of additional flagella (Ludington et al. 2012; Engel et al. 2009). As the flagella grow, the IFT trains being

transported out to the flagellar tips slow as the components are being exhausted. However the flagellar severing assay gives the most convincing evidence that this system is regulated by limiting components. If one of the two flagella is severed at the base, the remaining flagellum will correspondingly shrink to facilitate the sharing of limited components (Ludington et al. 2012).

Multiple groups also arrived at a similar conclusion when studying the mitotic apparatus encompassing the microtubule organizing centrosomes and microtubule-based cental spindle. *In vivo* and *in vitro* work demonstrated that both the centrosomes and central spindle are regulated by cytoplasmic volume and limiting components. Utilizing *Caenorhabditis elegans* embryos it was shown that as the embryos divide into smaller and smaller cells, their centrosomes and microtubule-based mitotic spindles shrink correspondingly with cytoplasmic volume and the rapidly dwindling amount of maternally supplied centrosome proteins (Greenan et al. 2010; Decker et al. 2011). Later Good et al. reconstituted this rapid and reductive cell division *in vitro* by encapsulating *Xenopus* egg or embryo cytoplasm into different volumes and shapes of hydrophobic droplets and then monitoring microtubule spindle size (Good et al. 2013). As predicted, the volume and not the shape of the droplet scaled with spindle size, reinforcing what was known from the *in vivo* studies. However the exact component that is limiting spindle size is undetermined.

SECTION 1.4 PRIOR REPORTS OF ACTIN ASSEMBLY FACTOR COMPETITION FOR MONOMERS

How cells build and utilize multiple dynamic F-actin networks in a crowded cytoplasm is an extremely important biological question. There are two non-mutually exclusive possibilities for

actin network size regulation: active control by signaling cascades that activate an actin assembly factor at the correct time and place, and passive control that limits the size of all of the actin networks through depleting a shared pool of actin monomers. Recently we hypothesized that much like the examples of centrosome, microtubule spindle and flagellar size regulation via a pool of limiting components, cells employ a similar regulatory mechanism for the actin cytoskeleton. If cells only use signaling cascades to determine F-actin network size and density, then modifying one actin network in a cell should have no effect on the other networks. Conversely, if cells do use competition for actin monomers as a regulatory mechanism to limit the size and density of actin networks, then depletion or modification of one network or the size of the actin pool should elicit a response from other networks.

Research suggesting actin is not limiting

Traditionally the concentration of actin in cells was not thought to be limiting, and that the availability of free barbed ends dictated the size and density of actin networks. Studies utilizing cell extracts from *Acanthamoeba castellanii* and nuetrophils concluded that actin filaments in the extracts do not elongate because their barbed ends are capped
(Zigmond et al. 1998; Mullins & Pollard 1999). If actin was limiting, adding factors to stimulate actin polymerization should have no effect, but this was not the case. Addition of exogenous uncapped actin filaments or the assembly factor activating Rho GTPase Cdc42 stimulated additional actin polymerization by the Arp2/3 mediated dendritic networks within the extracts. Recently many studies have shown the relationship between actin networks *in vivo*, and how depletion of one actin assembly factor can stimulate the function of others. Yet there is evidence that not all networks respond in the same way. Inhibition of the Arp2/3 complex in Jurkat T-cells

not only depletes the lamellipodia but the formin and Ena/VASP mediated filopodia as well (Young et al. 2015). This result can be interpreted in a different light since a generally accepted model of filopodia formation is through convergent elongation of the short branched filaments from the Arp2/3 mediated networks (Svitkina et al. 2003). Therefore if the quantity of barbed ends is decreased, one might predict if there was extra G-actin in the cytoplasm the barbed end elongation factors could not utilize it. However previous evidence shows that cells do not modulate the intracellular concentration of actin throughout the cell cycle, providing a constant, potentially limiting pool of actin monomers (Leavitt et al. 1987). Until my research systematically tested the effect of F-actin assembly factor depletion on actin network homeostasis, there had been multiple published studies on single to multi-cellular organisms that showed the modification of the amount of F-actin in one network changed the size and density of other actin networks.

Research suggesting actin is limiting

Studies from the single celled organisms fission and budding yeast showed that modification of the Arp2/3 complex mediated actin networks influenced actin cable formation. In budding yeast, Arp2/3 complex depletion stimulated the formation of thick, cable-like ectopic F-actin spanning from the mother cell to the bud, and over-expression of the Arp2/3 complex activator Las17p increased both the quanity and size endocytic actin patches to the detriment of the actin cables (Winter et al. 1997; Gao & Bretscher 2008). In fission yeast deletion of *dip1* (Wsp1p enhancer) causes fewer Arp2/3 complex-mediated endocytic patches to be formed and corresponds with an increase of ectopic cable-like F-actin (Basu & Chang 2011). A similar pheotype of fewer patches

and increased F-actin cables is observed when the Arp2/3 complex suppressor Gmf1p is over-expressed (Figure 1-2 B and D) (Nakano et al. 2010).

Depletion of the Arp2/3 complex leading to a reorganization of the actin cytoskeleton has been observed in multi-cellular animal models as well. Treatment of sea slug *Aplysia* neuronal growth cones with the small molecule Arp2/3 complex inhibitor CK-666 depletes the smooth outer lamellipodia while simultaneously increasing the quantity of the finger-like filopodia like protrusions (Nolen et al. 2009; Q. Yang et al. 2012). RNA interference experiments targeting subunits of the Arp2/3 complex in *Drosophila* S2 cells shows the same result of lamellipodia retraction and a corresponding increase in filopodia-like projections (Figure 1-2 C) (Rogers et al. 2003). Visualization of ArpC3-/- deletion mouse fibroblasts and rat MTLn3 rat carcinoma cells depleted of the Arp2/3 complex NPFs N-WASP/WAVE-2 showed lamellipodia retraction coupled with an increase of filopodia-like protrusions with the formins mDia1 and mDia2 localized to the ectopic actin protrusions (Figure 1-2 A) (Suraneni et al. 2012; Sarmiento et al. 2008; C. Wu et al. 2012). The interpretation from these studies is the inhibition or depletion of the Arp2/3 complex mediated actin networks leads to an increase in the overall cellular concentration of actin monomer. The other assembly factors, whether formins or Ena/VASP, are still competent to utilize this newly liberated monomer leading to the increase of long, straight bundles of F-actin. The focus of the previous studies was not on F-actin network competition, so therefore F-actin network homeostasis was implied from the results.

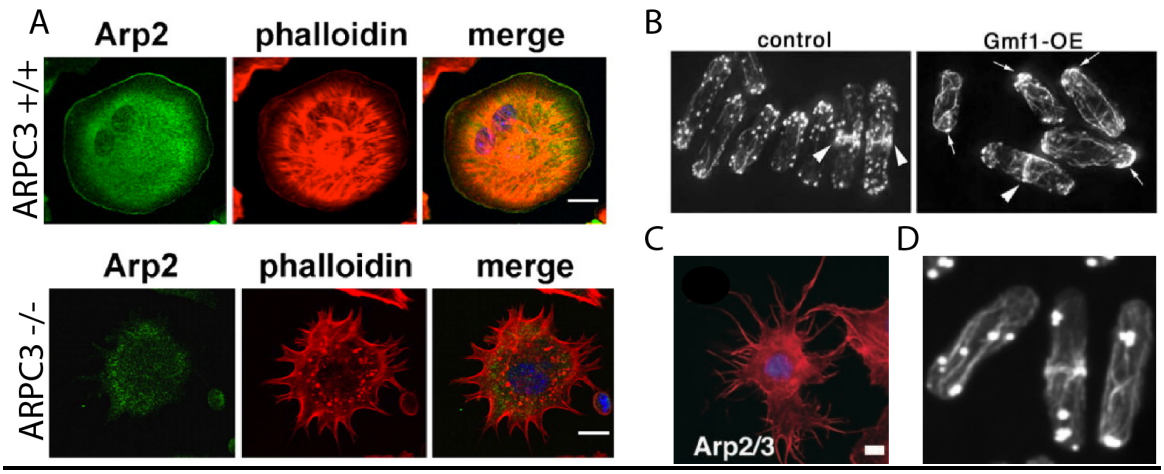

Figure 1-2: Examples of Arp2/3 depletion leading to ectopic F-actin formation
(A) Arp2/3 knockdown mouse fibroblasts labeled with phalloidin showing the decrease in lamellipodia and increase in filopodia like structures (Suraneni et al. 2012). (B) Over-expression of the Arp2/3 complex inhibitor Gmf1p in fission yeast showing a decrease in actin patches and an increase of ectopic cable-like F-actin. (Nakano et al. 2010) (C) Arp2/3 knockdown *D. melanogaster* S2 cell stained with phalloidin showing an increase in filopodia like protrusions (Rogers et al. 2003). (D) Deletion of the Arp2/3 co-activator *dip1* depletes actin patches while formin ectopic cable-like F-actin (Basu & Chang 2011).

SECTION 1.5 BACTERIAL CYTOTOXINS AND THE F-ACTIN CYTOSKELETON

Many species of infectious bacteria have obtained ways to exploit the host cell's actin cytoskeleton ranging from hijacking endogenous actin assembly factors for motility, interacting with upstream signaling pathways to disrupt endogenous actin networks, or simply by assembling actin monomers into unproductive F-actin (Aktories & Barbieri 2005). These bacterial cytotoxins are inherently disrupting the actin homeostasis in cells. *Rickettsia* uses Sca2 and *Listeria* uses ActA to either polymerize actin directly or to activate the endogenous Arp2/3 complex respectively to polymerize F-actin comet tails that promote their intra- and inter-cellular motility (Haglund et al. 2010; Welch et al. 1998). Other species secrete actin-modulating proteins that are only meant to disrupt the endogenous actin networks. Species of *Salmonella* secrete SipA and SipC, that when taken together polymerize and bundle F-actin both *in vitro* and *in vivo* (McGhie et al. 2001). *Chlamydia* use TARP (translocated actin recruiting

phosphoprotein) not only to gain entry into host cells via actin mediated endocytosis, and when oligomerized TARP can assemble unproductive F-actin with no other purpose than to consume available actin monomer (Jewett et al. 2006). *Legionalla* species secrete VipA, a protein that nucleates actin *in vitro*, localizes to F-actin rich puncta *in vivo* and disrupts multivesicular body trafficking (Franco et al. 2012). Most relevant to my thesis work are the actin assembly factors VopL and VopF secreted by *Vibrio* bacteria. VopL and VopF are part of the WH2-domain class of actin assembly factors (Dominguez 2016). VopL and VopF are highly potent F-actin nucleators *in vitro* and cause large-scale F-actin rearrangements in the epithelial cells of the host's small intestine. These VopL and VopF mediated rearrangements degrade the F-actin dependent tight junctions, which leads to intestinal inflammation and increases transmission of the bacteria (Liverman et al. 2007; Tam et al. 2010; Tam et al. 2007). The best hypothesis as to how the tight junctions are degraded is VopL and VopF polymerize large quantities of unproductive F-actin that some of the endogenous processes suffer due to a lack of actin monomer. VopL and VopF provide another example as to how disrupting F-actin homeostasis in cells is detrimental.

CHAPTER 2: ACTIN ASSEMBLY FACTORS COMPETE FOR A LIMITED POOL OF ACTIN MONOMERS

This chapter is adapted from (Burke et al. 2014). Contributions by Jenna R. Christensen (The University of Chicago, Chicago, IL), Elisabeth Barone and Vladimir Sirotkin (SUNY Upstate Medical University) will be noted in the figure legends.

SECTION 2.1 PREFACE

Controlling the quantity and size of organelles through competition for a limited supply of components is quickly emerging as an important cellular regulatory mechanism (Goehring & Hyman 2012). Cells assemble diverse F-actin networks for fundamental processes including division, motility, and polarization (Campellone & Welch 2010; Chesarone & Goode 2009; Chhabra & Higgs 2006). F-actin polymerization is tightly regulated by activation of assembly factors such as the Arp2/3 complex and formins at specific times and places. We directly tested an additional hypothesis that diverse F-actin networks are in homeostasis, whereby competition for actin monomers (G-actin) is critical for regulating F-actin network size. Here we show that inhibition of Arp2/3 complex in the fission yeast *Schizosaccharomyces pombe* not only eliminates Arp2/3 complex-mediated endocytic actin patches, but also induces a dramatic excess of formin-assembled F-actin. Conversely, disruption of formins increases the density of Arp2/3 complex-mediated patches. Furthermore, modifying actin levels significantly perturbs the fission yeast actin cytoskeleton. Increasing the concentration of actin favors Arp2/3 complex-mediated actin assembly, whereas decreasing the actin concentration favors formin-mediated contractile rings. Therefore, the specific actin concentration in a cell is critical, and competition for G-actin helps regulate the proper amount of F-actin assembly for multiple networks.

SECTION 2.2 THE FISSION YEAST ACTIN CYTOSKELETON

Fission yeast actin cytoskeleton

The fission yeast *Schizosaccharomyces pombe* provides an important model to study the actin cytoskeleton. Compared to mammalian cells that utilize upwards of twenty networks or processes, the fission yeast's relatively simple actin cytoskeleton relies on three actin networks during the asexual growth cycle: endocytic actin patches, polarity establishing actin cables, and the cytokinetic contractile ring (Figure 2-1) (Campellone & Welch 2010) (Kovar et al. 2011). Each of these networks is mediated by a single actin assembly factor: the Arp2/3 complex for actin patches, the formin For3p for actin cables, and the formin Cdc12p for the contractile ring. The biochemical mechanism of actin filament assembly for each of the assembly factors is well studied. The Arp2/3 complex makes short, branched filaments while formins make long, straight filaments that are well suited for specific processes (Pollard 2007). Fission yeast have a comparatively small genome with low redundancy which allowed for the identification of important genes involved in the organization of the actin cytoskeleton (Chang et al. 1996). Recently due to advances in fluorescent tagging of proteins and imaging techniques, the genetic tractability of fission yeast was further exploited by labeling actin assembly factors and actin binding proteins. Research from multiple groups has provided a thorough quantification of the composition and temporal assembly and disassembly dynamics of the three actin networks.

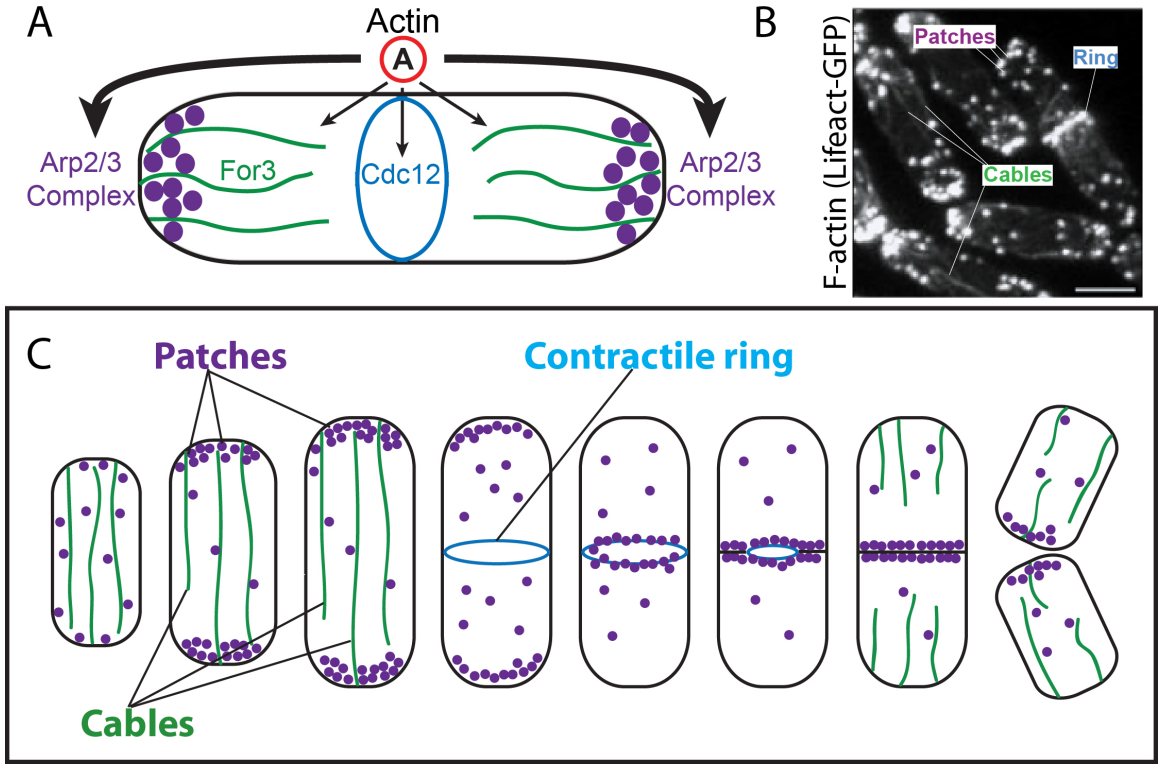

Figure 2-1: The three actin networks of the fission yeast *S. pombe*
(A) Cartoon showing the three F-actin networks in fission yeast, the Arp2/3 complex mediated actin patches, the formin For3p mediated actin cables, and the formin Cdc12p mediated contractile ring. (B) Fluorescently labeled actin networks from live fission yeast that correspond with the structures in (A). (C) Cartoon representation of the life cycle of the fission yeast. Interphase growth is followed by contractile ring formation and cell division. Source: adapted from D. R. Kovar

The Arp2/3 complex-mediated endocytic actin patches

The Arp2/3 complex was initially implicated in endocytic actin patch assembly by visualizing rhodamine phalloidin stained cells with the Arp2/3 complex subunits depleted. The Arp2/3 complex contains seven subunits, with Arp2p and Arp3p subunits providing the molecular mimicry necessary for its actin filament nucleation function (Pollard 2007). The Arp2p and Arp3p subunits are essential in fission yeast. Studies on cold-sensitive *arp2* and *arp3* mutants showed a marked depletion of endocytic actin patches as well as cytokinesis defects (Morrell et

al. 1999; McCollum et al. 1996). These studies also gave the first hints in regards to crosstalk between actin networks. Genetic depletion of the *arp2, arp3,* and *sop2* (ArcC1 subunit of the Arp2/3 complex) components of the Arp2/3 complex genetically suppress mutants of *cdc3*, the gene that encodes the actin monomer binding protein profilin, which was originally identified as a mutant that failed to undergo cytokinesis and is essential for formin-mediated assembly *in vivo* (Morrell et al. 1999; McCollum et al. 1996), (Balasubramanian et al. 1996) (Balasubramanian et al. 1994). Double mutants *arp2 cdc3*, *arp3 cdc3*, and *sop2 cdc3* all have increased viability at semi-permissive temperatures versus single mutants, implying a direct relationship between actin assembly at the endocytic actin patches and the contractile ring.

Research then focused on the identification and classification of the activators, or nucleation promoting factors (NPFs) for the Arp2/3 complex. Unlike for the formins For3p and Cdc12p it is currently unknown what, if any signaling cascades are upstream of the NPFs for the Arp2/3 complex in fission yeast. Actin assembly by the Arp2/3 complex in fission yeast is stimulated by two parallel NPF pathways: Wsp1p and Vrp1p (homologs of WASP and Verprolin) constitute one path, while Myo1p (a myosin-I motor) is the parallel pathway (Figure 2-2) (W. L. Lee et al. 2000; Vladmir Sirotkin et al. 2008). Each single *wsp1*, *vrp1*, and *myo1* mutant is viable, however the double *wsp1 myo1* mutant is lethal, further reinforcing the essentiality of Arp2/3 complex mediated actin assembly (Vladmir Sirotkin et al. 2008). The exact makeup of each actin patch was rigorously quantified in 2010. By fluorescently tagging known patch components along with an ectopic copy of GFP-actin, Sirotkin et al. showed that each patch underwent a regular pattern of assembly, actin binding protein recruitment, and disassembly with remarkably little variation between patches within a single cell and amongst a population of cells (Vladimir Sirotkin et al. 2010). Out of approximately 1.2 million actin

monomers in a cell, the endocytic actin patches utilize about 40-50% of the monomers at any time.

Formin For3p-mediated polarizing F-actin cables

The second F-actin network in fission yeast, the polarity establishing actin cables mediated by the formin For3p have been more recently studied. Their exact composition of actin binding proteins and amount of incorporated actin is not as well known due to their less robust nature compared to the endocytic actin patches and the cytokinetic contractile ring. However their function is important for normal interphase growth and morphology. *for3Δ* cells are viable, but are devoid of actin cables emanating from the cell poles, are misshapen, and the actin patches are more disperse throughout the cell (Feierbach & Chang 2001; Pelham & Chang 2001). Tracking individual For3p-3XGFP molecules showed short bursts of movement inward from the poles to the cell middle. The individual runs of processive elongation by For3p-3XGFP were too short to polymerize the entire length of the cable, implying that cables are assembled by the annealing of numerous For3p-mediated actin filaments (Martin & Chang 2006). Regulation of For3p localization and function is coordinated by two proteins, the microtubule associated protein Bud6 and the Rho GTPase Cdc42 (Figure 2-2) (Glynn et al. 2001; Martin et al. 2007). A *bud6Δ* mutant has thicker, more robust actin cables and a *cdc42-ts* mutant has fewer, thinner actin cables when stained with Alexa-488 phalloidin (Martin et al. 2007). Determining how much actin is incorporated into the For3p mediated actin cables is more challenging than for patches, but computer modeling based on the quantity of For3p molecules in cells and their average actin polymerization run lengths revealed an estimation of 5-10% of the total actin in cells (Wang & Vavylonis 2008).

Formin Cdc12p mediated-cytokinetic contractile ring

The third F-actin network, the cytokinetic contractile ring, is mediated by the formin Cdc12p. Cdc12p is essential for viability in fission yeast. Fission yeast can form a contractile ring through two mechanisms both dependent on functional Cdc12p: by utilizing the anillin homolog Mid1 to organize cytokinetic nodes that coalesce into a ring, or through the Septation Initiation Network pathway/leading spot pathway (Laporte et al. 2010; I.-J. Lee et al. 2012). Cdc12p was identified as a formin that interacts with the fission yeast profilin Cdc3p both genetically and directly from purified components *in vitro* (Chang et al. 1997). Depleting Cdc12p via a temperature sensitive mutation leads to cytokinetic failure due to decreased incorporation of actin into the contractile ring, implying that Cdc12p is responsible for actin assembly (Pelham & Chang 2001).

A combination of studies including quantitative fluorescence microscopy and electron microscopy shed light on the exact composition of the contractile ring in fission yeast in terms of actin incorporated as well as the quantity and dynamics of actin binding proteins associated with the actin network. During cytokinetic node-mediated contractile ring assembly, there are approximately 600 formin Cdc12p's at the contractile ring that polymerize around 10-15% of the total cellular actin pool (Kamasaki et al. 2007; J.-Q. Wu et al. 2003; J. Q. Wu 2005; J.-Q. Wu et al. 2006). Initiation of ring assembly through nodes comes from an upstream signal where the Polo-Like Kinase 1, Plo1p, phosphorylates multiple sites on the anillin homolog Mid1p setting off a cascade of ring assembly (Almonacid et al. 2011). If Mid1p is depleted Cdc12p can still assemble the contractile ring, albeit from a single spot and less efficiently than from condensing cytokinetic nodes (Bohnert et al. 2013; Y. Huang et al. 2008). Direct regulation of Cdc12p activity is less understood. Cdc12p needs fully functional FH1 and FH2 domains for proper

contractile ring assembly, but truncations or mutations in the putative regulatory DID/DAD domains did not alter function (Yonetani et al. 2008). However, over-expression of a Cdc12p C-terminal truncation tagged with GFP not only assembles actin during interphase but did so in a ring-like manner indicating an unidentified regulatory domain resides in the C-terminal 400 amino acids (Yonetani & Chang 2010).

Profilin is a multifunctional G-actin binding protein implicated in all three networks

Initial implications that there is indirect interaction between the three assembly factors and that their relationship between each other is competitive came from studies on fission yeast profilin. Profilin is an essential, multifunctional small G-actin binding protein that inhibits spontaneous nucleation, yet proflin-actin is competent to add freely to the barbed end of pre-existing filaments (Blanchoin et al. 2014). Formins utilize profilin-actin to catalyze processive elongation of actin filaments increasing the elongation rate 10-fold over actin alone. Formin function is dependent on the utilization of specific isoforms of profilin, and is a conserved property that has evolved in multiple organisms (Neidt et al. 2008; Kovar et al. 2006).

Traditionally the study of profilin has focused on its interaction with the formin class of assembly factors, however the research on profilin is bookended by results implicating and elucidating its interaction with the Arp2/3 complex. The fission yeast profilin, Cdc3p, was identified in a screen for cytokinesis mutants where *cdc3-124* temperature sensitive cells have gross actin cytoskeleton and cytokinetic defects (Balasubramanian et al. 1994). Cdc3p is important for the formation of the contractile ring, for the proper quantity and distribution of actin patches, *cdc12-112* and *cdc3-124* mutants are synthetically lethal, and Cdc3p and the formin Cdc12p interact through the poly-proline rich region of Cdc12p's FH1 domain (Chang et

al. 1996; Chang et al. 1997). More detailed observations of *cdc3* mutants elucidated the mechanism as to how profilin was affecting the cytoskeleton in fission yeast as well as how its absence affected all three networks. Cdc3p has multiple essential functions within the cell that include binding to proline-rich regions of actin assembly factors like formin, binding to G-actin, and catalyzing ADP to ATP nucleotide exchange on monomeric G-actin (Lu & Pollard 2001). Cdc3p is required for the proper function of all three networks in fission yeast. Depletion of Cdc3p causes the formin For3p-mediated actin cables to disappear, actin patches to become de-polarized and acquire defects in trajectory and turnover, and a loss of active actin polymerization at the contractile ring (Pelham & Chang 2001; Pelham & Chang 2002). In regards to the genetic interaction between the cytokinesis formin Cdc12p and Cdc3p, *in vitro* biochemical analysis investigating the mechanism of F-actin assembly by Cdc12p showed that Cdc12p is a barbed end binding protein that facilitates processive elongation of actin filaments in the presence of profilin (Kovar 2003; Kovar et al. 2005). Agreeing with the biochemical results, fission yeast need the profilin-binding poly-proline rich region FH1 domain for proper contractile ring formation and cytokinesis (Yonetani et al. 2008). Biochemical characterization of all three fission yeast formins showed that they share the trait of a Cdc3p-mediated increase in the rate of actin filament elongation over formin and actin alone (Scott et al. 2011).

Interestingly fission yeast profilin had been implicated in modulating Arp2/3 complex-mediated actin patches, although not in the direct way Cdc3p interacts with the formins Cdc12p and For3p. Genetic screens showed a rescue phenotype when the Arp2p subunit of the Arp2/3 complex was simultaneously depleted along with Cdc3p (Balasubramanian et al. 1994). This demonstrated a relationship between the Arp2/3 complex and profilin, although it would take nearly 20 years before the mechanism responsible for this relationship was revealed. Both *in vivo*

and *in vitro* studies have contributed to our understanding of the relationship between Arp2/3 complex and profilin. *In vivo* it was shown both in fission yeast and mammalian cells that profilin has an antagonistic relationship with the Arp2/3 complex. Arp2-/- mouse fibroblasts are relatively devoid of the Arp2/3 complex mediated lamellipodia, but depletion of the Profilin-1 isoform rescues this phenotype, and increasing the cellular concentration of Profilin-1 in WT mouse fibroblasts depletes the lamellipodia (Rotty et al. 2015). Studies in fission yeast using both cells and purified components demonstrated that not only does the fission yeast profilin Cdc3p inhibit the Arp2/3 complex through an interaction with the NPF Wsp1p, but depleting Arp2/3 complex-mediated actin patches via pharmacological inhibition with CK-666 rescues the cytokinetic defects in *cdc3-124* mutants (Suarez et al. 2015). Taken together the results on the function of profilin puts it in a very unique position, as it regulates multiple assembly factors independently from one another, assisting assembly of diverse F-actin networks in a crowded cytoplasm.

Adf1p/Cofilin is an actin severing protein that promotes F-actin network turnover

All three fission yeast actin filament structures are linked by the actin binding protein cofilin, which facilitates the turnover of actin polymer to monomer (H. Chen et al. 2000). The fission yeast cofilin, *adf1*, was first identified as an essential protein for viability and the formation of the contractile ring. Depletion of Adf1p in fission yeast essentially freezes the dynamics of the F-actin cytoskeleton, leading to severe cytokinetic and actin patch defects (Nakano & Mabuchi 2006b). Further characterization of Adf1p mutants indicated that the severing activity is essential for both assembly of the cytokinetic contractile ring as well as endocytic actin patch formation (Q. Chen & Pollard 2011; Q. Chen & Pollard 2013). All of the studies on Adf1p/cofilin in fission

yeast indicate a unique additional mechanism of the regulation of actin assembly besides the traditional thought that all networks are regulated through signaling cascades. If Adf1p/cofilin is depleted, the pool of available actin monomer (resulting from the disassembly of old networks) and the flow of monomer from one network to another is disrupted and all of the F-actin network's dynamics deteriorate. This implies a regulatory mechanism wherein all three networks share a common pool of actin monomers. As is evidenced above by the numerous genetic, quantitative fluorescence and confocal microscopy studies we have a significant understanding of each of the F-actin networks and their associated assembly factors in fission yeast. However, for all of the information gleaned about each F-actin network individually, we still do not know if the depletion of one network affects the others in fission yeast. Therefore, a systematic depletion of actin assembly factors coupled with fluorescent confocal microscopy allowed us to truly understand the F-actin inter-network competition for a common pool of actin monomers.

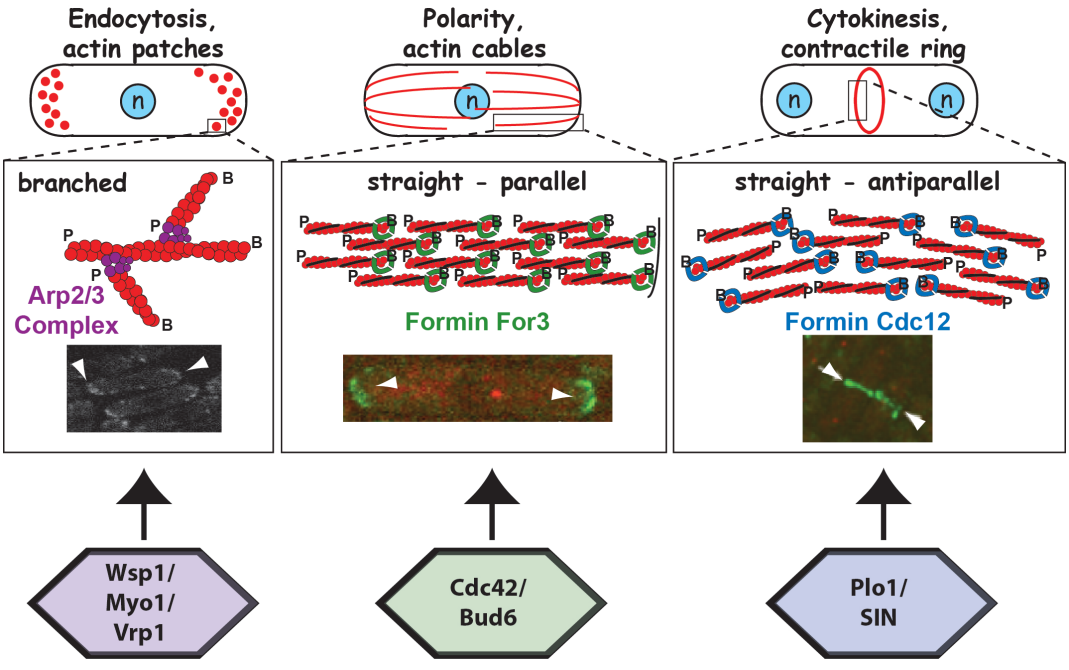

Figure 2-2: The three actin assembly factors of the fission yeast *S. pombe*
Cartoon showing the three F-actin networks in fission yeast, the Arp2/3 complex mediated actin patches, the formin For3p mediated actin cables, and the formin Cdc12p mediated contractile ring. Inset images are fluorescent micrographs indicating the *in vivo* distribution of each

assembly factor. Colored hexagons represent the upstream signals that were thought to be the only form of regulating actin assembly in fission yeast. Source: adapted from D. R. Kovar. (Vladmir Sirotkin et al. 2008; Martin et al. 2007; Bohnert et al. 2013; Ohkura et al. 1995; Almonacid et al. 2011)

Capping protein binds to barbed ends and is essential for proper actin networks

Capping protein binds to the barbed end of actin filaments preventing further elongation and in fission yeast is a hetero-dimeric protein consisting of two subunits, Acp1p and Acp2p. Capping protein localization is actin dependent, and depletion of one or both of the subunits leads to defects in the actin cytoskeleton: the endocytic actin patches are disrupted and are more numerous and contractile ring formation is disrupted leading to severe cytokinesis defects (Nakano et al. 2001; Kovar et al. 2005). Capping protein has been localized to the actin patches through fluorescent tagging and has been implied to localize to the contractile ring. However we now know that actin networks compete for actin monomers and the defects seen at the ring could be indirect via the Arp2/3 complex mediatedactin patches incorporating too much actin monomer. Much like cofilin, capping protein affects global F-actin levels within all structures. Over-expression of either subunit followed by staining with phalloidin gives no signal, indicating a total lack of F-actin(Nakano & Mabuchi 2006a). Overall, capping protein provides another link between F-actin networks within cells.

SECTION 2.3 INTRODUCTION

To control F-actin network density, actin polymerization is tightly regulated through the activation of assembly (nucleation) factors by GTPase signaling cascades, the rate at which F-actin barbed ends are capped, the rate at which assembly factors are turned off, and F-actin disassembly factors (Campellone & Welch 2010; Chesarone & Goode 2009; Michelot & Drubin 2011). The supply of unassembled G-actin is not generally considered to be limiting (Mullins &

Pollard 1999; Zigmond et al. 1998). Alternatively, it is possible that the actin cytoskeleton is homeostatic with a limited concentration of G-actin, which is competed for by assembly factors to help regulate its incorporation into diverse F-actin networks. However, this intriguing additional hypothesis has not been systematically tested.

Fission yeast forms three F-actin network structures by three different assembly factors (Kovar et al. 2011). The Arp2/3 complex assembles short-branched F-actin in endocytic actin patches, whereas the formins For3p and Cdc12p assemble long-straight F-actin in polarizing actin cables and the cytokinetic contractile ring, respectively. The amount of actin and other components incorporated into actin patches and contractile rings is remarkably consistent, varying less than 50% for each structure (Laporte et al. 2011; Vladimir Sirotkin et al. 2010; J. Q. Wu 2005). Although measuring the composition of actin cables has been technically challenging, they may be similarly consistent. Of the ~1 million actin molecules per cell, ~35 to 50% are evenly distributed between 30 to 50 actin patches, ~10% are incorporated into contractile rings, and perhaps as much as 15% are estimated to be consumed by actin cables (Laporte et al. 2011; Vladimir Sirotkin et al. 2010; J. Q. Wu 2005; Martin & Chang 2006; Wang & Vavylonis 2008).

To test this additional hypothesis of actin assembly factor competition for actin monomers within the cell I systematically depleted each F-actin network in fission yeast. Since we know how much actin is incorporated into each network, we can predict the outcome of depleting each network as it pertains to the relative G-actin concentration in cells. For example, by depleting all of the Arp2/3 complex mediated endocytic actin patches the G-actin concentration in cells will approximately double. Upon actin assembly factor depletion I discovered that inhibition of the Arp2/3 complex in fission yeast not only eliminates Arp2/3 complex-mediated endocytic actin patches, but due to the newly freed up actin monomer, also

induces assembly of a dramatic excess of formin-assembled F-actin. Conversely, disruption of the formins increases the density of Arp2/3 complex-mediated actin patches. Depletion of the F-actin severing protein cofilin prevents the turnover from F- to G-actin, and this disruption of the flux of monomer liberated by depleting an actin assembly factor prevents ectopic actin from forming. Furthermore, modifying actin levels significantly perturbs the fission yeast actin cytoskeleton. Increasing actin favors Arp2/3 complex-mediated actin assembly, whereas decreasing actin favors formin-mediated contractile rings. Therefore, competition for G-actin helps regulate the proper amount of F-actin assembly for diverse processes.

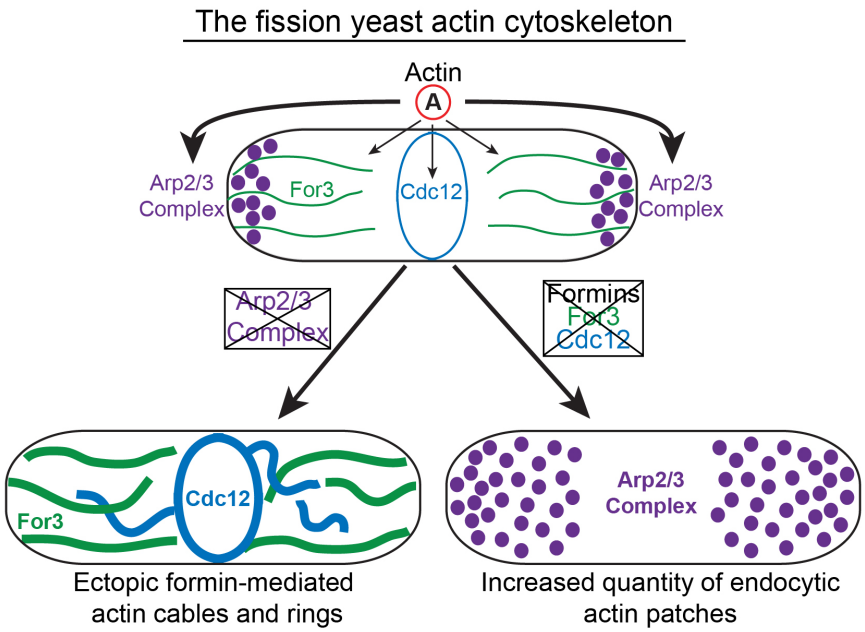

Figure 2-3: Graphical abstract demonstrating F-actin assembly factor competition for monomers in the fission yeast *S. pombe*
Cartoon showing the three F-actin networks in fission yeast, the Arp2/3 complex mediated actin patches, the formin For3p mediated actin cables, and the formin Cdc12p mediated contractile ring all sharing the common pool of actin monomers indicated by the A in the red circle. Depletion of the Arp2/3 mediated actin patches leads to ectopic formin-mediated actin cables

and rings while depletion of the two formins For3p and Cdc12p leads to an increased density of Arp2/3 complex mediated actin patches.

SECTION 2.4 RESULTS

Pharmacological inhibition and genetic depletion of the Arp2/3 complex stimulates ectopic F-actin assembly

To directly test the hypothesis that assembly factors compete for G-actin, we investigated the consequences of systematically disrupting individual actin assembly factors in fission yeast cells. Initially, we treated cells expressing the general F-actin marker Lifeact-GFP with a range of concentrations of the Arp2/3 complex inhibitor CK-666 (Nolen et al. 2009), causing a dose-dependent decrease in the number of actin patches (Figures 2-4 A and B and Figure 2-6 A) and reduction in patch lifetime and motility (Table 1). Strikingly, actin patch depletion coincides with the dramatic formation of new ectopic cable-like F-actin (Figure 2-4 A and 2-6 A), saturating at ~100 µM CK-666 (2-4 B).

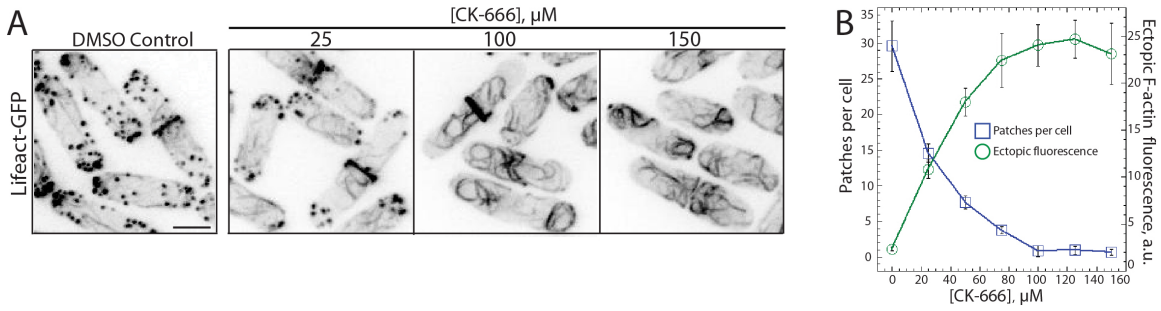

Figure 2-4: Pharmacological inhibtion of the Arp2/3 complex with the small molecule inhibitor CK-666 leads to a decrease in patches with a corresponding increase of ectopic F-actin

(A) Fluorescent micrographs of cells treated with DMSO (control) or a range of CK-666 concentrations. Scale bar, 5 µm. (B) Dependence of the number of actin patches (left) and Lifeact-GFP fluorescence intensity of ectopic F-actin (right) on the concentration of CK-666. Error bars, s.d.; n = 25.

The same dose dependent response can be seen in regards to viability of the fission yeast cells. As the concentration of CK-666 increases the viability of cells decreases correspondingly (Figure 2-5 A and B). CK-666 treatment facilitates ectopic F-actin assembly in both minimal and rich growth media, is visible with different general F-actin markers including rhodamine-phalloidin (Figures 2-6 A-F), and is inhibited by the G-actin sequestering drug LatA (Figure 2-6G).

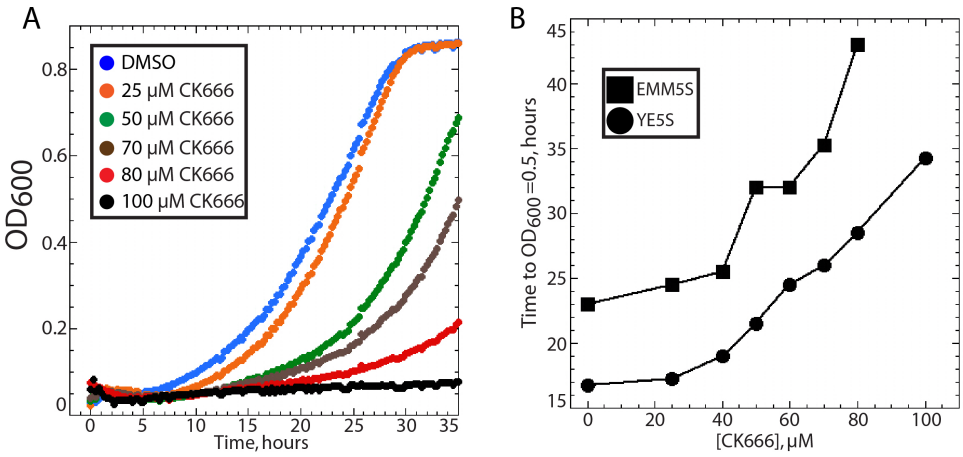

Figure 2-5: Pharmacological inhibtion of the Arp2/3 complex with the small molecule inhibitor CK-666 decreases cell viability
(A) OD timecourse of WT fission yeast grown in EMM5S media with increasing concentrations of CK-666. (B) Plot showing the effect of increasing concentrations of CK-666 on the time to OD = 0.5 (half maximal) for cells grown in EMM5S (square) and YE5S complete media (circle).

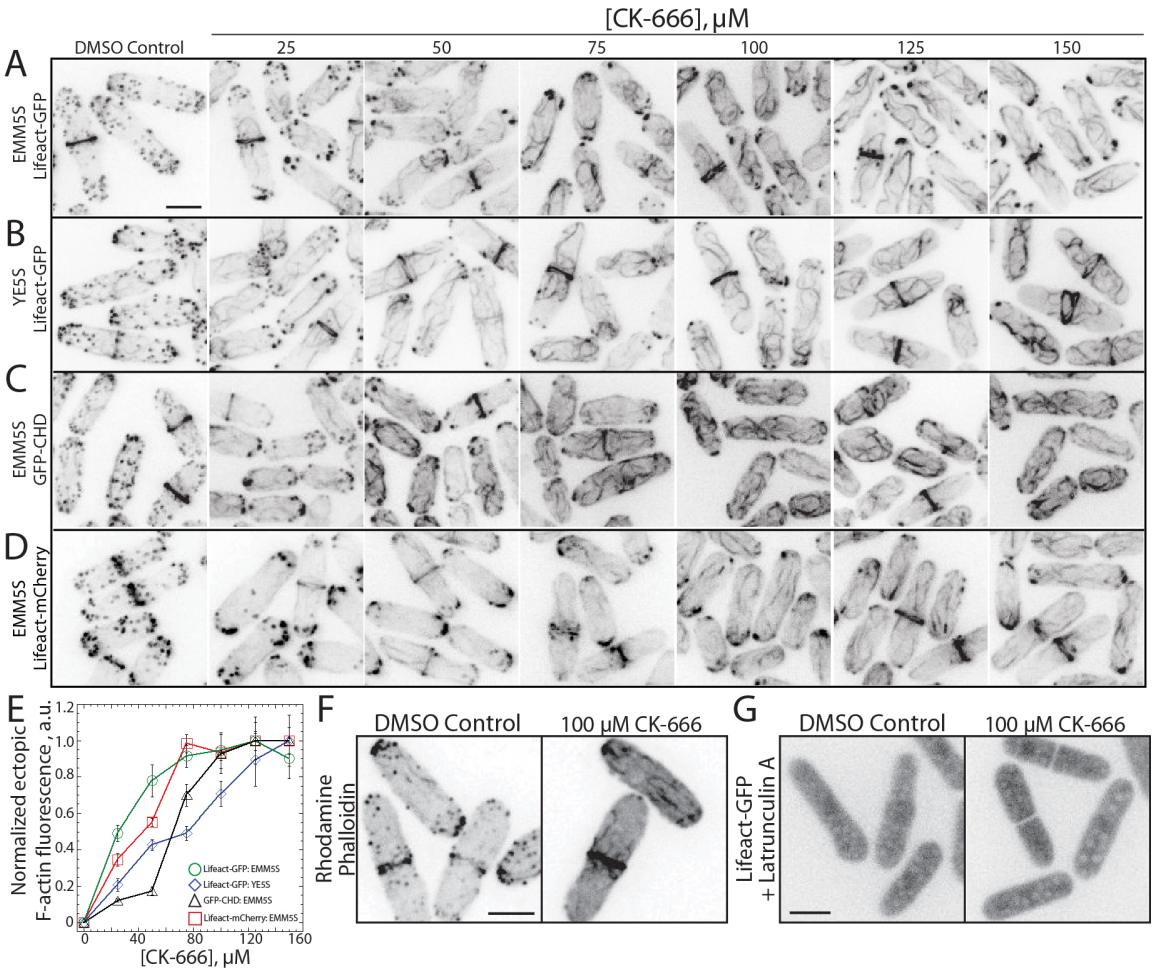

Figure 2-6: Visualization of CK-666 Stimulated Ectopic F-actin Assembly
(A-D) Fluorescence micrographs of cells expressing different general F-actin markers in minimal EMM5S and complete YE5S liquid media, and treated for 30 minutes with a range of concentrations of the Arp2/3 complex inhibitor CK-666. Scale bar, 5 µm. (A) Cells expressing Lifeact-GFP in EMM5S (B) Cells expressing Lifeact-GFP in YE5S. (C) Cells expressing GFP-CHD(rng2) in EMM5S. (D) Cells expressing Lifeact-mCherry in EMM5S. (E) Dependence of the normalized ectopic F-actin fluorescence per cell on the concentration of CK-666 for conditions in A-D. Error bars, s.d.; n = 25. (F) Rhodamine-phalloidin stained control and CK-666 treated cells that do not express a fluorescent F-actin marker. Scale bar, 5 µm. (G) Control and CK-666 treated cells expressing Lifeact-GFP were incubated with 25 µM LatA. Scale bar, 5 µm. Imaging from (2-6 C and D) was done by Jenna R. Christensen.

Observation of cells in a microfluidic chamber revealed that depletion of actin patches and the concomitant assembly of ectopic F-actin occurs in ~10-20 minutes after addition of saturating concentrations of CK-666 (Figure 2-7 A and B). Ectopic F-actin rapidly disassembles upon wash

out of CK-666 with a corresponding reassembly of actin patches in ~10-40 minutes (Figure 2-7 A and B). Actin patch proteins ArpC5-mCherry (Arp2/3 complex component) and Acp2-GFP (actin capping protein) are released into the cytoplasm by CK-666 treatment, but do not incorporate into the ectopic F-actin (Figure 2-8 A-C).

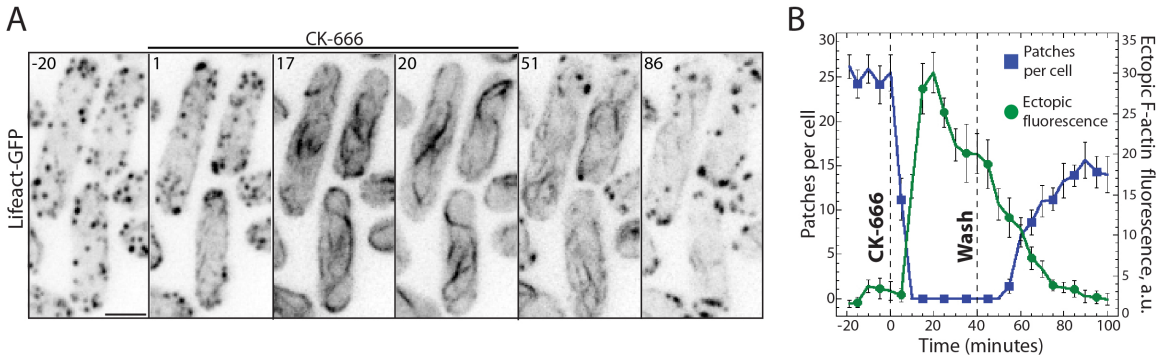

Figure 2-7: Effects of addition and washout of CK-666 on cells in a microfluidic chamber
(A) Time-lapse fluorescent micrographs after the addition of saturating CK-666 at zero minutes, and removal of CK-666 at 40 minutes. Scale bar, 5 µm.
(B) The number of actin patches (left) and ectopic F-actin (right) upon the addition and removal (dashed lines) of CK-666. Error bars, s.d.; n = 10.

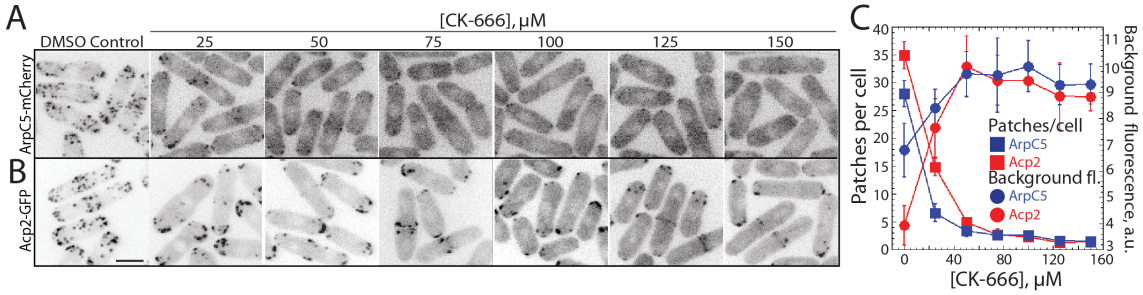

Figure 2-8: Visualization of actin patch components in Arp2/3 complex inhibited cells.
(A and B) Fluorescence micrographs of endocytic actin patch markers in cells treated for 30 minutes with a range of CK-666 concentrations. Scale bar, 5 µm.
(A) Cells expressing the Arp2/3 complex component ArpC5-mCherry. (B) Cells expressing actin capping protein Acp2-GFP. (C) Dependence of the number of ArpC5- and Acp2-labeled actin patches per cell (left) and background cytoplasm fluorescence (right) on the concentration of CK-666. Error bars, s.d.; n = 25. Imaging from (2-8 A and B) was done by Jenna R. Christensen.

Genetic disruption of Arp2/3 complex also leads to ectopic F-actin assembly, albeit less prominently than with CK-666 since actin patches are not reduced completely under these conditions (Figure 2-9 A-D). Compared to WT cells, at the restrictive temperature of 19°C Arp2/3 complex cold-sensitive mutant *arp3-C1* cells (McCollum et al. 1996) have approximately half the number of patches and a corresponding statistically significant 3-fold increase in ectopic F-actin ($p<0.0001$) (Figure 2-9 A and C). Similarly, reducing Arp2/3 complex expression by shutting off Arp3 (SO-arp3) for 46 hours also halves the number of patches per cell while increasing the amount of ectopic F-actin by more than 3-fold ($p<0.0001$) (Figure 2-9 B and D).

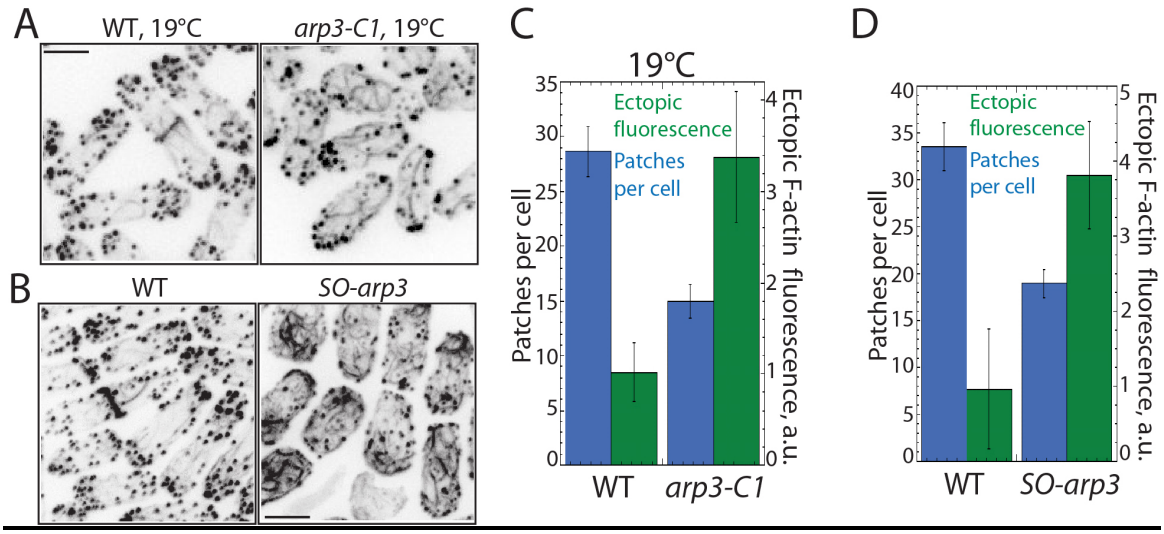

Figure 2-9: Genetic depletion of the Arp2/3 complex leads to ectopic F-actin formation
(A) Fluorescent micrographs of WT and Arp2/3 complex mutant *arp3-C1* cold sensitive cells following 4 hours at 19°C. Scale bar, 5 µm. (B) Fluorescent micrographs of WT and Arp2/3 complex shut off (*SO-arp3*) cells after inhibiting expression for 46 hours. Scale bar, 5 µm. (C) Actin patches per cell (blue) and Ectopic F-actin fluorescence (green) of cells from (A). Error bars, s.d.; n = 25. (D) Actin patches per cell (blue) and Ectopic F-actin fluorescence (green) of cells from (B). Error bars, s.d.; n = 25. The SO-arp3 line was generated by and imaging from (2-9 A and B) was done by Elisabeth Barrone and Vladimir Sirotkin.

Ectopic F-actin requires formin and profilin

We next investigated whether the cable-like ectopic F-actin is spontaneously assembled, or is dependent upon remaining actin assembly factors: the formins For3p and Cdc12p. 100% of single formin mutant cells (*for3Δ* or *cdc12-112* temperature sensitive) assemble ectopic F-actin when treated with CK-666 at the restrictive temperature of 36°C, whereas double formin mutant *for3Δ cdc12-112* cells do not (Figure 2-10 A-D top versus bottom rows). Disrupting the small G-actin binding protein profilin (*cdc3-124*), which is necessary for formin-mediated actin assembly *in vivo* (Chang et al. 1997; Kovar 2003), also prevents CK-666 mediated ectopic F-actin assembly (Figure 2-10 E).

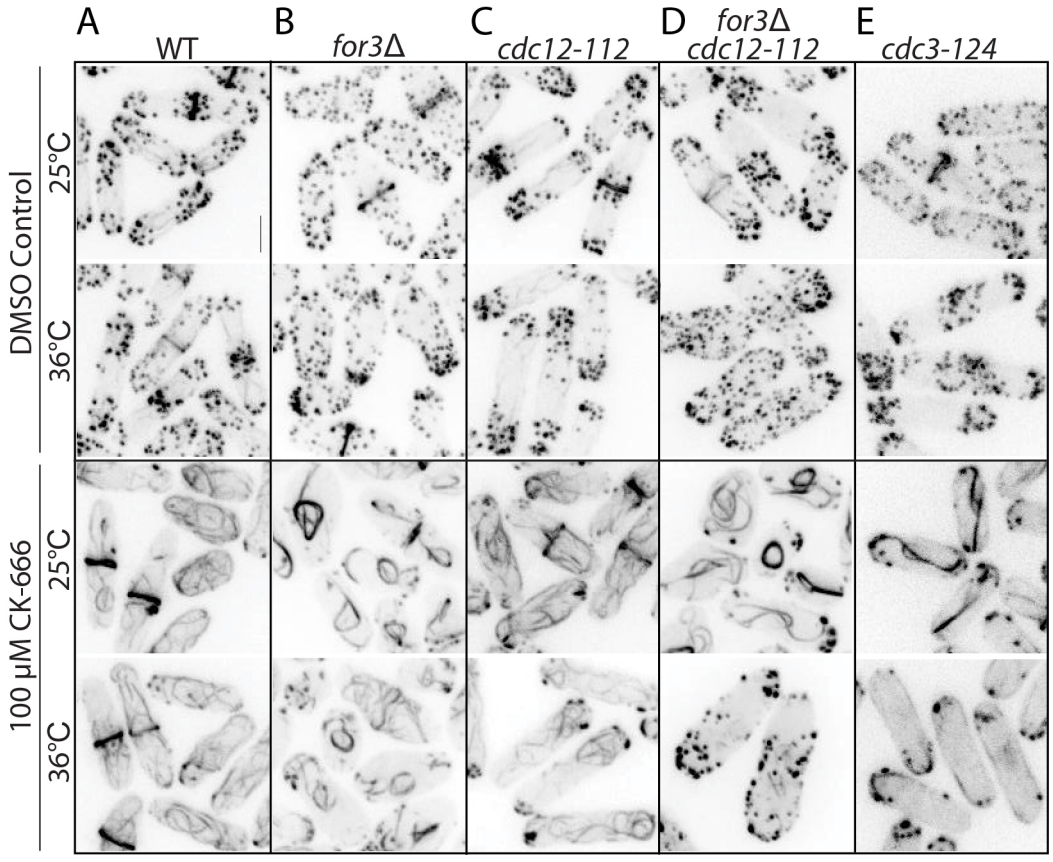

Figure 2-10: Ectopic F-Actin Assembly Requires Formin
(A-E) Fluorescence micrographs of Lifeact-GFP in WT and mutant cells incubated for 30 minutes with DMSO (control) or 100 µM CK-666 at 25 or 36°C. Scale bar, 5 µm. (A) WT cells.

(B) Polarity formin mutant *for3Δ* cells. (C) Cytokinesis formin mutant *cdc12-112* cells. (D) Double formin mutant *for3Δ cdc12-112* cells. (E) Profilin mutant *cdc3-124* cells.

Time-lapse imaging revealed that formin-mediated ectopic F-actin is highly dynamic, whereas smaller F-actin aggregates formed by inhibition of Arp2/3 complex in double formin mutant cells are immobile (Figure 2-11). Additionally, the F-actin binding protein tropomyosin (Cdc8p) (Balasubramanian et al. 1992), which associates with formin-assembled filaments (Balasubramanian et al. 1992; Skau & Kovar 2010; Skoumpla et al. 2007), localizes to the ectopic F-actin (Figure 2-12 A). Similarly, the formin-mediated contractile ring marker Rlc1-tdTomato localizes to robust rings in CK-666 treated cells (Figure 2-12 B).

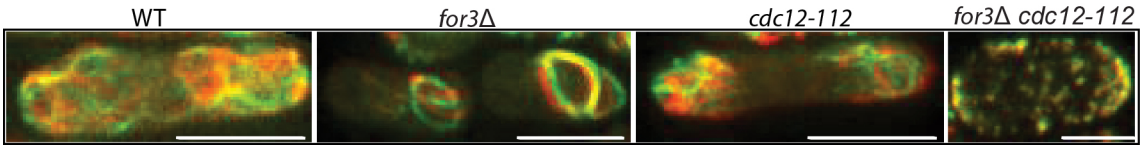

Figure 2-11: Formin mediated ectopic F-actin is dynamic versus F-actin aggregates in the double formin mutant.
Merged fluorescent micrographs of ectopic F-actin visualized with Lifeact-GFP at 0 seconds (green) and 180 seconds (red) for WT, *for3Δ, cdc12-112*, and *for3Δ cdc12-112* cells at 36°C. Scale bars, 10 µm.

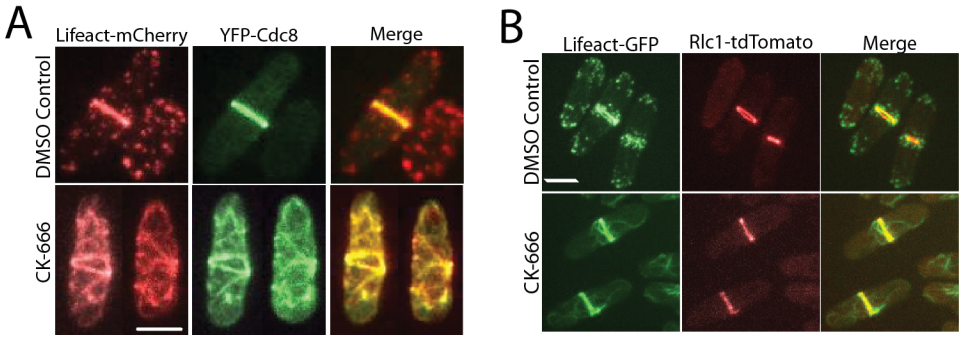

Figure 2-12: Formin mediated ectopic F-actin is bound by formin filament specific actin binding proteins
(A) Fluorescent micrographs of cells expressing both Lifeact-mCherry and tropomyosin YFP-Cdc8, incubated for 30 minutes with DMSO (control) or 100 µM CK-666. Scale bar, 5 µm. (B) Fluorescent micrographs of cells expressing both Lifeact-GFP and Rlc1-tdTomato incubated for 30 minutes with DMSO (control) or 100 µM CK-666. Scale bar, 5 µm.

These results indicate that inhibition of Arp2/3 complex amplifies formin-mediated actin assembly in fission yeast, suggesting an underlying homeostatic state whereby assembly factors compete for G-actin. Increased levels of G-actin produced by inhibiting Arp2/3 complex may allow intrinsically active formins to elongate filaments faster (Kovar et al. 2006), and/or turn on inactive formin molecules (Higashida et al. 2008) (Ramabhadran et al. 2013).

For3p primarily localizes to and forms actin cables from cell tips, whereas active Cdc12p forms contractile rings in the middle of dividing cells (Feierbach & Chang 2001; Chang et al. 1997). Consistent with these different cellular localizations, line scans of fluorescence intensity across the length of individual interphase cells treated with CK-666 revealed that single formin mutants assemble unique ectopic F-actin patterns (Figure 2-13). Ectopic F-actin is present in approximately three peaks at the tips and middle of WT cells, while it localizes primarily to poles in *cdc12-112* cells, and to the midzone in *for3Δ* cells. Ectopic F-actin in *for3Δ* cells is assembled by Cdc12p in the midzone rather than relocated there following its assembly elsewhere (Figure 2-14 A), indicating that Cdc12p is active in the midzone during interphase when the Arp2/3 complex is inhibited.

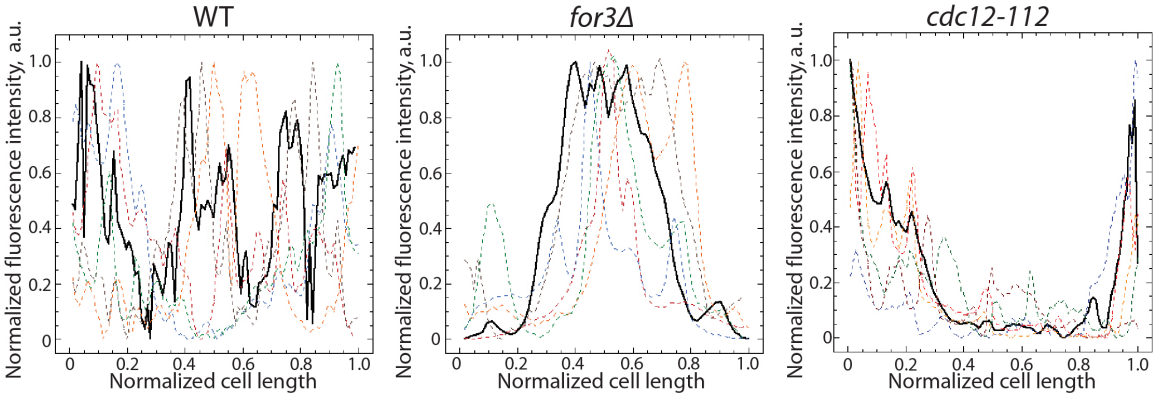

Figure 2-13: Each formin mediates a distinct pattern of ectopic F-actin
Line scans of ectopic F-actin intensity along the length of five representative cells (dashed colored lines), and the average of 20 cells (solid black line).

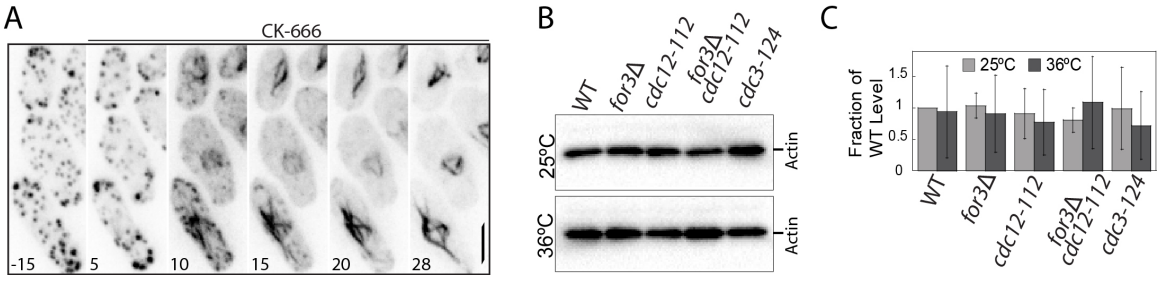

Figure 2-14: The formin For3p mediates circular ectopic actin and the actin levels in the formin mutants are unchanged versus wildtype
(A) Time-lapse fluorescent micrographs showing Lifeact-GFP in formin mutant *for3Δ* cells before and after the addition of CK-666 at zero minutes (Movie S2). Scale bar, 5 μm. (B) Western blots with an α-actin antibody showing the relative levels of actin in WT, *for3Δ, cdc12-112, for3Δ cdc12-112*, and *cdc3-124* cells at 25 and 36°C. (C) Quantification of the blots from (J), with values normalized to WT levels at 25°C. Error bars, s.d.; n = 3. Western blot analysis from (2-14 B and C) was done by Vladimir Sirotkin.

The fluorescence intensities of Lifeact-GFP and rhodamine-phalloidin in Cdc12-mediated contractile rings increase in WT cells treated with CK-666 (Figure 2-15 A and B). Contractile ring F-actin levels are also elevated in *for3Δ* cells, and even more so when *for3Δ* cells are treated with CK-666 (Figure 2-15 A and B). Therefore, Cdc12p assembles more robust rings upon inhibition of the other assembly factors, suggesting that the formin Cdc12p competes with both Arp2/3 complex and the formin For3p for G-actin.

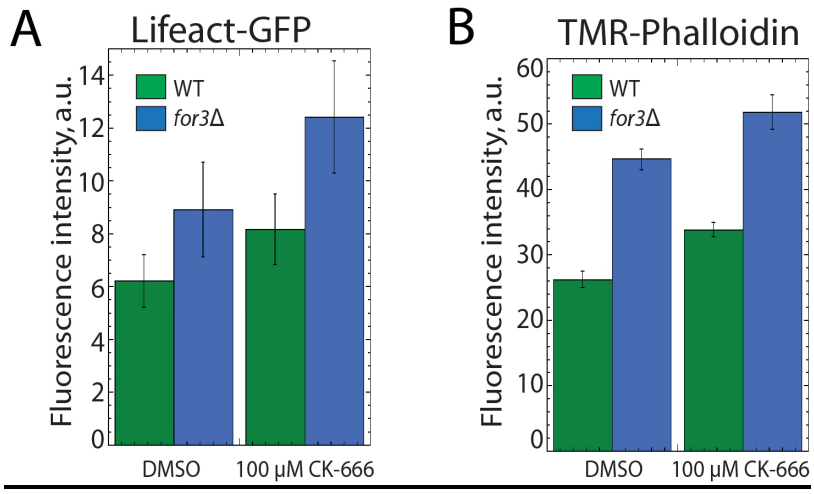

Figure 2-15: Contractile ring fluorescence intensity increases in CK-666 and *for3Δ* cells
(A and B) Mean fluorescence intensity of Lifeact-GFP (A) or rhodamine-phalloidin (B) in contractile rings of WT and *for3D* cells incubated with DMSO (control) or 100 µM CK-666. Error bars, s.d.; n ≥ 25.

Depletion of the formins Cdc12p and For3p increases the quantity of Arp2/3 mediated actin patches

We next investigated whether depleting the formins enhances Arp2/3 complex-mediated actin assembly (Figures 2-16 A and B). While formin mutant and WT cells have similar total amounts of actin (Figures 2-14 B and C), single (*cdc12-112* and *for3Δ*) and double (*cdc12-112 for3Δ*) formin mutant cells have increasingly higher densities of Arp2/3 complex-dependent actin patches (Figure 2-16 B). The density of Lifeact-GFP-labeled actin patches increases from ~1.0 (per µm2 of confocal Z-projections) in WT cells to ~1.6 in *cdc12-112 for3Δ* cells. However, in both single and double formin mutant cells, the amount of Lifeact-GFP fluorescence, lifetime, and motility of individual patches are relatively unchanged (Figure 2-16 B and Table 1). The assembly of an excess number of actin patches with similar dynamics suggests that the concentration of G-actin could be important for regulation of actin patch initiation by the Arp2/3

complex. Conversely, consumption of G-actin by individual patches may instead be limited by the number of activated Arp2/3 complexes, barbed end capping protein, and F-actin disassembly by cofilin (Vladimir Sirotkin et al. 2010; Q. Chen & Pollard 2013; Berro et al. 2010).

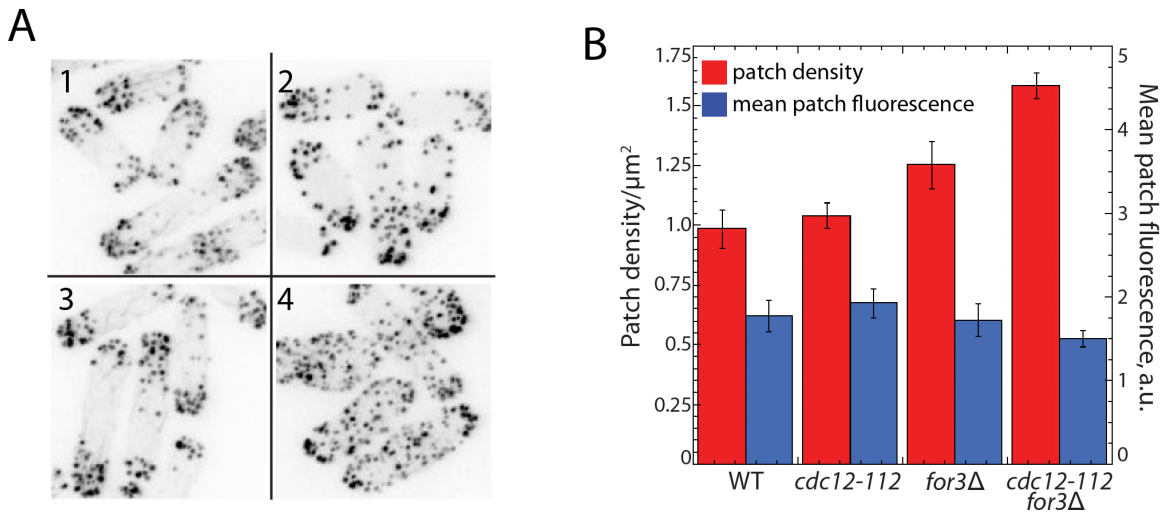

Figure 2-16: Depletion of the formins increases the endocytic actin patch density in fission yeast cells.
(A) Fluorescent micrographs showing Lifeact-GFP in formin mutant cells at 36°C. 1. WT, 2. *for3Δ*, 3. *cdc12-112*, 4. *for3Δ cdc12-112*. (B) The density (red) and mean fluorescence (blue) of Lifeact-GFP labeled actin patches in WT and formin mutant cells grown at 36°C for 3 hours. Error bars, s.d.; n = 25.

Depletion of the F-actin severing protein ADF/Cofilin prevents CK-666 mediated ectopic F-actin assembly

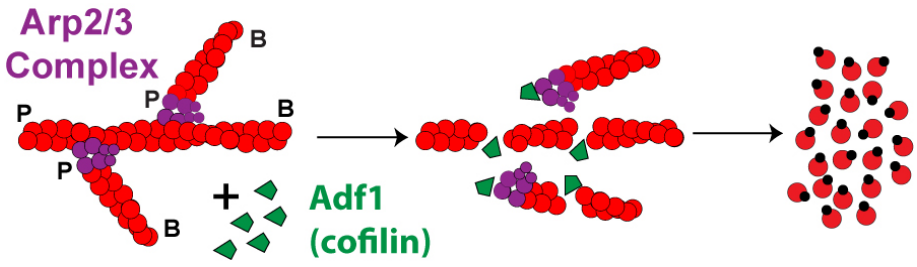

Figure 2-17: Cartoon depicting severing by the protein Adfp1/cofilin
Adf1/cofilin (green diamonds) bind to and sever actin filaments, hastening the transition back to ATP and potentially profilin bound G-actin

We hypothesize that inhibition of Arp2/3 complex liberates G-actin by preventing its incorporation into new patches, thereby increasing its availability for the formins (Figure 2-17). Because the F-actin severing protein cofilin is required for actin patch disassembly, depletion of cofilin increases the density and size of actin patches and prevents formin-mediated assembly of both rings and cables (Figures 2-18 A and C) (Nakano & Mabuchi 2006b; Q. Chen & Pollard 2013). Given that CK-666 inhibits nucleation by Arp2/3 complex but does not disassemble pre-existing branches (Hetrick et al. 2013), it is therefore not surprising that treatment of cofilin mutant cells (*adf1-1*) with 100 µM CK-666 at the restrictive temperature of 36°C does not deplete actin patches, and consequently does not induce formin-mediated ectopic F-actin assembly (Figure 2-18 A). Prevention of CK-666 mediated ectopic F-actin assembly appears to be specific to the cofilin *adf1-1* mutant, because deletion of the F-actin bundling endocytic actin patch component fimbrin (*fim1Δ*) does not prevent ectopic F-actin formation (Figure 2-18 B).

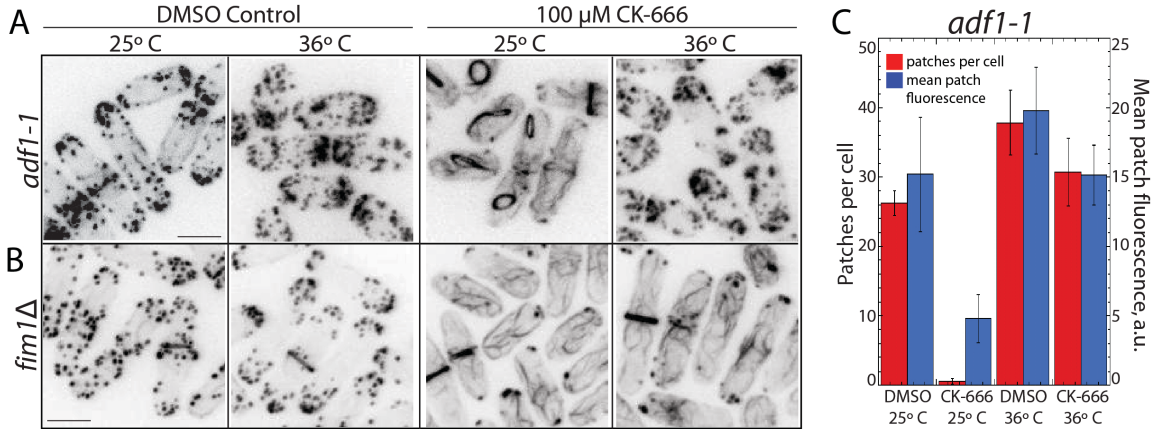

Figure 2-18. Depletion of ADF/Cofilin Prevents CK-666 Mediated Ectopic F-Actin Assembly.
(A-C) Mutant cells expressing Lifeact-GFP were grown at 25 or 36°C for 2 hours, and incubated with DMSO or 100 µM CK-666 for 30 minutes. (A) Fluorescent micrographs of cofilin mutant *adf1-1* cells at 25 and 36°C. Scale bar, 5 µm. (B) Fluorescent micrographs of fimbrin mutant *fim1Δ* cells at 25°C. Scale bar, 5 µm.

(C) Actin patches per cell (red) and mean patch fluorescence (blue) of cofilin mutant *adf1-1* cells from (A). Error bars, s.d.; n = 25.

Varying actin concentrations disrupts formin- and Arp2/3 complex mediated F-Actin assembly

Because the disruption of actin assembly factors and their associated structures leads to extraneous F-actin assembly by competing factors, we hypothesized that the specific cellular actin concentration is critical for proper F-actin network formation. We replaced the endogenous actin (act1) promoter with the thiamine-repressible Pnmt1 promoter, which in the presence or the absence of thiamine for 22 hours results in either a ~5-fold under- or ~5-fold over-expression of actin, respectively (Figure 2-19 A-C).

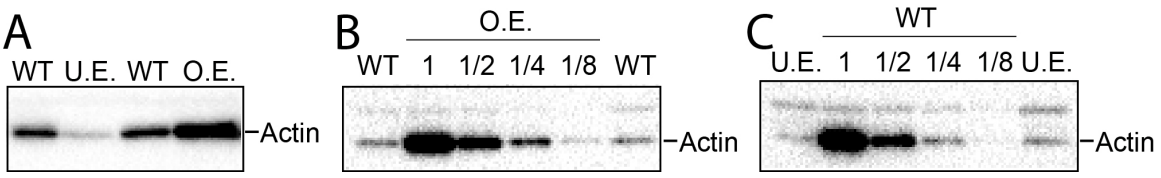

Figure 2-19: Western blots demonstrating the actin over or under-expression in fission yeast cells
(A-C) Western blots with an α-actin antibody showing the relative levels of actin in WT, actin under-expression (U.E.), and actin over-expression (O.E.) cells. (A) Blot from equivalent sample volumes. (B) Serial dilutions of the actin over-expression sample relative to WT (first and last lanes). (C) Serial dilutions of the WT sample relative to the actin under-expression sample (first and last lanes). Generation of and western blot analysis (2-19 A-C) of the actin over- and under-expression cells was done by Elisabeth Barone and Vladirmir Sirotkin.

Fluorescent images of Lifeact-GFP revealed that under- and over-expressing actin has contrasting effects; under-expression (U.E.) favors formin-mediated contractile rings whereas over-expression (O.E.) favors Arp2/3 complex-mediated actin patches (Figure 2-20 A). Because actin cables are difficult to image, we focused our quantitative analysis on actin patches and contractile rings. There are ~3-fold fewer actin patches per cell when actin is under-expressed

(Figure 2-20 B), but individual patch behaviors (lifetime, mean Lifeact-GFP fluorescence, and motility) are only affected slightly (Figures 2-20 C-E and Table 1). Conversely, actin over-expression cells contain at least 2-fold more actin patches per cell (Figure 2-20 B), an underestimate as individual patches are extremely difficult to discern within broad swaths of patch-like material (Figures 2-20 A-D) that colocalizes with the actin patch component fimbrin Fim1-mCherry (Figure 2-21). The lifetime of distinguishable individual patches in actin over-expression cells is ~2-fold longer, and they travel an ~3.5-fold shorter distance from the cortex during internalization (Figures 2-20 C-E and Table S1). Interestingly, actin patch dynamics are significantly altered in actin over-expression cells where actin is increased by ~500%, whereas patch dynamics are not altered in formin mutant cells where the available actin may be increased by only ~20% (Table 1).

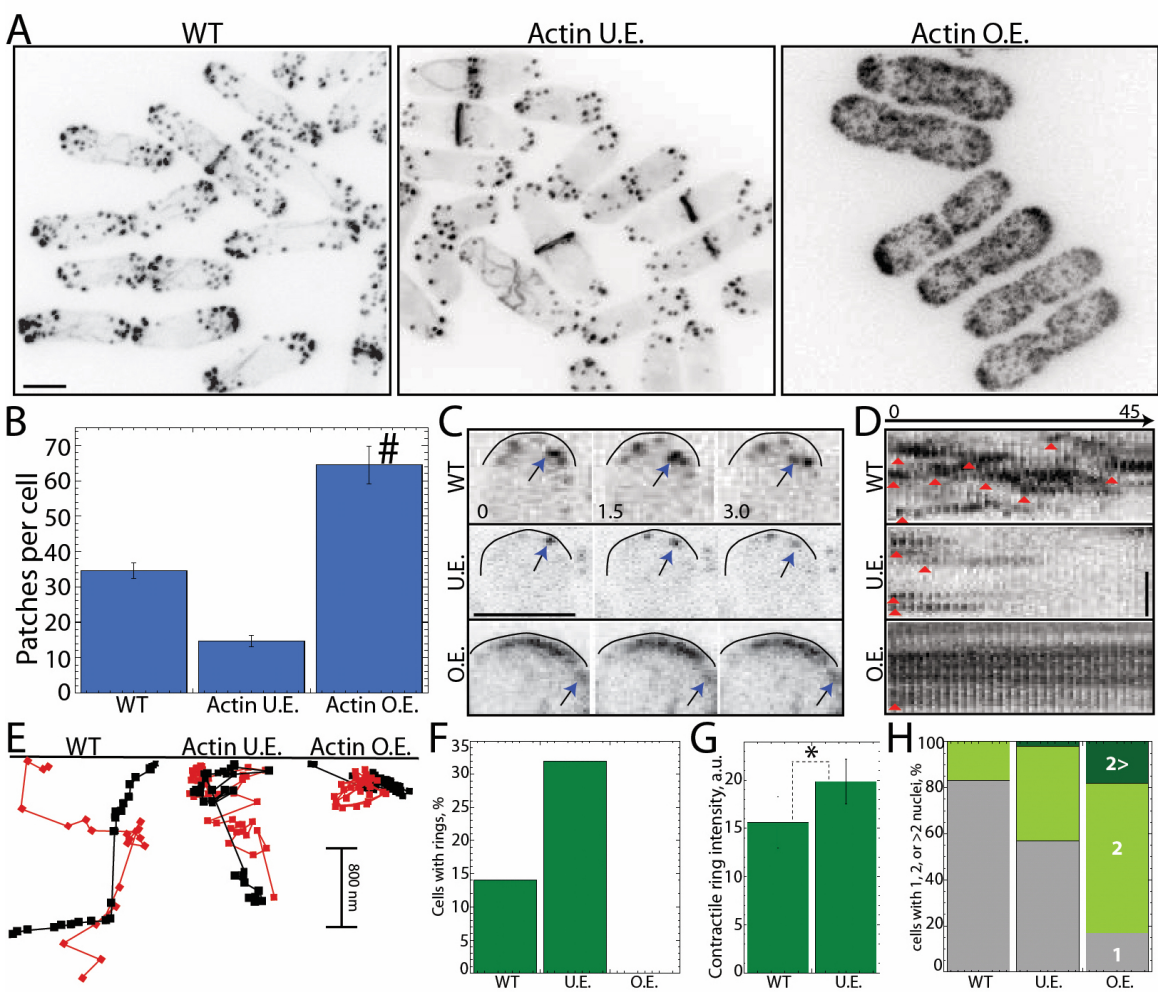

Figure 2-20. Varying Actin Concentrations Disrupts Formin- and Arp2/3 Complex-Mediated F-Actin Assembly.

(A-H) Comparison of Lifeact-GFP labeled F-actin networks in WT cells, and in cells under-expressing (U.E.) or over-expressing (O.E.) actin for 22 hours.

(A) Representative fluorescent micrographs. Scale bar, 5 µm. (B) Actin patches per cell. Error bars, s.d.; n = 25. Actin patches per O.E. cell is underrepresented due to patch aggregation (#). (C) Time-lapse (seconds) fluorescent micrographs of actin patches (arrows) (Movie S3). Scale bar, 5.0 µm. (D) Kymographs (Time = 0 to 45 seconds) of the cell tips shown in (C), revealing actin patch (red triangles) dynamics. Scale bar, 5 µm. (E) Plots of the position of two representative patches (red and black) over time (0.75 seconds per point). (F) Percent of cells with contractile rings. (G) Lifeact-GFP fluorescence intensity in rings. Error bars, s.d.; n = 25. P = 0.0098. (H) Percent of cells with 1, 2, or >2 nuclei.

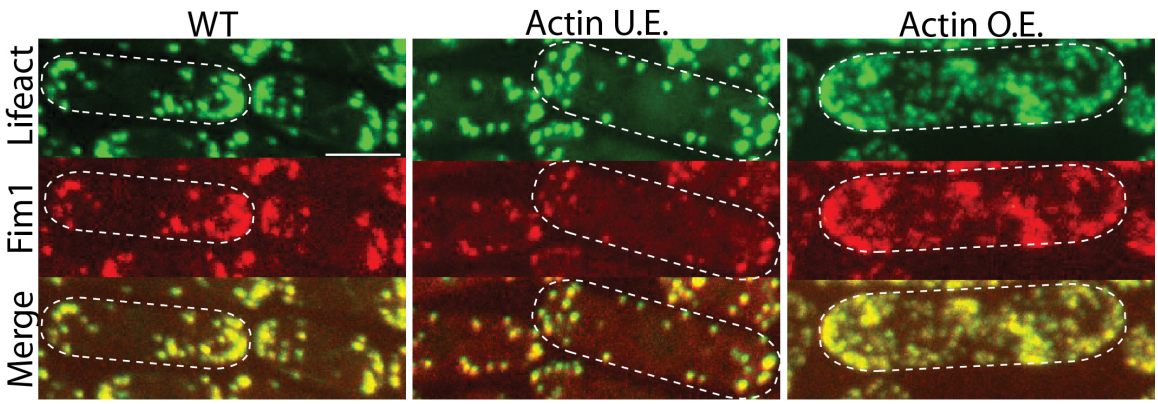

Figure 2-21: The endocytic actin patch binding protein Fimbrin localizes to cortical F-actin in actin under- and over-expression cells.
Fluorescent micrographs of WT, U.E., and O.E. cells expressing both Lifeact-GFP and the endocytic actin patch marker Fim1-mCherry. Representative cells are indicated with a dashed outline. Scale bar, 5 µm. Imaging from (2-21) done by Elisabeth Barone and Vladimir Sirotkin.

Formin-mediated contractile rings are not detected in cells over-expressing actin (Figures 2-20 A, 2-22 C), and >80% of these cells are multi-nucleate with malformed septa (Figure 2-20 H and Figures 2-22 A and B). The type II myosin regulatory light chain Rlc1-GFP contractile ring marker confirmed that multi-nucleate cells over-expressing actin fail to form normal contractile rings (Figure 2-22C). Conversely, ~2-fold more cells under-expressing actin have contractile rings compared to WT cells (Figure 2-20 F), and those rings have significantly more Lifeact-GFP fluorescence (actin) (Figure 2-20 G), resulting in >2-fold more bi-nucleate cells with deformed septa than WT cells (Figure 2-20 H and Figure 2-22 A and B).

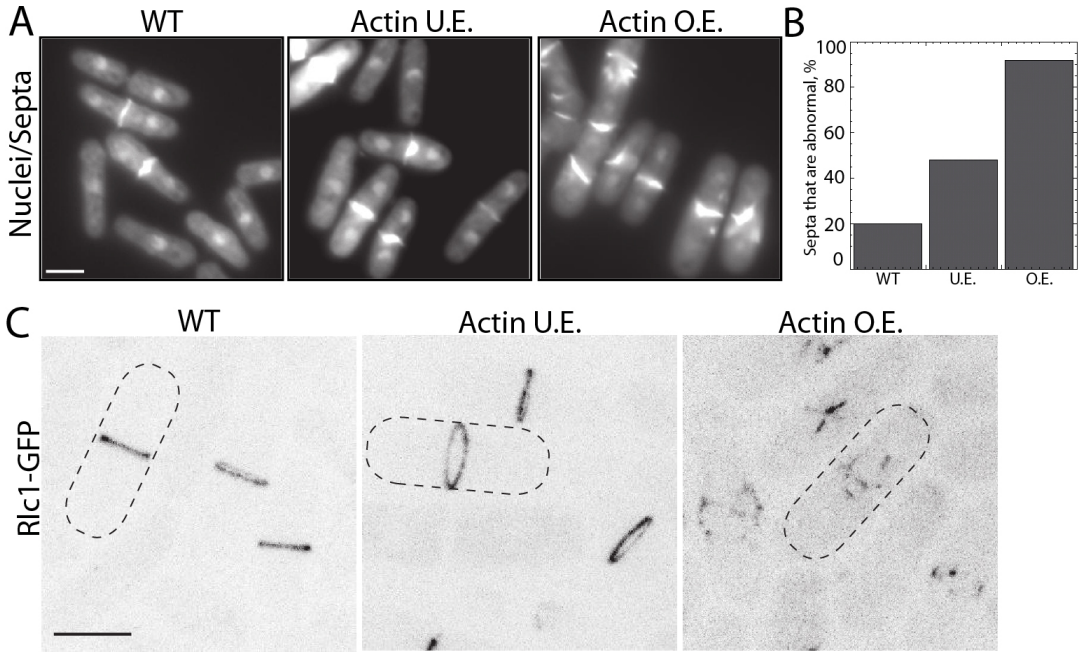

Figure 2-22: Comparison of nuclei, septa and Rlc1-GFP localization in WT, actin under-expression (U.E.), and actin over-expression (O.E.) cells.
(A) Fluorescent micrographs of cells fixed and stained with DAPI (nuclei) and Calcofluor (septa). Scale bar, 5 µm. (B) Percent of septa that are abnormal (misplaced, misaligned, broad, incomplete). (C) Fluorescent micrographs of WT, U.E., and O.E. cells expressing the contractile ring marker Rlc1-GFP. Representative cells are indicated with a dashed outline. Scale bar, 5 µm. Imaging from (2-22 C) was done by Vladimir Sirotkin.

Thus, reduced actin concentrations appear to decrease Arp2/3 complex-mediated actin patches and favor formin-mediated contractile rings, whereas elevated actin concentrations favors actin patches over contractile rings. Increased actin concentration may stimulate excessive actin patch initiation by Arp2/3 complex, which subsequently consumes the majority of actin at the expense of formins. Conversely, reduced actin concentration may increase the ratio of profilin to G-actin, which is critical for formin Cdc12 function (Kovar 2003). Lastly, treatment of cells under- or over-expressing actin with a range of concentrations of CK-666 supports our hypothesis that competition for a common pool of G-actin helps regulate the extent of F-actin network assembly (Figure 2-23 A and B). Cells under-expressing actin require a lower concentration of CK-666 to

fully disassemble the fewer number of actin patches, and form less formin-mediated ectopic F-actin than WT cells. On the other hand, cells over-expressing actin require ~2-fold more CK-666 to fully disassemble the excess of actin patches, and form >3-fold more ectopic F-actin.

We discovered that depletion of either Arp2/3 complex- or formin-dependent F-actin networks leads to enhanced F-actin assembly by the remaining actin assembly factors. Furthermore, raising actin levels favors Arp2/3 complex actin patches, whereas lowering actin levels favors formin contractile rings. These results suggest an important regulatory mechanism whereby the actin cytoskeleton is in homeostasis, characterized by an intrinsic competition for a common pool of G-actin that helps set the number and size of diverse F-actin structures in fission yeast. Consumption of G-actin by one F-actin network is critical to limit the amount of G-actin available for other networks, and that the F to G-actin levels are in homeostasis. This competition could explain why Arp2/3 complex mutations suppress profilin mutations in fission yeast (McCollum et al. 1996; Balasubramanian et al. 1996).

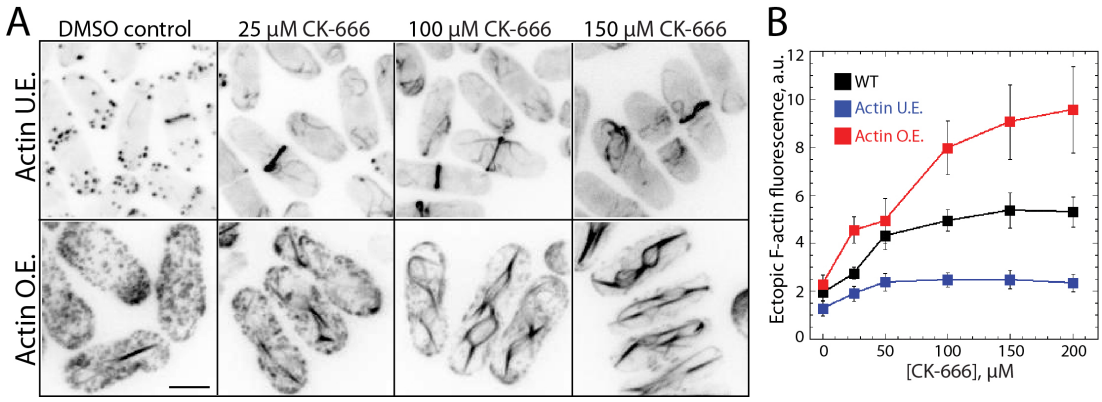

Figure 2-23: Actin under- and over-expression cells assemble different amounts of formin mediated ectopic F-actin.
(A) Fluorescent micrographs of cells incubated with DMSO (control) or a range of CK-666 concentrations for 30 minutes. Scale bar, 5 µm.
(B) Dependence of Lifeact-GFP fluorescence in ectopic F-actin structures per cell on the concentration of CK-666. Error bars, s.d.; n = 25.

Table 1: Comparison of Actin Patch Dynamics, Related to Results and Discussion

Strains and Conditions[a]	Patch Lifetime (sec)	Internalization From Cortex (nm)[e]	Mean Fluorescence Intensity (a.u.)[f]	Max Fluorescence Intensity (a.u.)[g]
DMSO[b]	11.73 ± 3.9	1060 ± 330	1211 ± 26	1595 ± 88
25 μM CK-666[b]	30.32 ± 6.5	460 ± 220	1191 ± 18	1470 ± 71
50 μM CK-666[b]	37.38 ± 9.8	0	1190 ± 17	1406 ± 51
WT[c]	15.4 ± 2.7	1284 ± 285	3550 ± 370	4810 ± 710
for3Δ[c]	19.1 ± 5.0	939 ± 175	3443 ± 275	3450 ± 290
cdc12-112[c]	17.3 ± 4.2	1333 ± 332	3834 ± 345	3850 ± 350
for3Δ cdc12-112[c]	17.5 ± 4.0	1313 ± 335	2982 ± 178	3000 ± 200
WT[d]	17.2 ± 5.5	1230 ± 218	1700 ± 65	2290 ± 160
Actin U.E.[d]	18.2 ± 9.1	1190 ± 275	1800 ± 130	2290 ± 160
Actin O.E.[d,h]	36.5 ± 10.5	270 ± 110	1730 ± 42	2110 ± 81

[a]All values are mean ± s.d., n ≥ 50 patches.
[b]Actin patch dynamics in WT cells expressing Fim1-mCherry that were treated with CK-666. Related to Figure 2-4 A and 2-6 A.
[c]Actin patch dynamics in formin mutant cells expressing Fim1-mCherry. Related to Figure 2-16.
[d]Actin patch dynamics marked with Lifeact-GFP in cells under- (U.E.) and over- (O.E.) expressing actin. Related to Figure 2-20.
[e]Patch displacement from initiation to disappearance.
[f]Mean fluorescence intensity of individual patches over the course of their lifetime.
[g]Maximum fluorescence intensity (peak fluorescence) of individual patches over the course of their lifetime.
[h]Data is from individual patches discernable by the particle tracking program.

SECTION 2.5 DISCUSSION

Although competition for G-actin had not been systematically tested before, and has only occasionally been suggested as a possible actin cytoskeleton regulatory mechanism (Chesarone & Goode 2009; Gao & Bretscher 2008; Kovar et al. 2011; Nakano & Mabuchi 2006b; Basu & Chang 2011) (Hotulainen & Lappalainen 2006), multiple Arp2/3 complex inhibition experiments from diverse cell types can be interpreted similarly. For example, depletion of actin patches by either over-expressing the Arp2/3 complex inhibitor Gmf1 or depleting the Arp2/3 complex activator Dip1p both lead to ectopic F-actin formation in fission yeast (Basu & Chang 2011; Nakano et al. 2010). Budding yeast Arp2/3 complex mutant cells have excessive formin-like F-actin cables (Winter et al. 1997). Furthermore, in insect and diverse animal cell types the inhibition of Arp2/3 complex leads to depletion of lamellipodia with a simultaneous increase in

the number of long, straight, bundled F-actin networks such as formin- and Ena/VASP-dependent filopodia-like structures (Hotulainen & Lappalainen 2006; Rogers et al. 2003; Sarmiento et al. 2008; Steffen et al. 2006; Suraneni et al. 2012; C. Wu et al. 2012; Q. Yang et al. 2012). Therefore, considerable care is required to interpret experiments that perturb actin assembly factors or actin levels.

Aside from reinterpretations of previous work that modified actin assembly factor levels and the evidence for F to G-actin homeostasis presented here, a question that still needs a complete answer is: do cells actively utilize competition for actin monomers to regulate unperturbed, endogenous F-actin networks? Shortly after the publication of the work described above (Burke et al. 2014), research from within the Kovar lab as well as our collaborators implicated the small G-actin binding protein profilin as a multifunctional protein fulcrum that ensured the correct incorporation of actin into different networks. Suarez et al. demonstrated that profilin both enhances formin-mediated actin assembly (as was previously known) and serves as an inhibitor of the Arp2/3 complex (Suarez et al. 2015). Elegant in vitro TIRF-M experiments showed that the addition of the fission yeast profilin Cdc3p to beads that were either coated with the Arp2/3 complex activator Wsp1 or the formin Cdc12p simultaneously dampened the Arp2/3 mediated assembly while facilitating the processive elongation of formin mediated filaments. More detailed analysis targeted this Arp2/3 complex inhibition to profilin disrupting the association of Wsp1p and actin monomers, preventing the formation of the simulated actin trimer between the Arp2, Arp3 and an actin subunit. As mentioned above, the over-expression of actin led to over assembly of the Arp2/3 complex mediated actin patches in fission yeast. In Suarez et al. this phenotype was rescued by a simultaneous over-expression of *cdc3*. At a certain level, actin over-expression cells are not viable and cannot undergo cytokinesis. Over-expression of

profilin rescued the cytokinesis defect as well as the endocytic actin patch defects to a certain extent, improving dynamics, lifetime, and internalization rates (Suarez et al. 2015). Conversely the addition of moderate amounts of the Arp2/3 complex inhibitor CK-666 rescued the cytokinesis defects of *cdc3-124ts* cells at the semi-restrictive temperature. Suarez et al. demonstrated *in vitro* and *in vivo* that the fission yeast actin cytoskeleton can be regulated by the competition between assembly factors for actin monomers, and that profilin was the multifunctional key facilitating some networks while dampening others.

In a companion study Rotty et al. demonstrated the relationship between the Arp2/3 complex and profilin was conserved in a mammalian system (Rotty et al. 2015). Utilizing murine fibroblasts that were devoid of the Arp2 subunit (Arp2-/-), they saw a marked decrease in the lamellipodia while stimulating stress fibers and other protrusive F-actin structures mediated by Ena/VASP such that the overall F-actin levels were relatively unchanged. Furthermore modifying the levels of Profilin-1 in fibroblasts heavily changed the F-actin distribution within cells. Increasing Profilin-1 decreased overall actin incorporation into the leading edge/lamellipodia, while decreasing Profilin-1 had the opposite effect wherein the lamellipodia was larger than WT cells. This directly implicates Profilin-1 as an Arp2/3 complex inhibitor in mammalian cells. One important commonality between Suarez et al. and Rotty et al. is both studies demonstrated that the ability of profilin to bind to G-actin was essential for Arp2/3 inhibition for the fission yeast profilin Cdc3p and the mammalian Profilin-1. Although Suarez et al. and Rotty et al. clearly show the Arp2/3 complex is inhibited by profilin and that the multifunctional properties of profilin are important for F to G-actin homeostasis and assembly factor competition, there is still a nascent area of study that is focusing on a variety of ways that profilin can be regulated. Whether profilin's ability to bind to the phospholipid PI4,5P2 or it's

ability to be phosphorylated on tyrosines has any effect on its ability to regulate F-actin networks has yet to be elucidated but provides completely new avenues of study. Whether or not signaling cascades like those that facilitate the creation of specific phospholipids or tyrosine phosphorylation directly affect the F-actin cytoskeleton are enticing targets of research now that we have a greater understanding of how they might affect actin assembly factors through the intermediary of profilin.

Besides the effect profilin has on F to G-actin homeostasis and assembly factor competition for actin monomers other groups have found ways that cells actively store or segregate pools of actin for specific processes like lamellipodial assembly and cell migration. In 2012 Suraneni et al. found the Arp2/3 complex was necessary for proper fibroblast migration and lamellipodial extension, but that cells could still migrate in a defective way (Suraneni et al. 2012). In a follow up study the same author demonstrated that this residual ability to migrate was due to the up-regulation of formin-mediated networks coupled with myosin contractility and that by inhibiting formins with the small molecule inhibitor SMIFH2 this residual ability was nearly abolished (Rizvi et al. 2009; Suraneni et al. 2015). Cells can also store actin in F-actin and myosin contractile networks. Lomakin et al. demonstrated that migratory cells can be stimulated to mobilize by inhibiting myosin motors and shifting the balance of F-actin from stress fibers to the dramatically more dynamic leading edge/lamellipodia (Lomakin et al. 2015). Their interpretation is cells can “lock away” actin in these dense networks of stress fibers until needed, and that cells utilize this mechanism to limit the available actin to regulate network dynamics. In an interesting turn of events a different study showed that cells can utilize multiple pools of G-actin for distinct processes, and that segregating actin monomer into multiple pools was important for proper network dynamics. Utilizing Cath. a-differentiated neuroblastoma cells

from mice it was shown that the formin mediated networks were dependent on a cytoplasmic pool of G-actin bound by thymosin-beta-4 while the Arp2/3 complex mediated lamellipodia was dependent on G-actin not bound by thymosin-beta-4 (Vitriol et al. 2015). The interpretation as to what function thymosin-beta-4 is serving is much like that of profilin. Without thymosin-beta-4 sequestering monomers, the Arp2/3 complex mediated dendritic networks would consume all available actin, but thymosin-beta-4 serves as a chaperone to deliver actin monomers past the Arp2/3 complex mediated networks to the formins and Ena/VASP proteins in the filopodia and other protrusive networks.

SECTION 2.6 MATERIALS AND METHODS:

Strain Construction, Growth Conditions, and CK-666: Table 2 lists the fission yeast strains used in this study. Cells were maintained on standard YE5S complete and EMM5S minimal growth media. All strains combining two or more markers or mutants were constructed by genetic crosses and tetrad dissection. All crosses, except those involving the 3xPnmt1-act1 allele and arp3 shut off allele, were made on SPA5S plates followed by tetrad dissection on YE5S plates.

To construct the actin under- and over-expression strain, –173 nt to +3 nt of the act1+ promoter was replaced with the pFA6a-kanMX6-P3nmt1 cassette [Bahler 1998] so that actin expression is controlled by the thiamine-repressible 3xPnmt1 promoter. This strain is viable in the presence of thiamine. The 3xPnmt1-act1 allele was combined with Lifeact-GFP and other markers by genetic crosses on ME plates with 5.0 μg/mL thiamine, followed by tetrad dissection on YE5S plates.

The shut off allele of arp3 was created by replacing –109 nt to +3 nt of the arp3 promoter in the wild type diploid strain with pFA6a-natMX6-P81nmt1 cassette constructed by replacing

kanMX6 in pFA6a-kanMX6-P81nmt1 [S7] with natMX6. The haploid arp3 shut off strain was isolated by sporulation on ME plates and tetrad dissection on EMM5S plates in the absence of thiamine. The haploid arp3 shut off cells are viable in the EMM5S lacking thiamine and die in 3-4 days after addition of thiamine. The arp3 shut off allele was combined with Lifeact-GFP by genetic crosses on ME plates and tetrad dissection on EMM5S plates in the absence of thiamine.

Stock solutions of 10 mM CK-666 (Sigma, St. Louis, MO) were prepared in DMSO. 500 μL of exponentially growing cells (OD of 0.2-0.6, 25°C unless stated otherwise) were incubated in a 1.5 mL eppendorf tube for 30 minutes with the indicated amount of CK-666. For experiments at restrictive temperature, cells were pre-incubated at 36°C for 3 hours, followed by an additional 30 minutes with 100 μM CK-666. The arp3-C1 mutant was incubated at 19°C for four hours before imaging. For arp3 shut off, the arp3 shut off and control wild type cells were grown for 2 days (46 hours) in EMM5S with 5 μg/mL thiamine. Actin under- and over-expression cells were grown for 24 hours in YE5S at 25°C, washed three times with EMM5S supplemented with (under-expression) and without (over-expression) 5 μg/mL thiamine, and grown at 25°C for 22 hrs before imaging.

Rhodamine-phalloidin staining of F-actin structures was done using 1 mL of exponentially growing cells following 24 hours in YE5S complete media. Cells were fixed by adding 100 μL of 16% formaldehyde (Polysciences, Warrington, PA) for 2 minutes. Cells were spun down and permeabilized in 1 mL of 1% Igepal CA-630 in PBS (Sigma) for 30 seconds. Cells were washed four times in 1 mL PBS, then resuspended in 20 μL of 50% glycerol with 2 μL of 0.1 mg/mL stock solution of rhodamine-phalloidin (Life Technologies, Grand Island, NY).

Immunoblotting:

Actin under- and over-expression cells were grown overnight in YE5S at 25°C, washed three times with EMM5S without thiamine, re-seeded into EMM5S with (under-expression) and without (over-expression) 5 μg/mL thiamine, grown at 25°C for 22 hrs, and harvested by centrifugation. To compare actin levels in wild type, formin and profilin mutants, we collected samples of cells grown overnight in YE5S at 25°C and cells grown overnight in YE5S at 25°C and then shifted to 36°C for 3 hours.

Cells were disrupted by glass bead lysis in a FastPrep-24 (MP Biomedicals, Solon, OH) in Lysis Buffer U (50 mM Hepes, pH 7.5, 100 mM KCl, 3 mM MgCl2, 1 mM EGTA, 1 mM EDTA, 0.1% Triton X-100, 1 mM DTT, 1 mM PMSF, and Complete protease inhibitors (Roche, Fishers, IN). Samples were separated on SDS-PAGE gels, transferred onto PVDF membranes, and actin was detected by immunoblotting with anti-actin C4 monoclonal antibody (Sigma, St. Louis, MO) and secondary HRP-conjugated anti-mouse IgG antibody with SuperSignal West-Dura ECL reagent (Thermo-Pierce, Rockford, IL). Actin levels in actin under- and over-expressing cells were quantified in ImageJ from images of blots of serial dilutions of protein samples in the linear range. The actin levels in formin and profilin mutants relative to the wild type were measured in Image Lab (Bio-Rad, Hercules, CA) from three blots of the same protein samples.

Imaging Details:

For imaging, cells were grown in YE5S liquid media overnight at 25°C, subcultured into EMM5S liquid media for at least 24 hours at 25°C, and then spotted onto glass slides. Images of cells were acquired with a 100x, 1.4 NA objective on a Zeiss Axiovert 200M equipped with a

Yokogawa CSU-10 spinning-disk unit (McBain, Simi Valley, CA) illuminated with a 50-milliwatt 473-nm DPSS laser, and a Cascade 512B EM-CCD camera (Photometrics, Tucson, AZ) controlled by MetaMorph software (Molecular Devices, Sunnyvale, CA). Unless otherwise stated, fluorescent micrographs are maximum intensity projections of Z-series acquired at 0.50 μm intervals that span the entire cell. Epifluorescence images acquired for DAPI (nuclei) and Calcofluor (septa) analysis (quantified for at least 100 cells) were collected using an Orca-ER camera (Hamamatsu, Bridgewater, NJ) on an IX-81 microscope (Olympus, Tokyo, Japan) equipped with a 60x, 1.4 numerical aperture Plan Apo objective.

To acquire endocytic actin patch movies, cells were cultured as above, and then spotted onto EMM5S pads containing 25% gelatin on glass slides and sealed with VALAP (1:1:1 Vaseline:Lanoline:Parafin). Confocal images were collected with a Cascade 512BT camera (Photometrics, Tucson, AZ) on a Zeiss Axioimager M1 equipped with 63x, 1.4 numerical aperture oil-immersion lens and a Yokogawa CSU-X1 spinning-disk unit (Solamere, Salt Lake City, UT) with a Tempcontrol-37 objective heater (Zeiss, Thornwood, NY) controlled by MetaMorph software. Time-lapse movies were acquired at 750 ms intervals.

Rlc1-GFP in actin under- and over-expressing cells, LifeAct-GFP combined with Fim1-mCherry in actin under- and over-expressing cells, and LifeAct-GFP in arp3 shut off and control wild type cells were imaged using UltraView VoX (PerkinElmer, Waltham, MA) spinning disk confocal system equipped with C9100-50 EMCCD camera (Hamamatsu), installed on a Nikon Ti-E microscope with a 100×/1.4 N.A. PlanApo lens, and controlled by Volocity software. Cells were mounted on pads of 25% gelatin in EMM5S with or without 5 μg/mL thiamine and sealed with VALAP. Z-stacks of images spanning the entire cell depth at 0.4 μm intervals were collected for each strain.

CK-666 flow in and wash out experiments were performed in an Onix microfluidic perfusion chamber (CellASIC Corporation, Hayward, CA). Residual PBS was flushed from the culture/imaging chamber by running a flow of EMM5S with DMSO under 5 psi for two minutes. Cells (OD595 of 0.2-0.6) were loaded into the Y04C microfluidic plate for 3 sec at 8 psi. Flows at 5 psi of either EMM5S with DMSO or EMM5S with 2 mM CK-666 were applied. Onix plates contain polydimethylsiloxane, which absorbs hydrophobic small molecules such as CK-666. Therefore a high concentration of CK-666 was required for flow experiments. Confocal Z-stack time-lapse images were acquired at 1.0 minute intervals utilizing the 100x, 1.4 NA objective on a Zeiss Axiovert 200M equipped with the Yokogawa CSU-10 spinning-disk unit mentioned above, and the amount of patches per cell and Lifeact-GFP labeled ectopic F-actin fluorescence were measured every 5 minutes.

Quantification of Ectopic Fluorescence:

Mean fluorescence was measured with ImageJ using a 3.6 µm-wide circular selection tool placed over the middle of interphase cells (sum intensity Z-projections, 0.50 µm slices). Background fluorescence, measured with a 1.5 µm-wide circular selection tool in a region that lacked visible F-actin structures, was subtracted from the mean ectopic F-actin fluorescence. For quantification of ectopic F-actin distribution in Figure 2B, a fluorescent intensity profile was produced from a 3 µm-wide line drawn through the middle of the long axis of each cell. Cell length and Lifeact-GFP fluorescence were normalized independently for each strain.

Actin Patch Tracking:

Tracking of actin patches labeled with Lifeact-GFP or Fim1-mCherry was done with TrackMate particle tracker using the ImageJ program Fiji [Schindelin 2012]. Only patches that originated and disappeared during the course of the movie were quantified. Of these, at least 50 patches

chosen at random for each strain were measured for fluorescence intensity over time, patch lifetime, patch displacement, and speed. Kymographs to track actin patches on portions of the cell cortex over time were created by JFilament (http://athena.physics.lehigh.edu/jfilament/) [Smith 2010]. Patch density in Figure 2-16 was calculated as the number of patches per cell per μm2 area.

Table 2: Fission Yeast Strains Used in This Study, Related to Experimental Procedures

Strain Name	Genotype	Reference
VS703-C1	*h+, Pnmt41X-GFP-CHD(rng2)-Leu1+, ade6-M216 ura4-18, leu1-32*	This study
VS887-A1	*h+, act1::KanMX6-3xPnmt1-act1, ade6-M210 ura4-D18, his3-D1, leu1-32*	This study
MBY6843	*h+, pAct1 Lifeact-mCherry::Leu+, ade6-m216; leu1-32; ura4-D18*	(J. Huang et al. 2012)
MBY6656	*h-, pAct1 Lifeact-GFP::Leu+, ade6+, leu1-32, ura4-D18*	(J. Huang et al. 2012)
VS888-3	*h-, fim1-mCherry:: natMX6, leu1-32, ura4-D18, his3-D1*	This study
KV69	*h-, cdc12-112, his7-366, ura4-D18, leu1-32, ade6-M216*	(Chang et al. 1997)
KGY491	*h+, cdc3-124, ade6-216, ura4-D18, leu1-32*	(Balasubramanian et al. 1994)
FY527	*h-, leu1-32, his3-D1, ura4-D18, ade6-M216*	Liang et al. 1999
BFY9	*h-, for3Δ::kanMX6, ura4-D18, leu1-32, ade6*	(Feierbach & Chang 2001)
KV354	*h-, rlc1-gfp-KanR, ade6-M216, leu1-32, ura4-D18*	Lord et al. 2004
KV609	*h+, fim1Δ:: kanMX6, lifeact-GFP::Leu+, ade6-m216, leu1-32, ura4-D18*	This study
KV624	*h+, cdc3-124, pAct1 Lifeact-mCherry::Leu+, ade6-m216, leu1-32, ura4-D18*	This study
KV661	*h+, cdc12-112, Lifeact-GFP::Leu1+, ade6-m216, leu1-32, ura4-D18*	This study
KV662	*h?, for3Δ::KanMX6 cdc12-112, Lifeact-GFP::Leu+, ade6, leu1-32, ura4-D18*	This study
KV680	*h?, capB-GFP::kanMX6, Lifeact-mCherry::Leu+, ade6-M216; ura4-D18, leu1-32*	This study
KV681	*h?, adf1-1-ura+, Lifeact-mcherry::Leu+, ade6, leu1-32, ura4-D18*	This study
KV692	*h?, ARPC5-mCherry-natMX6, Lifeact-GFP Leu+, ade6-M216, leu1-32, his3-D1, ura4-D18*	This study
KV696	*h+, pAct1 Lifeact-GFP::Leu+, Sad1-mCherry::Nat, ade6-m216, leu1-32, ura4-D18*	This study
KV705	*h?, for3Δ::kanMX6, pAct1 Lifeact-GFP::Leu+, Sad1-mCherry::Nat ade6-m216, leu1-32, ura4-D18*	This study
KV800	*h?, arp3-C1, pAct1 Lifeact-GFP::Leu+; ura4-D18 ade6-M210, leu1-32*	This study
VS1589-10B	*h-, Lifeact-GFP::Leu+, act1::KanMX6-3xPnmt1-act1, ade6+, ura4-D18, his3-D1, leu1-32*	This study
VS1590-1A	*h-, leu1-32::Pact1-LifeAct-GFP-leu1+, ade6-M210, ura4-D18, his3-D1*	This study
VS1610-6	*h+/h-, natMX6-81xPnmt1-arp3/arp3+, ade6-M210/ade6-M216, leu1-32, ura4-D18, his3-D1*	This study
VS1680-6B	*h+, natMX6-81xPnmt1-arp3, ade6-M216, leu1-32, ura4-D18, his3-D1*	This study
VS1724-5B	*h-, natMX6-81xPnmt1-arp3, leu1-32::Pact1-LifeAct-GFP-leu1+, ade6-M216, ura4-D18, his3-D1*	This study
VS1765-1A	*h-, kanMX6-Pnmt1-3x-act1, fim1-mCherry-natMX6, leu1-32::Pact1-LifeAct-GFP-leu1+, ade6-M210, ura4-D18, his3-D1*	This study
VS1767-7D	*h+, kanMX6-Pnmt1-3x-act1, rlc1-gfp-KanR, ade6-M216, leu1-32, ura4-D18, his3-D1*	This study
VS1770-6D	*h+, fim1-mCherry-natMX6, leu1-32::Pact1-LifeAct-GFP-leu1+, ade6-M210, ura4-D18, his3-D1*	This study

CHAPTER 3: THE MECHANISM OF ACTIN FILAMENT ASSEMBLY BY VopL AND VopF

SECTION 3.1 PREFACE

VopL and VopF are WH2-domain actin assembly factors utilized by the infectious bacteria that cause cholera *Vibrio parahaemolyticus* and *Vibrio cholerae* (Tam et al. 2007; Liverman et al. 2007). Unlike other infectious bacteria that secrete proteins to activate host-cell nucleation factors such as Listeria (ActA) and Shigella (IcsA) to hijack the host-cell's F-actin cytoskeleton for motility, VopL and VopF nucleate the host cell's F-actin directly (Cossart 2000; Tam et al. 2007; Liverman et al. 2007). VopL and VopF are F-actin nucleators and are categorized into a unique group of assembly factors such as Spire, Cobl, and Sca2 that rely on multiple G-actin binding WH2 domains for their activity (Chesarone & Goode 2009; Quinlan et al. 2005; Haglund et al. 2010; Dominguez 2016). WH2 (WASP-homology domain 2) domains are small (~20 a.a) domains that bind ATP-bound G-actin in a 1:1 ratio with nanomolar affinity and are found in multiple F-actin assembly related proteins (Paunola et al. 2002; Chesarone & Goode 2009; Dominguez 2016). VopL and VopF are both homodimers, and their domain organization is conserved with 72% protein sequence similarity. From N to C-terminus both have two proline-rich regions, three WH2 domains, followed by a dimerization inducing Vop C-terminal Domain domain that causes a U shaped configuration (Liverman et al. 2007; Tam et al. 2007; Namgoong et al. 2011; Pernier et al. 2013). The F-actin nucleation capabilities of VopL and VopF are undisputed, however recent studies have been in conflict over the exact mechanism employed. Two proposed mechanisms have emerged: VopL binding to the pointed end of the filaments it nucleates, and VopF nucleating and binding to barbed ends of actin filaments (Namgoong et al.

2011; Pernier et al. 2013). Given their high similarity in protein sequence and domain organization, we predict VopL and VopF will have the same mechanism of actin filament assembly. Using multi-color TIRF microscopy we have shown that in the presence of actin monomers, VopL and VopF are purely actin filament nucleators that associate briefly with the pointed end of actin filaments before dissociating and do not bind to pre-existing filaments. In the absence of monomer VopL and VopF are competent to bind to both the pointed and barbed ends of actin filaments. We also observed a small fraction of events in conditions with saturating profilin where VopL and VopF can bind the barbed ends of pre-assembled actin filaments, greatly reducing the elongation rate. However in the light of their pathogenic nature, we believe that the primary function of VopL and VopF are to be high efficiency nucleators that promote the assembly of unproductive F-actin in the host cell thereby disrupting the F to G-actin homeostasis.

SECTION 3.2 VIBRIO'S F-ACTIN MODULATING VIRULENCE FACTORS

Vibrio bacteria are gram-negative bacteria and are the causative agent of the transmittable disease cholera. Members of the genus *Vibrio*, which total more than 100 species are mostly associated with aquatic habitats. Human infection usually occurs through ingesting contaminated seafood or water. *Vibrio* bacteria colonize the host's small intestine by adhering to the microvilli of the epithelium (Reidl & Klose 2002). The *Vibrio* serogroups O1 and O139 possess the pathogenicity island that contains the traditional cholera toxin (CT) that disrupts the CFTR ion channel homeostasis. In its most fulminant form, the gastrointestinal syndrome is characterized by a severe and unrelenting purging (1 liter per hour) of the bowel contents. These symptoms can cause massive outbreaks that can lead to severe morbidity if not mortality within hours (Reidl &

Klose 2002; Faruque et al. 1998; ABMM et al. 2015). However non-O1, non-O139 *Vibrio* devoid of the pathogenicity island conferring the ability to produce cholera toxin embody a genetically diverse group of strains that can cause outbreaks of disease in a CT-independent manner. Although these strains rarely cause pandemic disease, it has recently been revealed that certain non-O1, non-O139 strains of *V. cholerae* and *V. parahaemolyticus* can cause similar, if not ameliorated symptoms much like the O1 and O139 subgroups (ABMM et al. 2015). Frequently these non-O1, non-O139 serogroups are acquired by the host through infected fresh water or by consuming uncooked shellfish harvested from an infected area and their symptoms are often misdiagnosed as other common forms of food-borne illness. How these non-O1, non-O139 serogroups cause gastrointestinal symptoms was a major question. However recent studies have found that *V. cholerae* and *V. parahaemolyticus* utilize type-III secretion machinery to export virulence factors into the host's intestinal epithelial cells (Galán & Wolf-Watz 2006).

Several of these recently identified effectors, some identified by their "Vop" nomenclature (Vibrio Outer Protein), directly affect the host-cell's actin cytoskeleton. By doing so these virulence factors disrupt G to F-actin homeostasis in cells, leading to the degradation and depletion of endogenous F-actin networks. These effectors can bind to the endogenous networks, activate or poison host-cell actin assembly factors, or assemble actin by themselves. VopV contains multiple F-actin binding sites, can bundle F-actin *in vitro*, and strains expressing VopV will shorten and dull the microvilli of rabbit intestinal epithelial cells (Hiyoshi et al. 2011). VopO activates the RhoA-ROCK pathway in cells, activating the host cell's F-actin assembly factors and induces the formation of ectopic F-actin stress fibers (Hiyoshi et al. 2015). The actin crosslinking domain (ACD) of the MARTX toxin (an effector of a type-I secretion system) can cross-link actin monomers into poisonous oligomers that affect the formin class of

actin assembly factors (Ma & Mekalanos 2010; Kudryashov et al. 2008; Heisler et al. 2015). Most relevant to this discussion are the actin assembly factors VopL and VopF that can assemble host cell actin directly with high efficacy causing the breakdown of the epithelial tight junctions, leading to inflammation and gastro-intestinal symptoms (Tam et al. 2007; Liverman et al. 2007; Tam et al. 2010) (Figure 3-1 A-C).

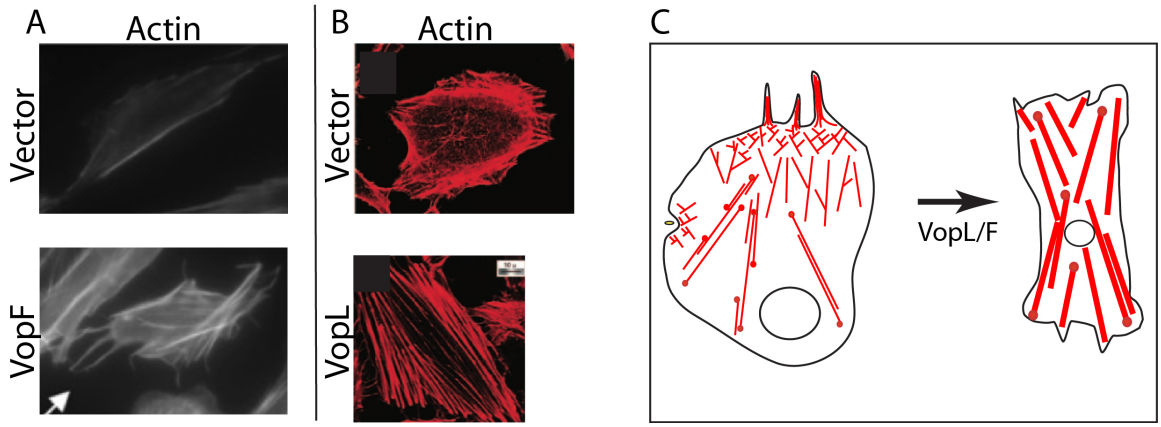

Figure 3-1: VopL and VopF reorganize the host cell's actin cytoskeleton
(A) Adapted from (Tam et al. 2007). Phalloidin stained CHO cells expressing an empty vector (top) or a vector containing VopF (bottom). The white arrow indicates the ectopic finger-like protrusions only seen in VopF transfected cells. (B) Adapted from (Liverman et al. 2007). Phalloidin stained HeLa cells expressing an empty vector (top) or a vector containing VopL (bottom). Notice the increase in the parallel thick actin bundles in the VopL transfected cell. (C) Cartoon depicting a generalized VopL or VopF mediated reorganization of the host cell's actin cytoskeleton into thick stress-fiber like networks.

SECTION 3.3 TANDEM WH2 DOMAIN ACTIN ASEEMBLY FACTORS

Cannonical methods of actin assembly: The Arp2/3 complex and formins

The actin cytoskeleton is utilized for a wealth of cellular processes including endocytosis, migration/motility, polarity establishment and cytokinesis. To achieve the rapid assembly and remodeling of actin networks necessary for these dynamic processes, cells express actin assembly factors to overcome the thermodynamically unfavorable reaction of de novo actin polymerization and to regulate where and when actin is polymerized (Chesarone & Goode 2009;

Amann & Pollard 2000). Investigating the biochemical mechanisms of how these assembly factors function is a cornerstone of the actin cytoskeleton research field and provides insights into how cells use specialized molecular machines to bring about a multitude of cytoskeletal structures. The Arp2/3 complex and the formins were the first two actin assembly factor classes to be identified and studied (Figure 3-2). The Arp2/3 complex makes short, branched filaments by binding to the side of pre-existing “mother” filaments, nucleating a new branched "daughter" filament through two subunits, Arp2 and Arp3, that employ mimicry of actin monomers, while remaining bound to the pointed end of the newly nucleated filament (Rotty et al. 2013; Pollard 2007). Cells then use this dense, dendritic branched network for multiple processes like endocytosis and membrane ruffling for motility (Campellone & Welch 2010). Formins make long, straight filaments by both promoting filament nucleation and elongation through the concerted mechanisms of their formin-homology 1 and formin-homology 2 domains (Pollard 2007). Formins processively elongate and protect filaments from premature capping by remaining continuously bound to the elongating barbed end (Breitsprecher & Goode 2013). Formin-mediated filaments are used for processes like cytokinesis, establishing polarity, and cell adhesion and migration (Goode & Eck 2007).

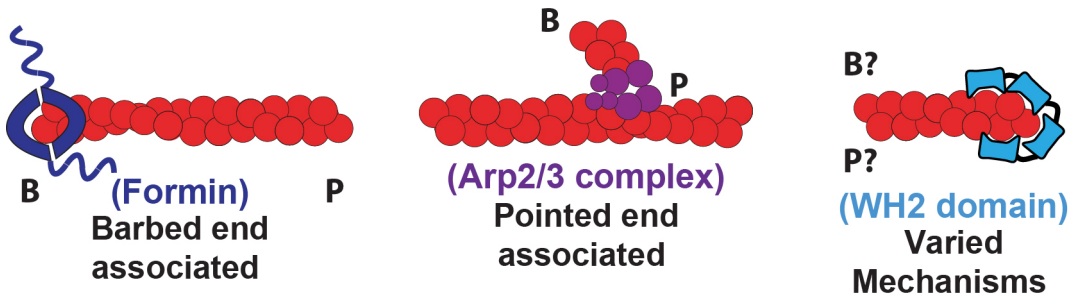

Figure 3-2: Cartoon the Formin, Arp2/3 complex, and WH2-domain assembly factors
Cartoon displaying the mechanism of F-actin assembly by Formins, the Arp2/3 complex, and the WH2-domain class of actin assembly factors. Generally formins bind to the barbed end of actin

filaments and stimulate runs of processive elongation in the presence of profilin, the Arp2/3 complex makes branched filaments from the sides of pre-existing mother filaments and remains bound to the pointed end, and the relatively newly discovered WH2-domain class of assembly factors has a wide variety of actin assembly capabilities ranging from nucleation of new actin filaments and pointed end binding to riding processively on the barbed end of pre-existing filaments like a formin.

The actin monomer binding WH2 domain is ubiquitous: sequestering actin monomers and assisting in assembly factor activation

Altogether, much time and effort has been spent on investigating the biochemical mechanism of actin filament assembly by the Arp2/3 complex and formins, and a general consensus of how these two classes function has been reached. However, there is a more newly discovered class of actin assembly factors that utilize the Wiskott-Aldrich syndrome protein homology 2 (WH2) domain (Figure 3-2) (Paunola et al. 2002; Qualmann & Kessels 2009). The WH2 domain is an abundant actin monomer-binding motif comprising of approximately 17 amino acids and contains the actin binding LKKV consensus sequence (Dominguez 2016; Paunola et al. 2002; Carlier et al. 2011). Arguably the most abundant WH2 domain protein is thymosin beta-4 (Tβ4). Tβ4 is a small protein (43 amino acids) that binds ATP G-actin with an affinity of ~ 0.15 μM and is present in concentrations up to 600 μM in cells (Carlier et al. 1993; Safer et al. 1991). Tβ4 renders actin monomers incompetent for assembly by sequestering them. However WH2 domains can be utilized for the direct assembly of actin filaments and are utilized by the mechanisms of actin filament assembly by the Arp2/3 complex and formins as well. WH2 domains are essential for the activation of the Arp2/3 complex; the nucleation promoting factors N-WASP and WAVE2 both contain WH2 domains and are responsible for bringing an actin monomer to the Arp2 and Arp3 subunits to promote the formation of an actin nucleus or trimer (Padrick et al. 2011; Ti & Pollard 2011; Helgeson et al. 2014). Some formins, like INF2 contain

putative WH2 domains in their auto-regulatory domains. When an actin monomer binds the WH2 domain, the N to C-terminal auto-inhibition is disrupted and INF2 becomes active (Ramabhadran et al. 2013).

Cells utilize WH2 domains in tandem for the direct assembly of F-actin

Unlike the Arp2/3 complex and formin utilization of WH2 domains, cells utilize proteins with WH2 domains in tandem arrays where the WH2 domain occurs in repeats of three to four domains with varying lengths of linkers in between to facilitate actin polymerization directly (Figure 3-2). Some WH2 domain containing assembly factors can also dimerize, further increasing the amount of monomers they can recruit, thereby increasing the efficiency of actin filament assembly (Namgoong et al. 2011; Pernier et al. 2013). Due to the great variation in this class of proteins, the mechanism as to how they assemble actin is largely unclear with multiple conflicting reports between studies of the same proteins.

The first protein shown to assemble actin by a mechanism different than that of the Arp2/3 complex or formins was Spire (Quinlan et al. 2005). Initial studies reported that Spire is monomeric and utilizes its four WH2 domains to promote actin filament nucleation and associates with the pointed ends of filaments. Later studies showed that Spire acquires the ability to dimerize upon binding to the formin Cappuccino, and these two assembly factors act synergistically where Spire recruits the actin monomers through its WH2 domains and remains bound to the pointed end, while the formin processively-elongates the newly nucleated filament (Quinlan et al. 2005; Quinlan et al. 2007). Multiple isoforms of Spire have been studied and are utilized for various cellular processes. This Spire-Cappuccino interaction is physiologically relevant, as the two assembly factors cooperate for the formation of the actin mesh necessary for

cytoplasmic streaming in *Drosophila* oogenesis (Quinlan 2013). Two isoforms of Spire in mice (Spire1 and Spire2) were identified as factors important for proper asymmetric cell division and polar-body extrusion (Pfender et al. 2011). The actin binding capability of Spire is essential, as truncating the WH2 domains from Spire in drosophila embryos causes enlarged cardiac cells, cytokinetic defects, and overall cardiac malformation (Xu et al. 2012).

Although the majority of studies implicate a pointed-end mechanism for Spire's actin assembly, there is evidence from Montaville et al. that Spire is actually a barbed-end capping protein (Montaville et al. 2014). They describe a "ping-pong" mechanism of filament elongation and capping when an N-terminal truncation of Spire containing the WH2 domains is added to assays with profilin and the formin Fmn2. Results from single color TIRF-M indicate that Spire can bind to Fmn2 bound rapidly elongating barbed ends and displace Fmn2 leading to arrests in filament elongation. Montaville et al. claim that this displacement and "ping-pong" mechanism of Spire replacing Fmn2 and vice versa happens to approximately half of the filaments analyzed. However they do not report the percentage of relative arrests in filament elongation with Fmn2 alone. Without that important control it is impossible to say whether the Spire or the experimental conditions themselves are leading to these results.

Similar to Spire, Cordon-bleu (Cobl) contains a tandem repeat of three WH2 domains and its mechanism of actin filament assembly is also disputed. Cobl was originally identified as a barbed end associated actin assembly factor enriched in the brain and involved in neuronal morphology (Ahuja et al. 2007; Haag et al. 2012). Other biochemical studies using a more complete construct and potentially non-physiological concentrations of Cobl implied that Cobl is a weak nucleator and primarily acts to sequester actin monomers and severs filaments (Husson et al. 2011; Carlier et al. 2011).

WH2 domain assembly factors: unresolved molecular mechanisms of actin assembly

Spire and Cobl are but just two examples of WH2 domain assembly factors mentioned above, and contrary to the numerous studies on the Arp2/3 complex and formins, there are not only great differences in the mechanisms of actin filament assembly between the two, but groups studying Spire and Cobl have not yet come to a consensus about how either protein stimulates actin filament assembly. The cell biological importance of understanding the mechanisms of how WH2 domain assembly factors assemble actin is further strengthened by studies revealing that certain pathogenic bacteria have appropriated this powerful mechanism and have made their own WH2 domain based assembly factors to hijack the host-cells actin cytoskeleton for their own bidding. *Rickettsia* bacteria express Sca2, a monomeric barbed-end binding protein containing three WH2 domains. Sca2 is exported to the bacteria's outter surface where it facilitates host-cell actin polymerization into a comet tail for intracellular motility (Haglund et al. 2010; Madasu et al. 2013). Some pathogens like *Vibrio* bacteria inject WH2 domain assembly factors into the host cell through a type-III secretion system with a different sinister intent. VopF and VopL are actin assembly factors utilized by the infectious bacteria, *Vibrio cholerae* and *Vibrio parahaemolyticus* that cause cholera (Tam et al. 2007; Liverman et al. 2007). Once secreted, VopF and VopL assemble host cell actin into non-productive networks that disrupt the F to G-actin homeostasis in cells leading to a degradation of the F-actin dependent tight junctions between intestinal epithelial cells (Tam et al. 2010). This can cause intestinal inflammation and irritation facilitating the passing of the bacteria. VopF and VopL share a nearly identical domain organization and have 72% protein sequence similarity (Figure 3-3), and their actin nucleation capabilities are undisputed. However much like Spir and Cobl, the mechanism by which VopL and VopF

stimulate actin assembly are in conflict (Namgoong et al. 2011; Pernier et al. 2013; Yu et al. 2011; Zahm et al. 2013; Avvaru et al. 2015).

SECTION 3.4 VopL and VopF

VopL: A WH2 domain actin assembly factor that promotes the virulence of *Vibrio parahaemolyticus*.

VopL is a 484 amino acid protein that is part of the type III secretion system in *V. parahaemolyticus* (Figure 3-3). Expressing VopL within cells increases F-actin assembly *in vivo* and recombinanatly purified VopL nucleates F-actin *in vitro* via bulk pyrene actin polymerization assays (Liverman et al. 2007). Mutational analysis showed the WH2 domains of VopL are necessary for actin assembly (Liverman et al. 2007; Namgoong et al. 2011). Truncating WH2 domains from six to four, to two, and to zero (VCD only) decreases the actin assembly capabilities correspondingly, with the VCD only truncation having the poorest actin assembly capability. Studies also indicated that dimerization of VopL, mediated by the VCD domain, was necessary for F-actin assembly and that the VCD of VopL associates with the pointed end of the filament (Namgoong et al. 2011). Single molecule TIRF experiments utilizing recombinantly purified VopL conjugated to quantum dots showed VopL nucleates actin filament assembly from the pointed end (Namgoong et al. 2011). However there are caveats of that interpretation to consider: only 3.9% of quantum dots were active, and while most filaments had an elongation rate equal to that of the control (~8 sub/sec), 7.6% of filaments elongated at double the control rate (~ 18 sub/sec) which were hypothesized to be associated with the barbed end of the filament like a formin. The addition of the small G-actin binding protein profilin decreases

the nucleation efficiency but does not change the elongation rate of actin filaments bound by VopL (Namgoong et al. 2011).

Crystallographic and mutational analysis of the VCD as well as the VCD complexed with an unpolymerizable G-actin mutant indicates that the dimerized VCD of VopL stabilizes short pitch (lateral) interactions between three actin monomers with their pointed ends oriented toward the base of the VCD (Zahm et al. 2013). The same study implied that the WH2 domains are primarily used to increase the local G-actin concentration so that the VCD may nucleate a filament (Yu et al. 2011; Zahm et al. 2013). The results generated from studies on VopL have generated the "filament template nucleation" model, where VopL stimulates rapid cycles of nucleation through the VCD and associates with the pointed end of the newly formed filament for a short period of time before filament release. These results and the model imply that VopL is purely a nucleation factor and does not bind to pre-assembled actin filaments.

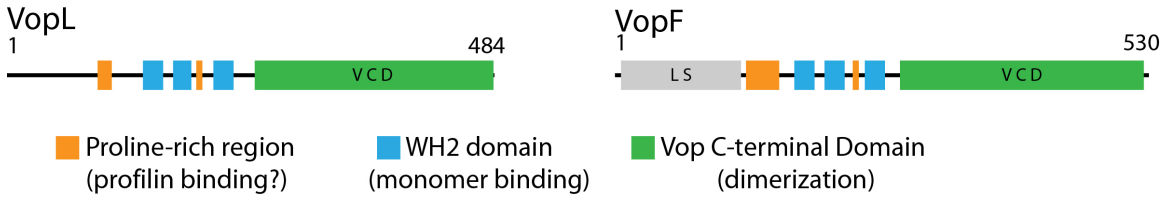

Figure 3-3: Domain organization of VopL and VopF
Total size in amino acids of VopL and VopF. Both VopL and VopF dimerize via the VCD domain and each dimer has six total WH2 domains that are each competent to bind an actin monomer. VopL and VopF facilitate nucleation of actin filaments through the cooperation of these two domains. It is unclear as to how the orange proline-rich region affects VopL and VopF function. The grey "LS" box marks the localization signal for the type-III secretion machinery of *V. cholerae*.

VopF: A WH2 domain actin assembly factor that promotes the virulence of *Vibrio cholerae*.

VopF is a 530 amino acid protein also identified as a part of a type III secretion system in *V. cholarae* with a similar domain organization as VopL (Figure 3-3) (Tam et al. 2007). VopF stimulates F-actin assembly in mammalian cells infected with bacteria expressing VopF, in cells transfected with VopF, or in bulk pyrene assembly assays *in vitro* (Tam et al. 2007). Cells expressing VopF or rabbits infected with bacteria expressing VopF had weakened F-actin dependent tight junctions, causting intestinal inflammation (Tam et al. 2010). Further work verified VopF's nucleation ability and the necessity of dimerization, the contributions of the WH2 domains via truncation analysis like VopL, as well as some capabilities that differ from those reported for VopL. Results of depolymerization assays utilizing gelsolin to cap the barbed end of filaments and adding VopF show no difference in the disassembly rate, indicating that VopF, unlike VopL, does not bind to the pointed end (Pernier et al. 2013). The same study also found VopF severs and caps filaments using static timecourse assays and fluorescence microscopy. Using single color TIRF microscopy and pyrene assembly assays, it was suggested that VopF's barbed end association will un-cap filaments bound by capping protein (Pernier et al. 2013). Additionally, small-angle X-ray scattering analysis of progressively smaller VopF truncations complexed with actin showed VopF stabilizes linear actin strings that differ from canonical actin filament organizations (Avvaru et al. 2015). These results suggest a model whereby VopF can associate with the side of a growing filament and potentially ride processively on the barbed end, adding monomers and preventing capping. The main mechanism of VopF-mediated F-actin assembly is contrary to that of VopL, however there are caveats to the VopF data: all of the mechanistic conclusions come from indirect assumptions from bulk assays, the constructs used for each of the experiments vary greatly, VopF does not interact directly with

capping protein indicating some unknown uncapping mechanism, and a potentially non-physiological ratio of profilin to actin was used in the uncapping assay.

In summary, the mechanisms of actin filament assembly by WH2 domain assembly factors is still a nascent area of study with not only various and divergent mechanisms between different assembly factors but between studies on the same assembly factor (Figure 3-4). To clarify the situation, I utilized recombinantly purified and fluorescently labeled VopL and VopF and directly visualized their dynamics on single actin filaments in an attempt to create a consensus on the actin filament assembly mechanisms between the two.

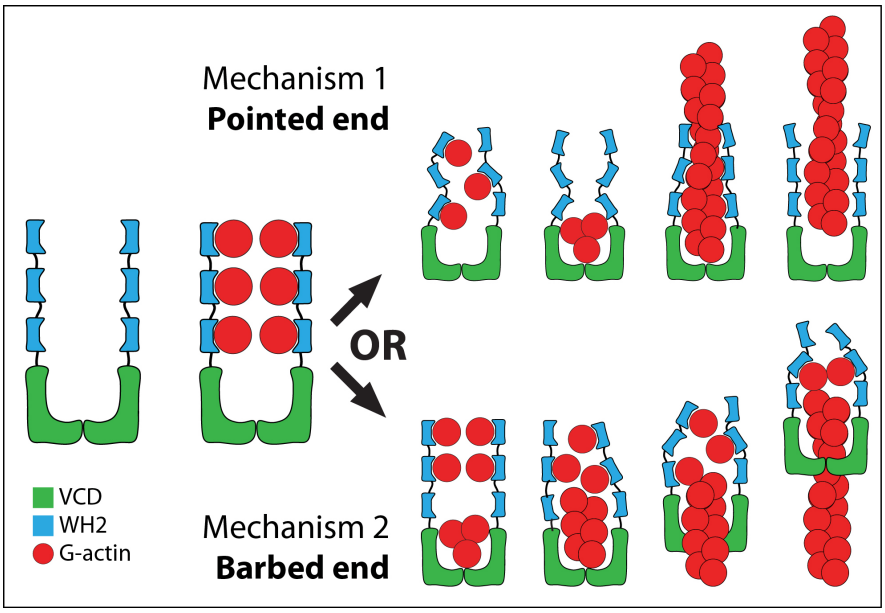

Figure 3-4: Opposing actin assembly mechanisms proposed for VopL and VopF. VopL and VopF contain a Vop C-terminal Domain (VCD) that is essential for dimerization and facilitates actin assembly along with the WH2 (Wasp homology 2) domains. VopL (top) has been reported to facilitate rapid cycles of nucleation and binds to the pointed end of F-actin (Namgoong et al., 2011, Yu et al., 2011, Zahm et al., 2013). VopF (Pernier et al., 2013 Avvaru et al., 2015) has been reported to associate with the barbed end of F-actin.

SECTION 3.5 INTRODUCTION

Diverse actin filament networks are assembled, maintained, and disassembled by different sets of actin binding proteins with complementary biochemical properties. These networks are initiated

by actin nucleation and assembly factors that enhance the transition from actin monomer to filament, filament elongation, or both. Although many valuable studies continue to sort out the particular details, the general mechanism of actin filament assembly by the Arp2/3 complex and formins are clear (Campellone & Welch 2010; Chesarone & Goode 2009; Chhabra & Higgs 2006; Pollard 2007). The Arp2/3 complex associates with the side of an actin filament and nucleates a new filament from the pointed end, leaving the barbed end to elongate freely before it is capped, generating short-branched filaments. Alternatively, formin remains processively associated with the barbed end, facilitating rapid elongation of profilin-actin, which produces long-straight filaments. However our understanding of the actin nucleation and assembly mechanisms of a third major class, the WH2 domain assembly factors, is relatively unstudied. This is mainly due to a wide range of isoform diversity within the class. These factors utilize different configurations of the actin monomer binding WH2 domain to stimulate nucleation and/or facilitate elongation (Paunola et al. 2002; Dominguez 2007; Qualmann & Kessels 2009). For example, the *Rickettsia parkerii* protein Sca2 is monomeric, contains three WH2 domains, and nucleates and elongates actin filaments by remaining processively bound to the barbed end (Madasu et al. 2013; Haglund et al. 2010). The conserved vertebrate protein Spire is a monomeric protein but can dimerize, containing eight total WH2 domains, and binds the pointed end of actin filaments (Quinlan et al. 2005; Rasson et al. 2015; Quinlan et al. 2007). Similar to Spire, Cordon-bleu (Cobl) contains a tandem repeat of three WH2 domains. Cobl was originally identified as a barbed end associating actin assembly factor enriched in the brain and involved in neuronal morphology (Ahuja et al. 2007; Haag et al. 2012). Sca2, Spire, and Cobl are just a few of many examples of WH2 domain assembly factors that display varied assembly mechanisms. Additionally, there is dissention within the study of individual WH2 domain assembly factors:

one report claims Spire it is actually a barbed-end capping protein, and other biochemical studies imply that Cobl is a weak nucleator and primarily acts to sequester actin monomers and severs filaments (Husson et al. 2011). This uncertaintly only adds to the necessity for further study to clarify the mechanisms of WH2 domain assembly factors.

Due to different assays employed and the resulting interpretations, there is disagreement in the field of how highly homologus WH2 domain assembly factors assemble actin. For example, studies on VopL and VopF (72% homologous) proteins have come to opposite conclusions as to the mechanism employed for actin assembly. VopL and VopF are effectors of type III secretion systems in the infectious bacteria *Vibrio parahaemolyticus* and *Vibrio cholerae*, respectively. VopL and VopF assemble actin directly, reorganizing the host-cell's actin cytoskeleton (Tam et al. 2007; Liverman et al. 2007). VopL is a 483 a.a. protein with three WH2 domains, two proline-rich domains, and a C-terminal dimerization domain (VCD). VopL utilizes six WH2 domains in total along with important residues within the VCD to stimulate actin assembly (Namgoong et al. 2011; Yu et al. 2011). Actin assembly by VopL is dependent upon its ability to dimerize, and truncating WH2 domains decreases the efficacy of VopL's assembly capabilities. VopF is a 530 a.a. protein with a nearly identical domain organization of VopL. VopF's actin assembly capabilities are also dependent upon dimerization and the amount of WH2 domains (Pernier et al. 2013).

The results showing VopL and VopF assemble actin are undisputed, however studies on the mechanism employed have come to opposite conclusions. Biochemical analysis of recombinantly purified VopL's actin assembly properties utilizing TIRF microscopy and X-ray crystallography have revealed that VopL stimulates rapid cycles of actin filament nucleation and associates with the pointed end of actin filaments (Namgoong et al. 2011; Yu et al. 2011; Zahm

et al. 2013). Studies on recombinantly purified VopF utilizing bulk biochemical assays came to the opposite conclusion, inferring that VopF binds to the barbed end and processively elongates actin filaments much like a formin (Pernier et al. 2013; Avvaru et al. 2015). Given the high homology between VopL and VopF, we hypothesize that both proteins employ the same mechanism of actin assembly. To determine whether VopL and VopF initiate assembly from the barbed or pointed end, we used multi-color total internal reflection fluorescence microscopy (TRIFM) to observe the assembly of single actin filaments in the presence of fluorescently labeled VopL or VopF. We found that both VopL and VopF share a conserved, multifunctional mechanism of actin filament assembly. In the presence of G-actin, VopL and VopF associate with the pointed end of the filaments they nucleate and do not associate with pre-formed filaments. However in the presence of pre-formed filaments in the absence of G-actin both VopL and VopF can associate with both the pointed and barbed ends of filaments. Finally, in conditions with saturating profilin, a small population of VopL and VopF associate briefly with the barbed ends of filaments while the majority of events are still nucleation based. Given the virulent nature of these effectors, this multifunctional mechanism allows for rapid cycles of actin filament nucleation when possible without binding to endogenous filaments, thus depleting the cytoplasmic pool of VopL or VopF.

SECTION 3.6 RESULTS

VopL and VopF nucleate and then associate with one end of actin filaments

To determine the mechanism by which VopL and VopF stimulate actin assembly, we purified constructs for each containing two proline-rich domains, three WH2 domains and the VCD domain (Figure 3-6 A). These truncations correspond to the longest of the VopL and VopF

constructs previously characterized with their N-terminal localization domain removed (Pernier et al. 2013; Namgoong et al. 2011). SNAP tags were added at their N-termini for labeling with fluorescent dyes, hereafter referred to as SNAP-VopL and SNAP-VopF. We initially compared the activity of unlabeled and fluorescently labeled versions of SNAP-VopL and SNAP-VopF by assessing their ability to facilitate the assembly of Mg-ATP-actin monomers in bulk pyrene actin assays (Figure 3-6). Labeled and unlabeled SNAP-VopL and SNAP-VopF accelerate spontaneous actin monomer assembly in nearly identical concentration dependent manners (Figures 3-6 A-C). The time to half maximal pyrene fluorescence is similar to what was previously published for similar unlabeled VopL and VopF constructs (Tam et al. 2007; Liverman et al. 2007; Namgoong et al. 2011; Pernier et al. 2013).

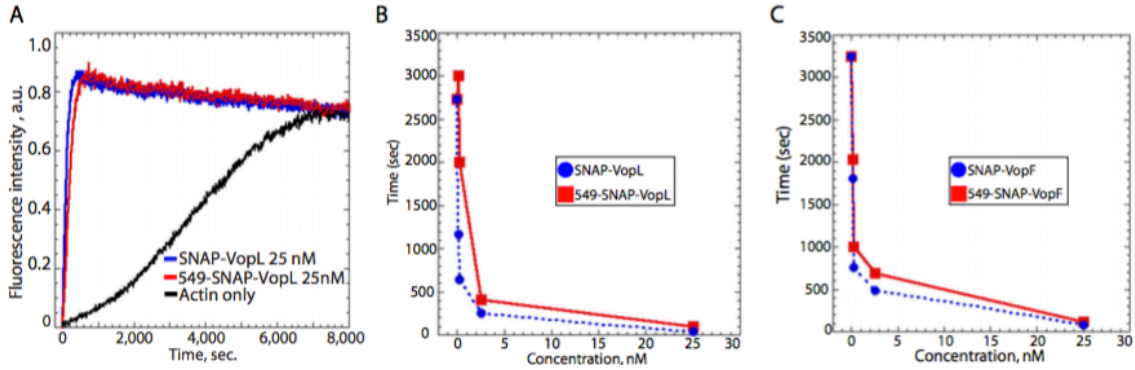

Figure 3-5: SNAP-VopL/VopF and 549-SNAP-VopL/VopF constructs stimulate actin assembly similarly.
(A-C) Spontaneous assembly of 1.0 µM Mg-ATP actin monomers (10% pyrene-labeled) over a range of labeled and unlabeled SNAP-VopL/VopF concentrations. (A) Time course of actin assembly in the absence (black) or presence of 25 nM SNAP-VopL (blue) or 549-SNAP-VopL (red). (B+C) Dependence of the time to half-maximal pyrene fluorescence increase on the concentration of the indicated SNAP-VopL/VopF (blue) or 549-SNAP-VopL/VopF (red) constructs.

VopL and VopF are potent actin nucleators, but the mechanism is disputed (Namgoong et al. 2011; Pernier et al. 2013; Avvaru et al. 2015). To clarify the discrepancies, we used multi-color TIRFM to directly visualize actin filament assembly in the presence of fluorescently labeled SNAP-VopL and SNAP-VopF. We followed the spontaneous assembly of 1.5 μM Mg-ATP-actin monomers (15% Oregon-green actin) in the presence of 0.2 nM red-labeled 549-SNAP-VopL and 549-SNAP-VopF (Figure 3-6 B and C). Both 549-SNAP-VopL (Figure 3-6 B) and 549-SNAP-VopF (Figure 3-6 C) stimulate actin assembly and then remain bound to one end of the actin filament, which continues to elongate. Since actin filaments elongate ~10 fold fold faster at their barbed ends (k_{on} = 11.6 μM^{-1} s^{-1}) than from their pointed ends (k_{on} = 1.3 μM^{-1} s^{-1}) (Pollard et al. 2000), proteins that remain continuously associated with elongating barbed, such as formin (Kovar 2006), typically modify the filament elongation rate. Plots of filament lengths over time revealed that 549-SNAP-VopL- and 549-SNAP-VopF-bound actin filaments elongate at ~13.0 sub s^{-1}, the same rate as unbound control filaments and the rate that filaments elongate after dissociation of SNAP-VopL or SNAP-VopF (Figure 3-6 D and E).

We previously reported that the elongation rate was increased ~two-fold for a small percentage of actin filaments associated by their end to VopL clustered on a quantum dot (Namgoong et al. 2011). However, we attributed this behavior to the dense clustering of WH2 domains, as has also been reported for N-WASP WWCA on nanowires (Khanduja & Kuhn 2013). We therefore determined the number of 549-SNAP-VopL and 549-SNAP-VopF molecules associated with nucleated filament ends in our experiments by determining the number of photobleaching steps following continuous imaging (Figure 3-7 A and B). 88% of VopL and VopF molecules bleached in two or fewer steps, consistent with a functional dimer

(based on ~75% labeling efficiency), as previously reported (Pernier et al. 2013; Namgoong et al. 2011).

We next determined the average association time of 549-SNAP-VopL and 549-SNAP-VopF on nucleated actin filaments. The average time that 549-SNAP-VopL and 549-SNAP-VopF were directly observed on filaments before their dissociation is 21.9 and 24.7 seconds (Figure 3-6 F, gold columns). However, these filaments were not visible immediately following their nucleation because of (1) the dead time required for the reaction to flow into the chamber (~ 20 seconds), and (2) for filaments to reach a critical length (~0.5 μm) to be spatially discerned and remain continuously in the TIRF imaging plane. Therefore, assuming that VopL and VopF were bound to these filaments from their inception, we determined their actual average association time to be ~76 seconds (Figure 3-6 F, blue columns), during which time ~1,000 actin subunits were added to the filament. Furthermore, a plot of the dependence of 549-SNAP-VopL and 549-SNAP-VopF residence times on their fluorescence intensity revealed that association with nucleated filament ends does not increase with an increase in oligomeric state (Figure 3-7 C and D).

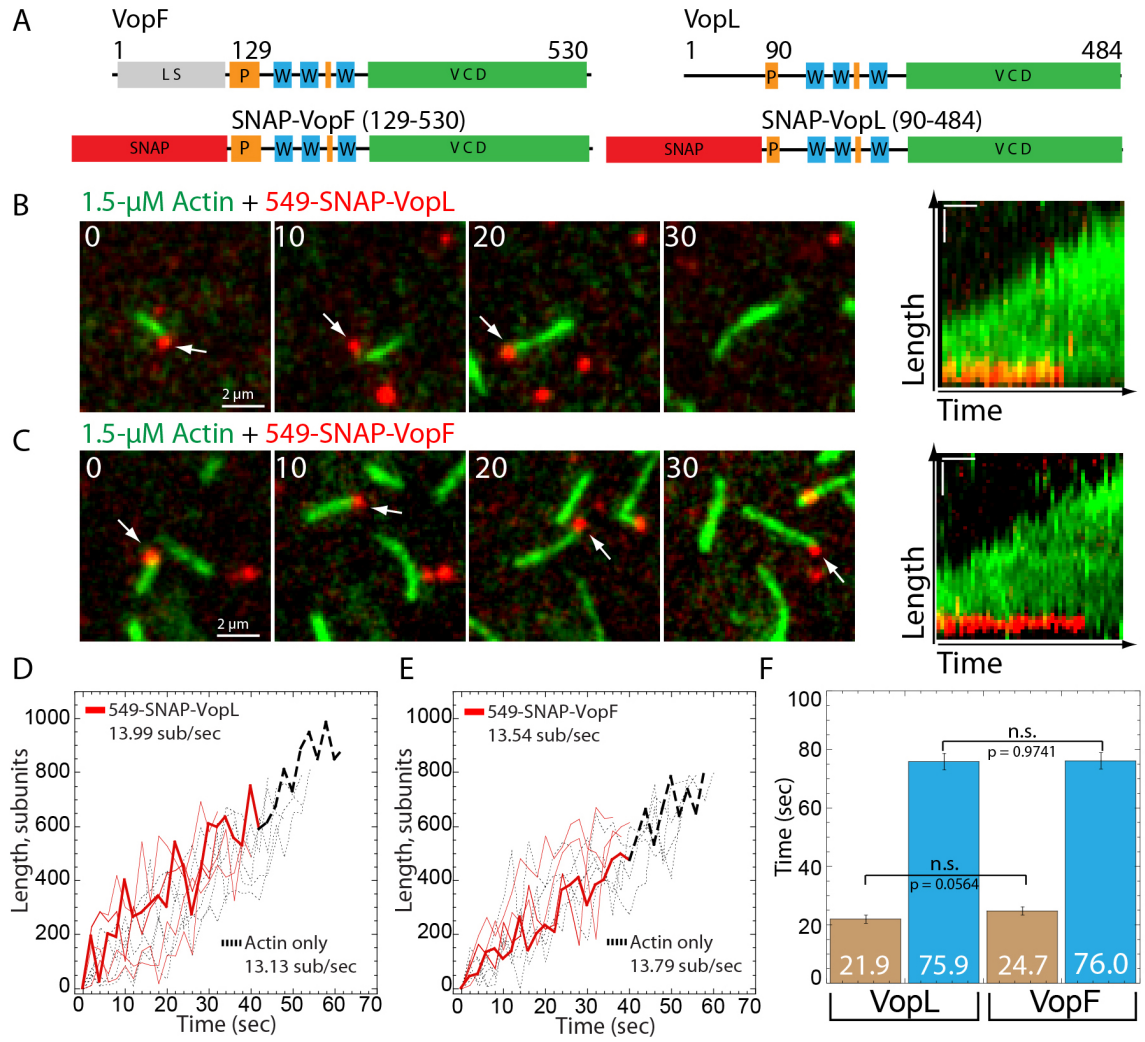

Figure 3-6: 549-SNAP-VopL/F nucleate actin assembly and associate with one end of an actin filament.

(A) (Top) Domain organization of VopF and VopL. P, proline-rich region (orange); W, WH2 domain (blue); VCD (Vop C-terminal domain) dimerization domain (green). (Bottom) VopF and VopL constructs used in this study. SNAP tag (red) for labeling with fluorescent dyes. (B-F) Two-color TRIFM of the assembly of 1.5-µM Mg-ATP-actin (15% Oregon green-actin) with 0.2 nM 549(red)-SNAP-VopL or 549-SNAP-VopF. (B and C, left) Merged time-lapse micrographs (in seconds) of individual filaments with 549-SNAP-VopL (B) and 549-SNAP-VopF (C) indicated with white arrows. Scale bars, 2 µm. (B and C, right) Merged kymographs of filament length (y-axis, scale bar: 1 µm) over time (x-axis, scale bar: 10 sec) of the corresponding 549-SNAP-VopL (B) or 549-SNAP-VopF (C) bound filaments. (D and E) Traces of the length of individual filaments over time that are control free (dashed black), or associated with either 549-SNAP-VopL (D) or 549-SNAP-VopF (E) (solid red), which revealed the indicated elongation rates. The filaments shown in (B and C) are bold. (F) Average residence time of 549-SNAP-VopL and 549-SNAP-VopF on filament ends. Brown columns: observed residence time. Blue columns: residence time assuming 549-SNAP-VopL and 549-SNAP-VopF are associated with filaments from their nucleation. Error bars indicate SEM; $n \geq 75$ events.

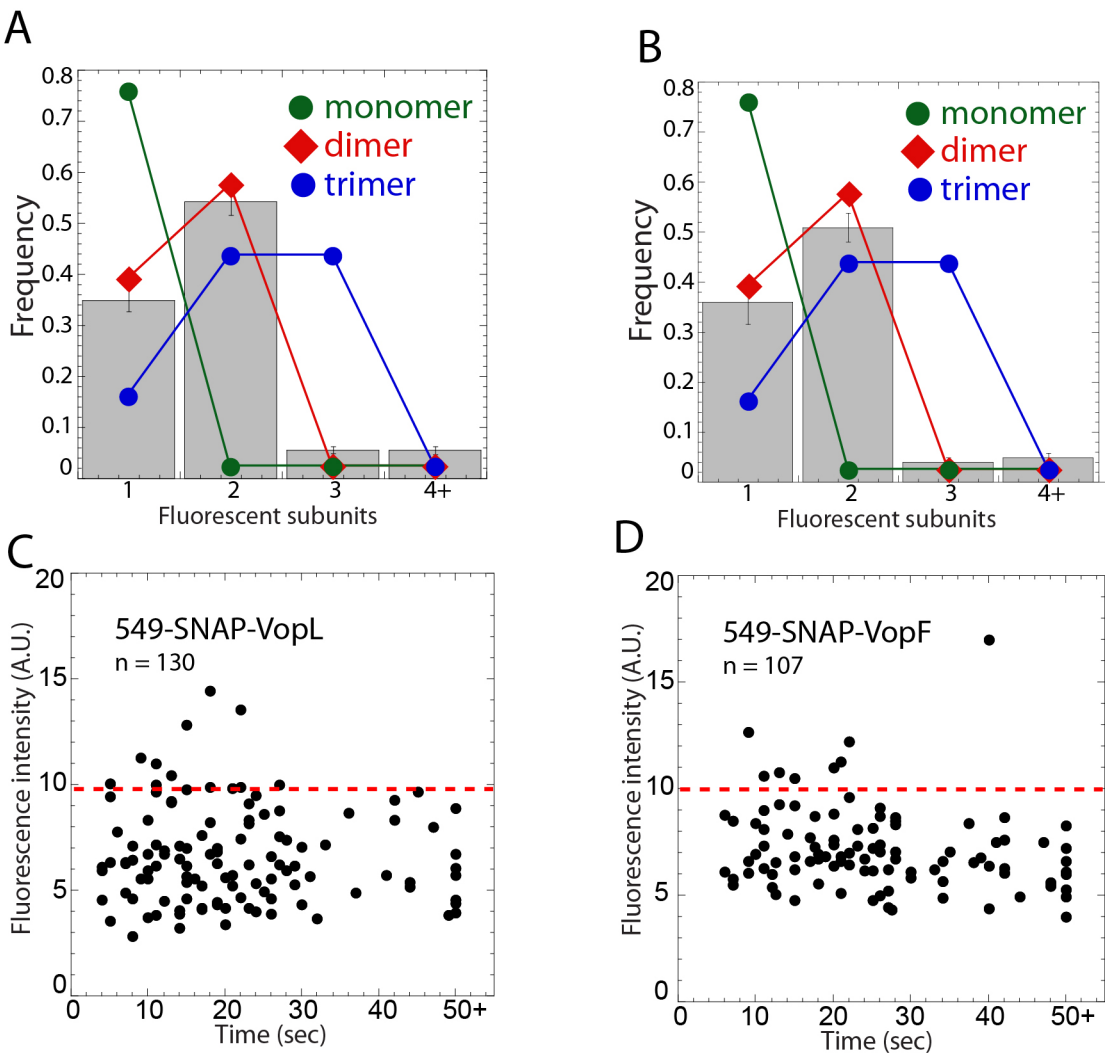

Figure 3-7: 549-SNAP-VopL/F constructs are dimers in solution.
(A+B) Histograms showing photobleaching steps for 549-SNAP-VopL (A) and 549-SNAP-VopF (B) bound particles. Colored lines represent predicted photobleaching distributions based on a binomial model where the measured subunit-labeling stoichiometry is 0.75. (C+D) Dependence of 549-SNAP-VopL (C) and 549-SNAP-VopF (D) residence time with actin filament ends on their fluorescence intensity. Dashed red lines indicate fluorescence intensity corresponding to 549-SNAP-VopL and 549-SNAP-VopF particles larger than dimers.

VopL and VopF associate with the dim, pointed ends of filaments

VopL and VopF nucleate filaments and subsequently remain associated with one end for ~76 seconds. Similar elongation rates between control and VopL- or VopF-associated filaments

implies, but does not verify, that they are associated with the pointed end. Therefore, we sought additional experimental evidence to decisively determine the actin filament end bound by VopL and VopF. Given that actin monomers add ~10-fold more quickly to the barbed end, rapid imaging of actin filaments assembled from fluorescently labeled monomers bleaches the pointed end significantly faster than the barbed end (Figure 3-8 A) (Kovar et al. 2006). Therefore we used rapid TIRF imaging (every one second) to visualize the spontaneous assembly of 1.5 μM Mg-ATP-actin monomers (15% Oregon-green actin) with 0.2 nM 549-SNAP-VopL or 549-SNAP-VopF (Figure 3-8 B-D). Linescans measuring the fluoresence intensity of filaments along their length revealed a steady decrease in intensity from the barbed to the pointed end (Figure 3-9 A). Both 549-SNAP-VopL and 549-SNAP-VopF are bound to the dimmer, pointed ends of the partially bleached nucleated filaments (Figure 3-8 B and C). Linescans of 549-SNAP-VopL and 549-SNAP-VopF bound filaments confirmed that in all cases VopL and VopF are bound to the dimmer, pointed end of nucleated filaments (Figure 3-9 B and C, $n > 75$). We also analyzed VopL and VopF with C-terminal SNAP tags to address whether the position of the SNAP tag influences their behavior. All VopL-SNAP-549 and VopF-SNAP-549 events were detected at the dim, pointed end of nucleated filaments as well (data not shown). Conversely, formins are actin assembly factors that remain processively associated with the elongating actin filament barbed end (Kovar 2006). As expected, 549-SNAP-mDia2 therefore localizes exclusively to the bright, barbed end of actin filaments (Figure 3-8 D and 3-9 D), confirming the validity of the assay. Rapid dual-color TIRFM imaging of actin filaments nucleated by 549-SNAP-VopL or 549-SNAP-Vop revealed that VopL and VopF localize to the slower growing pointed end of filaments, whereas the formin mDia2 localizes to the barbed end.

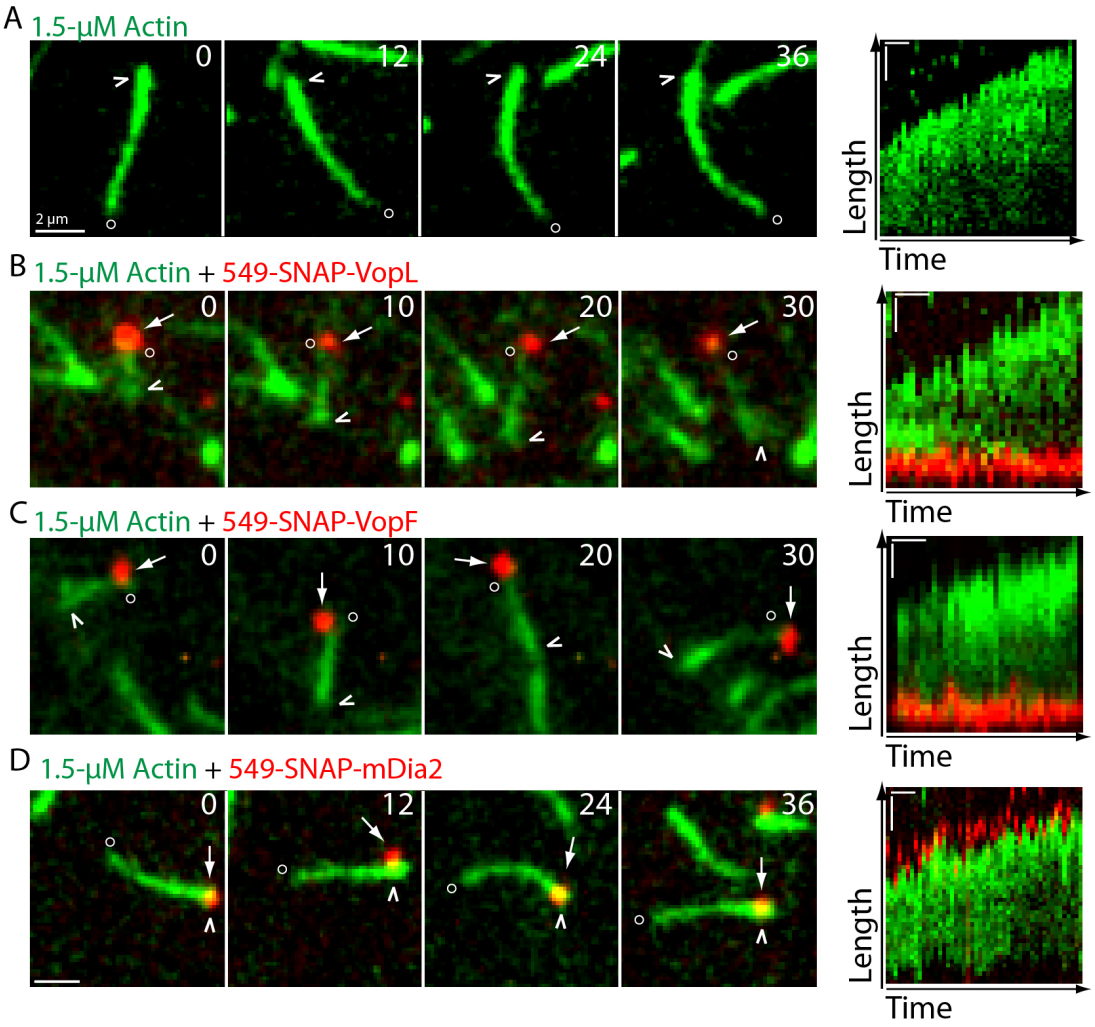

Figure 3-8: VopL and VopF associate with the bleached, pointed end of actin filaments they nucleate.

Rapid acquisition (every second) two-color TIRFM of the assembly of 1.5-μM Mg-ATP-actin (15% Oregon green-actin) assembled with 0.2 nM 549(red)-SNAP-VopL, 0.2 nM 549-SNAP-VopF or 2 nM 549-SNAP-mDia2. (A-D, left) Merged time-lapse micrographs (in seconds) of individual filaments. White arrowheads and open circles indicate bright and dim filament ends. White arrows indicate 549-SNAP-VopL (B), 549-SNAP-VopF (C) or formin 549-SNAP-mDia2 (D). Scale bars: 2 μm. (A-D, right) Merged kymographs of filament length (y-axis, scale bar: 1 μm) over time (x-axis, scale bar: 10 sec) of the corresponding filaments. (E-H) Line scans of the normalized fluorescence intensity of the indicated individual actin filaments measured from their bright to dim (bleached) ends. Red dots indicate position of 549-SNAP-VopL (F), 549-SNAP-VopF (G), or 549-SNAP-mDia2 (H) on the filament traces. Shaded red regions indicate where 100% of VopL, VopF, or mDia2 bind to filaments in regards to actin fluorescence intensity ($n \geq 75$ as indicated).

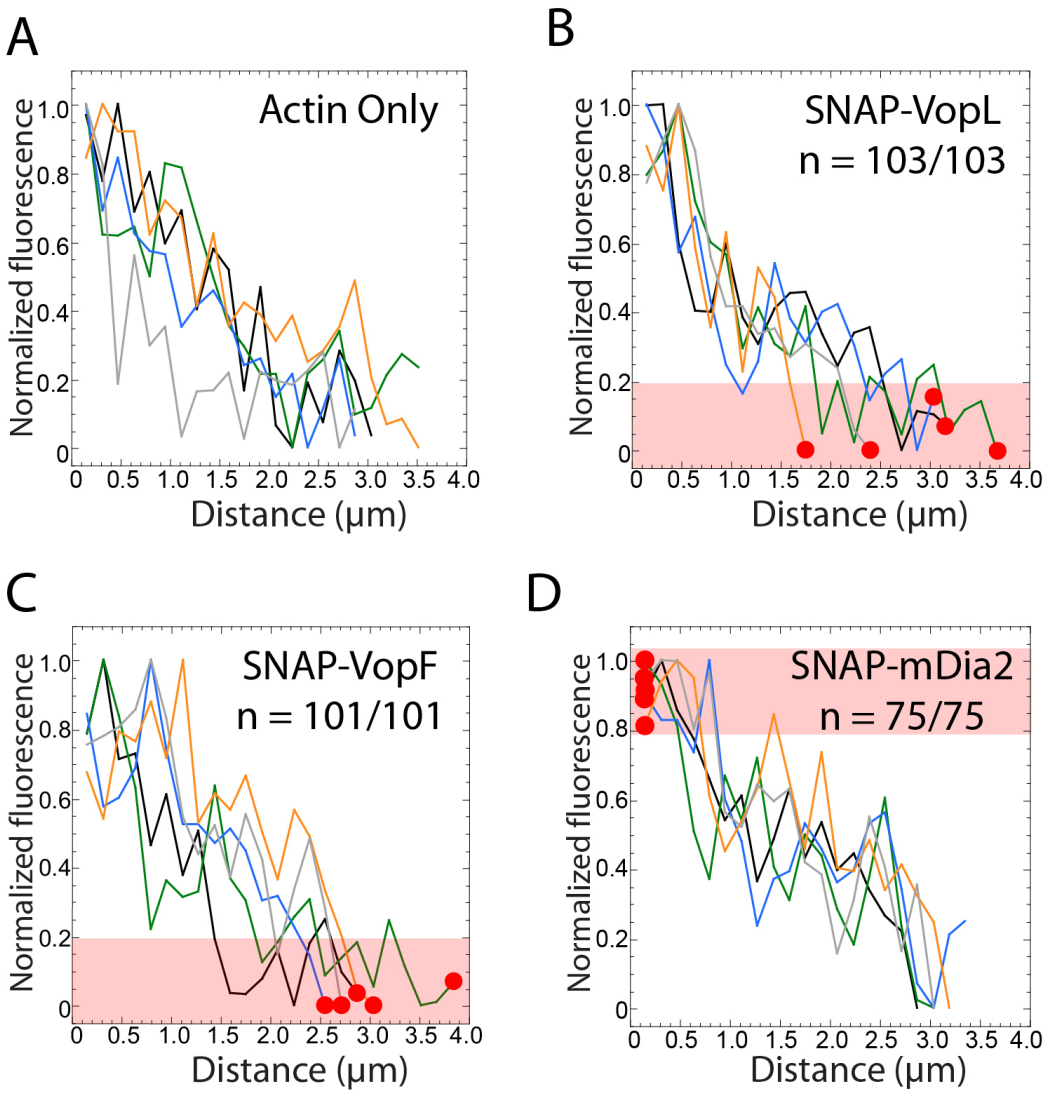

Figure 3-9: Linescans of 549-SNAP-VopL/F or 549-SNAP-mDia2 associated bleached actin filaments.

(A-D) Line scans of the normalized fluorescence intensity of the indicated individual actin filaments measured from their bright to dim (bleached) ends. Red dots indicate position of 549-SNAP-VopL (B), 549-SNAP-VopF (C), or 549-SNAP-mDia2 (D) on the filament traces. Shaded red regions indicate where 100% of VopL, VopF, or mDia2 bind to filaments in regards to actin fluorescence intensity ($n \geq 75$ as indicated).

VopL- and VopF-nucleated filaments can simultaneously be bound at their opposite ends by formin or capping protein

Given that VopL and VopF localize to the pointed end of nucleated filaments, it should be possible to visualize the barbed end binding proteins formin and capping protein on the opposite end. We therefore utilized three-color TIRFM to directly visualize the assembly of 1.5 μM Mg-ATP-actin (15% Oregon-green actin) monomers with 549-SNAP-VopL or 549-SNAP-VopF and blue labeled capping protein 647-SNAP-CP or formin 647-SNAP-mDia2 (Figure 3-10). As expected, 647-SNAP-mDia2 or 647-SNAP-CP associate with the opposite end of 549-SNAP-VopL or 549-SNAP-VopF on nucleated actin filaments (Figure 3-10 A-D). 647-SNAP-mDia2 and 647-SNAP-CP are bound to the opposite end of the filament to where the 549-SNAP-VopL or 549-SNAP-VopF are associated in 100% of observed cases (Figure 3-10 E). Furthermore, we never observed events where a 647-SNAP-mDia2 or 647-SNAP-MmCP replaced a dissociated 549-SNAP-VopL or 549-SNAP-VopF (data not shown). These results confirm that both VopL and VopF bind to the pointed end of nucleated actin filaments.

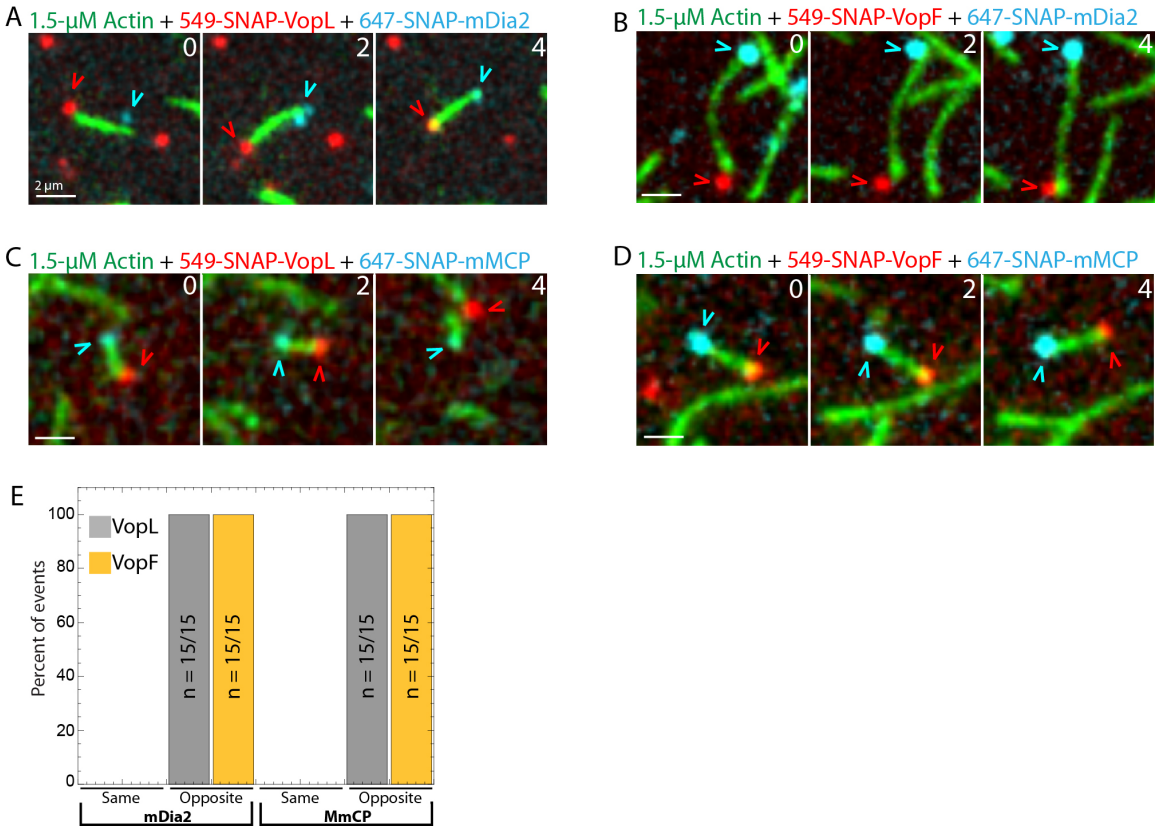

Figure 3-10: The formin mDia2 and capping protein MmCP bind the opposite end of VopF- or VopL-nucleated filaments.
Three-color TIRFM of the assembly of 1.5-μM Mg-ATP-actin (15% Oregon green-actin) assembled with 0.2 nM 549(red)-SNAP-VopL or 549-SNAP-VopF, and either 2 nM 647(blue)-SNAP-mDia2 or 2 nM 647-SNAP-MmCP. (A-D) Merged time-lapse micrographs (in seconds) of individual filaments. Scale bars: 2 μm. Red arrowheads indicate 549-SNAP-VopL (A and C) or 549-SNAP-VopF (B and D). Blue arrowheads indicate 647-SNAP-mDia2 (A and B) or 647-SNAP-MmCP (C or D). (E) Percentage of 549-SNAP-VopL (gray) or 549-SNAP-VopF (gold) to the same or opposite end of mDia2 or MmCP. n = 15.

VopL and VopF bind the ends of preassembled actin filaments in the absence of actin monomers

In the spontaneous actin monomer assembly assays described above (Figures 3-5 to 3-10), VopL and VopF only associate with the pointed end of filaments they nucleate. Unlike the formin mDia2, VopL and VopF were never observed to either (1) bind the ends of internal control filaments that spontaneously assembled, or (2) re-bind the end of a nucleated filament it had dissociated from. These observations contradict previous studies indicating VopF can bind to

both free and capped barbed ends (Pernier et al. 2013). Therefore, we directly tested the ability of VopL and VopF to bind the ends of preassembled filaments (Figure 3-11). Actin filaments were preassembled in a TIRFM chamber from 1.5 μM Mg-ATP-actin (10% Alexa-488 actin), and then 549-SNAP-VopL (Figure 3-11 A and C), 549-SNAP-VopF or formin 549-SNAP-mDia2 (Figure 3-11 B and D) was flowed into the chamber with or without 1.5 μM Mg-ATP-actin monomers (10% Alexa-488 labeled). The length of each filament bound by VopL, VopF or mDia2 was measured to determine whether they had associated with a long preassembled filament or a short filament recently nucleated by the assembly factor (Figure 3-11 E).

Consistent with the spontaneous assembly reactions described above (Figures 3-5 to 3-10), flowing in the presence of actin monomers revealed a marked difference in the lengths of filaments bound by 549-SNAP-VopL and 549-SNAP-VopF compared to 549-SNAP-mDia2 (Figure 3-11 A and B). As expected, because mDia2 can associate with the barbed ends of filaments it nucleated and with preassembled filament barbed ends (Kovar et al. 2006), 549-SNAP-mDia2 bound to filaments with a large distribution of lengths from short (nucleated) to long (preassembled) (Figure 3-11 B and E, mDia2 red dots). Conversely, 549-SNAP-VopL (Figure 43-11 A and E, VopL red dots) and 549-SNAP-VopL (Figure 3-11 E, VopF red dots) are only bound to short nucleated filaments ~1.5 μm long. Furthermore, 549-SNAP-VopL and 549-SNAP-VopF were only visualized on one end of these short nucleated filaments. These results are consistent with our previous observations that VopL and VopF nucleate actin monomer assembly and remain associated with the pointed end of the resulting filaments for ~75 seconds.

Conversely, we found that 549-SNAP-VopL, 549-SNAP-VopF and 549-SNAP-mDia2 all bind preassembled actin filaments ends when actin monomers are not included in the reaction (Figure 3-11 C and D). 549-SNAP-mDia2 binds to the barbed ends of preassembled actin

filaments over a wide length distribution (Figure 3-11 E, mDia2 black dots), and 117 out of 118 remained bound throughout the 10 minute experiment. Strikingly, both 549-SNAP-VopL (Figure 3-11 C) and 549-SNAP-VopF can also bind to preassembled actin filament ends in the absence of actin monomers (Figure 3-11 E, VopL and VopF black dots). Interestingly, VopL and VopF associate with both the barbed and pointed ends (Figure 3-11 F), and with an average residence time of 29 seconds (Figure 3-11 G).

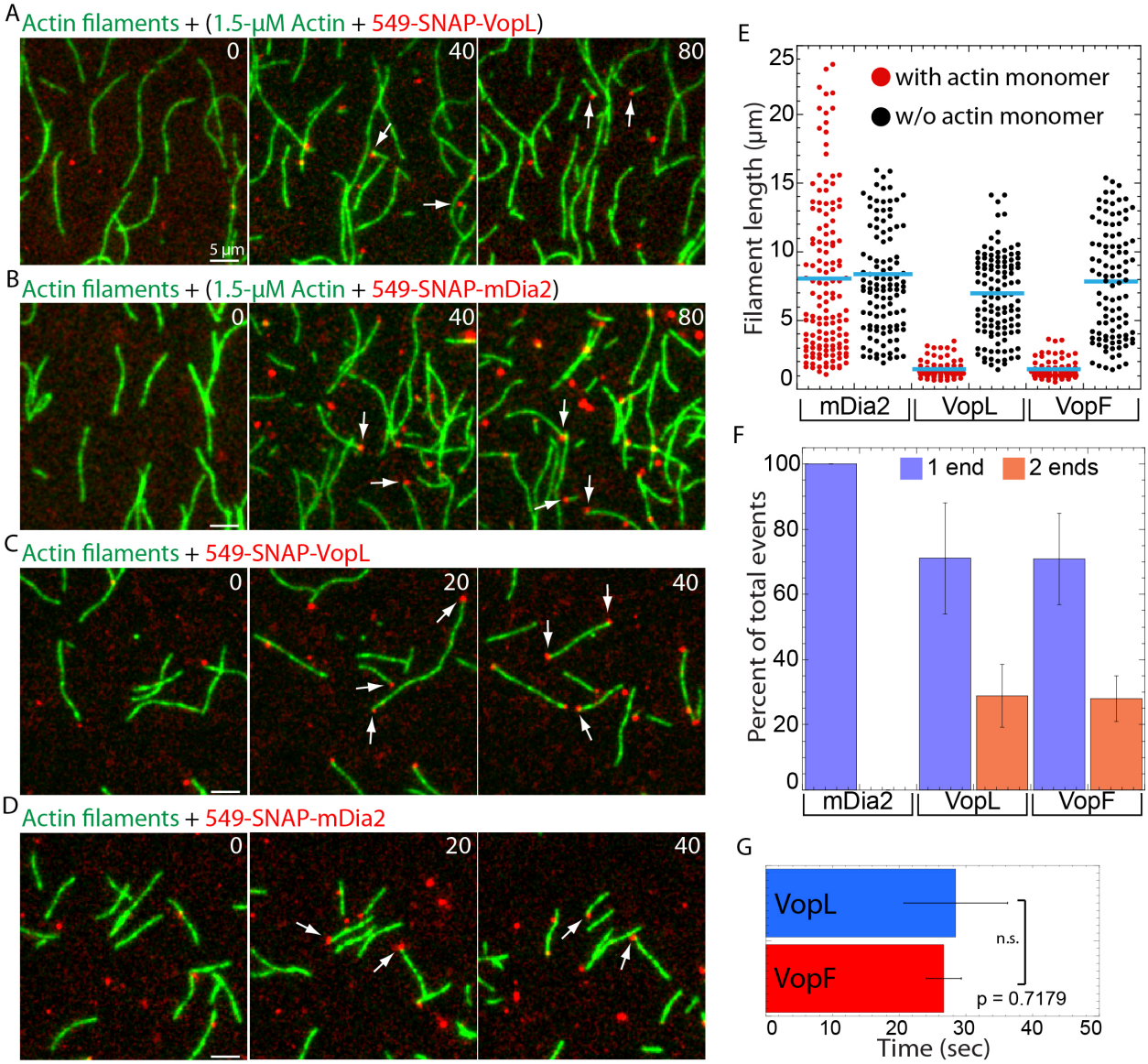

Figure 3-11: In the absence of actin monomers VopF and VopL bind preassembled filament ends.

Two color TIRFM visualization of the addition of 0.6 nM 549(red)-SNAP-VopL, 549-SNAP-VopF or 549-SNAP-mDia2 to pre-assembled actin filaments (10% Alexa-488) in either the absence or presence of 1.5 μM Mg-ATP-actin (10% Alexa-488) monomers. (A-D) Merged time-lapse micrographs (in seconds) of fields of filaments. White arrows indicate representative 549-SNAP-VopL (A and C) and formin mDia2 (B and D). Time zero indicates immediately after flow. Scale bars: 5 μm. (A) Flow in of 549-SNAP-VopL and actin monomers. (B) Flow in of 549-SNAP-mDia2 and actin monomers. (C) Flow in of 549-SNAP-VopL without actin monomers. (D) Flow in of 549-SNAP-mDia2 without actin monomers. (E) Dot plot of the length distribution of bound filaments after flow in the presence (red) and absence (black) of actin monomers. Blue lines indicate the average filament length for that population. $n \geq 50$ events. (F) Percent of total bound filaments that are bound on one (purple) or two (red) ends. Error bars indicate SD; $n \geq 50$. (G) Average association time of 549-SNAP-VopL and 549-SNAP-VopF on actin filament ends in the absence of monomer. Error bars indicate SEM; $n \geq 100$ events.

VopL and VopF primarily nucleate actin filament assembly in the presence of profilin

In reactions with actin monomers, regardless of the inclusion of preassembled actin filaments, VopL and VopF exclusively nucleate actin filament assembly from the monomers and remain associated with pointed ends for ~75 seconds. Conversely, without actin monomers VopL and VopF can associate with both the barbed and pointed ends of preassembled actin filaments for ~25 seconds. Because cells contain a mixture of existing actin filaments and actin monomers bound to profilin, we modified our preassembled actin filament TIRFM assay to flow in actin monomers labeled in a second color in both the absence and presence of profilin. Green actin filaments were preassembled in a TIRFM chamber from 1.5 μM Mg-ATP-actin (10% Alexa-488 actin), and then red actin assembly factors (549-SNAP-VopL/VopF/mDia2) were flowed into the chamber with 1.5 μM cyan Mg-ATP-actin monomers (10% Alexa-647 actin) in either the absence or presence of a 2:1 (3.0 μM) or 5:1 (7.5 μM) ratio of profilin to actin (Figure 3-12 A). This experimental setup allows decisive determination of the association of assembly factors with (1) actin filaments they nucleated from monomers, pure cyan (Alexa-647)-labeled filaments, and/or (2) preassembled actin filaments, green (Alexa-488)- and cyan-labeled

filaments. Furthermore, the preassembled filament end occupied by the assembly factor can easily be determined because addition of cyan-labeled monomers distinguishes the barbed end (Figure 3-12 A, right).

Representative fluorescent time-lapse images (Figure 3-12 B, left) and associated kymographs (Figure 3-12 B, right) of a reaction with 549-SNAP-VopL and 7.5 μM profilin demonstrates the effectiveness of this assay, allowing quantification of (1) the percent of nucleated or preassembled filaments associated by the assembly factor (Figure 3-12 C), (2) the lifetimes of assembly factors on nucleated and preassembled filament ends (Figure 3-12 D), and (3) the barbed end elongation rates of nucleated and preassembled filaments bound by the assembly factors (Figure 3-12 E). As expected, in the absence of profilin both VopL and VopF exclusively associate with the bleached pointed ends of filaments they nucleate (Figure 3-12 C) for ~75 seconds (Figure 3-12 D), which elongate at the control barbed end rate of ~10 sub s^{-1} (Figure 3-12 E). Conversely, formin mDia2 associates with the barbed end of both nucleated and preassembled filaments (Figure 3-12 C), slowing the barbed end elongation rate to ~2.5 sub s^{-1} (Figure 3-12 E) (Kovar et al. 2006). In the presence of excess profilin, the vast majority (>85%) of VopL and VopF are also associated with the pointed end of filaments they nucleate (Figure 3-12 C) for ~75 seconds (Figure 3-12 D), which elongate at ~10 sub s^{-1} (Figure 3-12 E). However, in reactions with 2-fold and 5-fold profilin 5 to 15% of VopL and VopF association events are with preassembled actin filament barbed ends (Figure 3-12 C) for ~25 seconds (Figure 3-12 D), which essentially cap barbed end elongation (Figure 3-12 E). In contrast to flow-in experiments without actin monomer (Figure 3-11), VopL and VopF were not observed to interact with the pointed end of preassembled actin filaments in the presence of profilin. By comparison, inclusion of profilin also slightly increases the percentage of formin mDia2 associated with preassembled

actin filaments (Figure 3-12 C), because profilin inhibits formin-mediated nucleation (Kovar 2003), which elongate their barbed ends at ~15 sub s^{-1} (Kovar et al. 2006). Therefore, although the inclusion of excess profilin allows VopL and VopF to associate with and cap actin filament barbed ends (Pernier et al. 2013), the vast majority of events (~85%) are nucleation from the pointed end.

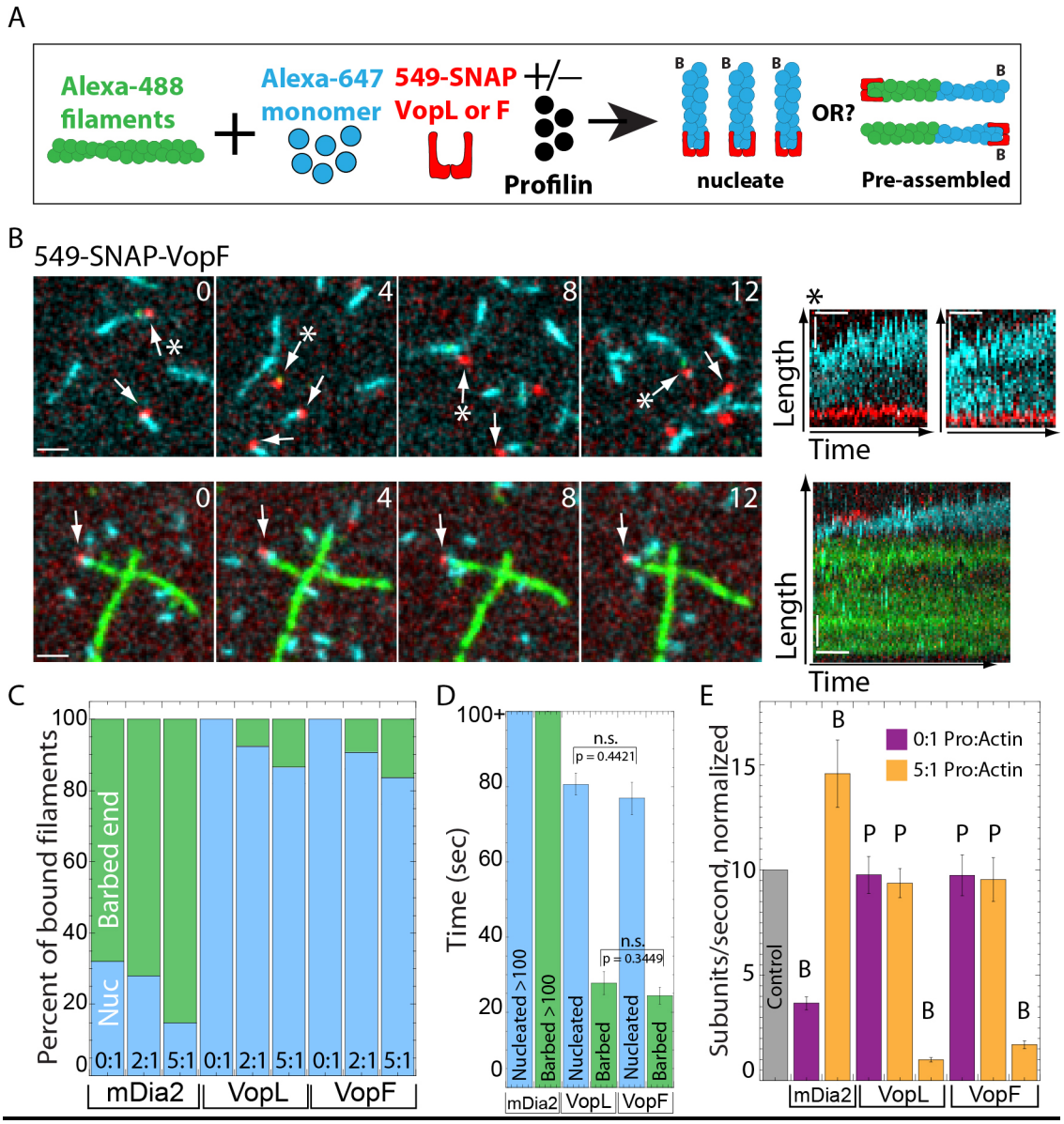

Figure 3-12: Association of VopF and VopL on the ends of nucleated and preassembled filaments in the presence of profilin.

Three color TIRFM visualization of the addition of cyan-labeled 1.5 µM Mg-ATP-actin monomers (15% Alexa-647-actin) to pre-assembled green actin filaments (10% Alexa-488-

actin), in the presence of 0.2 nM 549(red)-SNAP-VopF, 549-SNAP-VopL or 549-SNAP-mDia2, with 0, 3.0 or 7.0 μM profilin HsPRFN1. (A) Cartoon depicting the experimental setup and potential outcomes. (B) Flow of 549-SNAP-VopF in the presence of 7.0 μM profilin. (Left) Merged time-lapse micrographs (in seconds) of actin filaments. White arrows indicate 549-SNAP-VopF bound to filaments ends. Scale bar: 2 μm. (Right) Merged kymographs of filament length (y-axis, scale bar: 2 μm) over time (x-axis, scale bar: 10 sec) of the corresponding filaments. (Top) Representative examples of the predominant filament population, association of 549-SNAP-VopF with the pointed end of nucleated filaments. (Bottom) Example of 549-SNAP-VopF binding to the barbed end of a pre-assembled filament.. (C) Quantification of the percent of 549-SNAP-mDia2, 549-SNAP-VopL, or 549-SNAP-VopF association events with nucleated (blue; pointed end for VopL and VopF, barbed end for mDia2) or pre-assembled filament barbed ends (green) for different profilin:actin ratios. (D) Average association time of 549-SNAP-VopL, 549-SNAP-VopF, and 549-SNAP-mDia2 with the barbed end of pre-assembled filaments with a 5:1 profilin:actin ratio. Error bars indicate SEM; $n \geq 20$ events. (E) Elongation rates of 549-SNAP-mDia2-, 549-SNAP-VopL- and 549-SNAP-VopF-associated filaments with a 0:1 ratio (purple) or 5:1 ratio (yellow) of profilin:actin. Rates were normalized to the control rate of 10 subunits/sec. Error bars indicate SEM; $n = 20$ filaments.

SECTION 3.7 DISCUSSION

VopL and VopF stimulate rapid cycles of actin nucleation and associate with the pointed ends of filaments in the presence of actin monomers

We have utilized multi-color TIRFM to visualize the mechanism of actin filament assembly by the *Vibrio* virulence factors VopL and VopF. In the presence of available actin monomers, individual VopL or VopF dimers nucleate and then remain associated with the slow growing pointed end of actin filaments before dissociating, leaving the barbed end to elongate freely. In the presence of saturating profilin a majority of events were purely nucleation based with a small percentage of events binding briefly to the barbed end. Our results reflect results obtained from studies on both VopL and VopF, however we strongly agree with the previous studies that have focused on the *in vitro* biochemical studies on VopL (Namgoong et al. 2011; Yu et al. 2011; Zahm et al. 2013). Collectively our results converge on a pointed end mechanism for filament assembly for VopL and VopF. Some results from single color TIRFM VopL studies

implied a potential barbed end assembly mechanism, but we attribute that small fraction of events to VopL dimers attached to microspheres leading to a gain-of-function mechanism which we attribute to the clustering of multiple WH2 domain containing proteins (Namgoong et al. 2011; Khanduja & Kuhn 2013). All of the VopL or VopF nucleated filaments exhibited an elongation rate the same as control filaments (Figure 3-6 D and E) and bound to the dim, pointed end of photo-bleached filaments (Figures 3-8 B and C and 3-9 B and C). Remarkably, unlike other end-binding proteins like formin and capping protein, in the presence of monomer VopL and VopF can only associate with the end of actin filaments they are currently nucleating, and not with actin filaments that are already assembled. We determined this by flowing in VopL or VopF with actin monomers to TIRF chambers with preassembled filaments. By doing so we were able to determine that VopL and VopF do not bind to the longer, preassembled filaments like the formin mDia2. Flowing in VopL and VopF with Alexa-647 labeled actin monomers to chambers with preassembled Alexa-488 labeled filaments reinforced this point. In agreement with our model that VopL and VopF are purely nucleation factors, we observed VopL and VopF only associated with Alexa-647 labeled actin filaments.

However we did find that VopL and VopF both have the capability to bind pre-assembled actin filaments, but only in the absence of actin monomer or with saturating profilin. Upon addition of VopL and VopF to preassembled filaments without monomer, we visualized VopL and VopF binding transiently to both ends of actin filaments. Given that WH2 domains bind to ATP-actin with a 50 fold higher affinity than ADP-actin and that the VCD of VopL has the potential to bind F-actin, this behavior of VopL and VopF is not completely unexpected. In the absence of its preferred binding partner, the six WH2 domains of VopL or VopF are capable of binding ADP-Pi or ADP actin (Carlier et al. 1993). Additionally we observed rare events of

VopL and VopF binding to preassembled filaments in the presence of saturating profilin. It has been previously reported that the G-actin binding protein profilin competes with the WH2 domains in VopL for actin monomers (Namgoong et al. 2011). If present in high enough concentrations, profilin could "mask" the available monomers in solution and the WH2 domains of VopL and VopF could behave as we observed when actin monomers were absent. Taken together, this information could explain how studies on VopF inferred a barbed-end binding mechanism of actin assembly, as those experiments were done in conditions of a 5:1 ratio of profilin:actin. It is worth noting for this and other in vitro biochemical studies on actin that the ratio of profilin:actin can influence results and interpretations of certain mechanisms. Recently two studies on the mechanism of inhibition of the Arp2/3 complex by profilin came to different conclusions over the molecular mechanism based on the amount of profilin that was utilized. Suarez et al. found a 1:1 ratio of profilin:actin was sufficient for Arp2/3 complex inhibition through profilin and actin competing for the same binding site on the VCA domain of the fission yeast homolog of WASP Wsp1p (Suarez et al. 2015). Pernier et al. agrees that profilin inhibits the Arp2/3 complex, but concluded that profilin was competing with the Arp2/3 complex for a binding site on the barbed end of actin filaments under conditions of a 20:1 ratio of profilin to actin (Pernier et al. 2016). Also it is still unclear as to how studies on VopF excluded pointed end binding from their proposed assembly mechanism, as we show that: 1) pointed end binding is the only mechanism for both VopL and VopF in the presence of monomer 2) in the absence of monomer, VopL and VopF can bind to both ends of actin filaments and 3) even with saturating profilin, a majority of VopL and VopF binding events were pointed end nucleation based (Figure 3-13).

These new results adds significantly to our understanding of how VopL and VopF assemble filaments. It is logical that secreted virulence factors like VopL and VopF have evolved to have the highest efficacy possible. Being unable to bind pre-assembled filaments in the presence of available monomer promotes the pathogen's ultimate goal of disrupting the host-cell's actin cytoskeleton by assembling the greatest amount of non-productive actin filaments thereby disrupting the F-actin homeostasis.

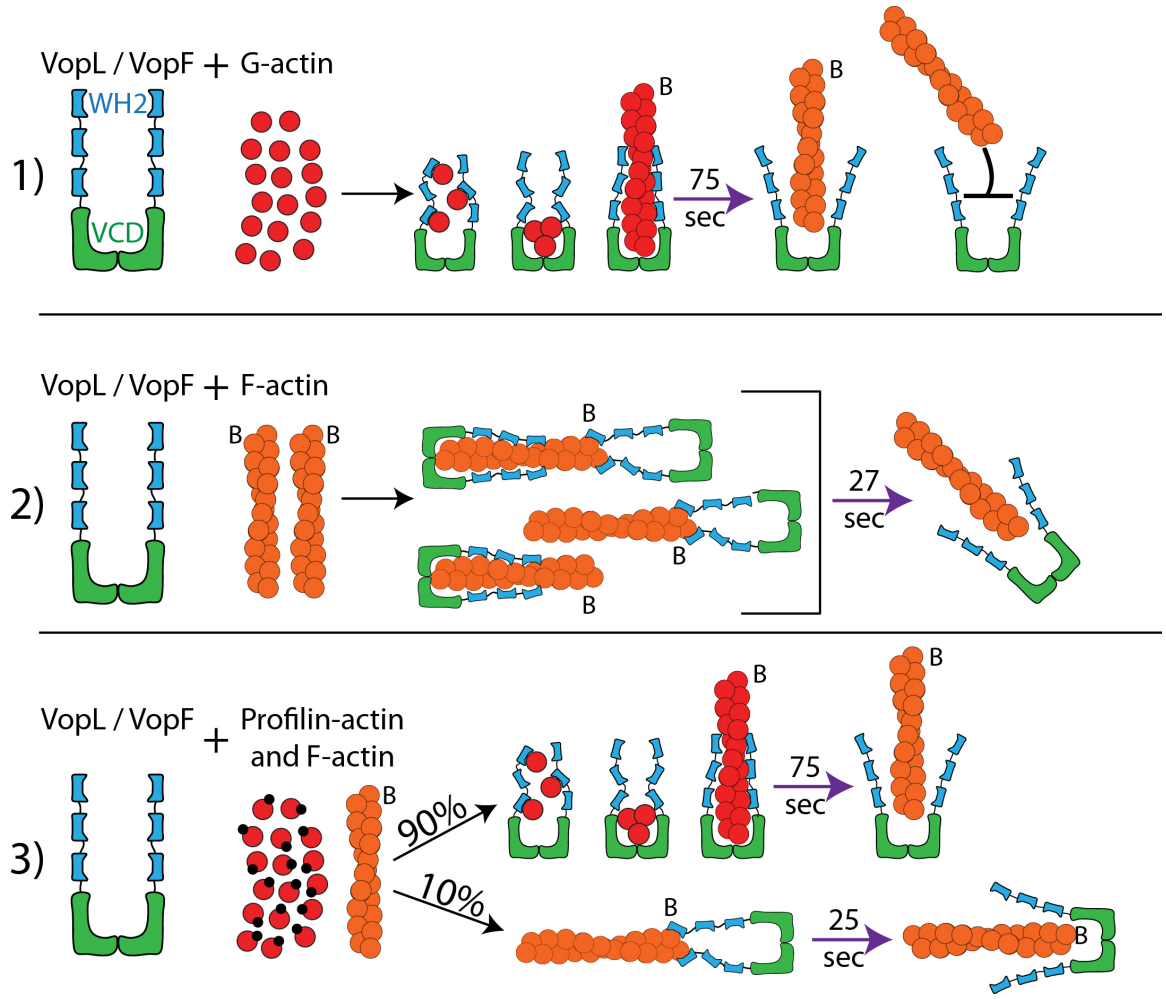

Figure 3-13: Observed actin assembly and binding properties of VopL and VopF
Cartoon representation of the data reported for VopL and VopF. 1) In the presence of actin monomer VopL/F nucleate and remain associated with the pointed end of the newly nucleated filament for approximately 75 seconds before releasing. In these conditions VopL/F cannot bind pre-assembled actin filaments or re-bind actin filaments nucleated by VopL/F. 2) In the absence

of monomer but in the presence of actin filaments VopL/F can bind both the barbed and pointed ends of actin filaments for approximately 27 seconds. 3) In the presence of actin monomers and saturating profilin, VopL/F still predominantly nucleate actin filaments and behave as in (1), but a small percentage of VopL/F events bind to the barbed ends of pre-assembled filaments and cap them for approximately 25 seconds.

SECTION 3.8 MATERIALS AND METHODS

TIRFM. TIRFM images were collected at 1- to 4-s intervals with an iXon EMCCD camera (Andor Technology) using an Olympus IX-71 microscope fit with through-the-objective TIRF illumination. Photobleaching TIRFM images were collected continuously (10–20 frames/s) in the 561-nm channel, with the 488- nm shutter opened every 20–40 frames to visualize actin. Mg-ATP-actin (15% Oregon Green-actin) was mixed with 2× TIRF buffer [1×: 10 mM imidazole (pH 7.0), 50 mM KCl, 1 mM $MgCl_2$, 1 mM EGTA, 50 mM DTT, 0.2 mM ATP, 50 μM $CaCl_2$, 15 mM glucose, 20 μg/mL catalase, 100 μg/mL glucose oxidase, and 0.5% (400 centipoise) methylcellulose] and SNAP-VopL and SNAP-VopF constructs was transferred to a flow cell for imaging at 23 °C. For two and three-color TIRFM, we cyclically imaged Oregon-green actin or Alexa-488 actin (one frame, 488-nm excitation for 50 ms), 549-SNAP-VopL or 549-SNAP-VopF (one frame, 561-nm excitation for 50 ms), and 640-SNAP-MmCP, 640-SNAP-mDia2, or Alexa-640 actin (one frame, 640-nm excitation for 50ms).

Plasmid Construction. VopL and VopF constructs were prepared by infusion (Clontech) following PCR amplification (iProof; Bio-rad) from plasmid DNA supplied by Dr. Roberto Dominguez for VopL and from codon-optomized plasmid DNA supplied by Dr. Eugen Kerkhoff for VopF with a 6xHis tag included in the reverse primer. PCR products were cloned into the SNAP-tag-T7-2vector (New England Biolabs) at the XmaI/PacI sites, but the PacI site is not maintained. A flexible linker (GGSGGS) was included in the forward primer sequences of the SNAP constructs.

Protein expression and purification. Recombinant SNAP-VopL-6xHIS and SNAP-VopF-6xHIS proteins were purified by expressing in *Escherichia coli* strain BL21-Codon Plus (DE3)-RP (Stratagene) with 0.5-mM isopropyl β-D-1-thio- galactopyranoside for 16 h at 16 °C. Cells were lysed with an Emulsi-Flex-C3 (Avestin) in extraction buffer [50 mM NaH_2 PO_4 (pH 8.0), 500 mM NaCl, 10% glycerol, 10 mM imidazole, 10 mM B-mercaptoethanol] and were clarified. The extract was incubated for 1 h at 4 °C with Talon Resin (Clontech) and was loaded onto a column and washed with extraction buffer, and VopL and VopF were eluted with 250 mM imidazole. SNAP-VopL and SNAP-VopF were dialyzed against buffer [20 mM Hepes (pH 7.4), 200 mM KCl, 0.01% NaN3, and 1 mM DTT]. SNAP-tagged VopL and VopF were labeled with SNAP-Surface 549 following the manufacturers' protocols (New England Biolabs, Ipswitch, MA). Concentrations of SNAP-tagged proteins and the degree of labeling were determined by densitometry of Coomassie- stained bands on SDS/PAGE gels compared with standards and by measuring fluorophore absorbance in solution using the extinction coefficient SNAP-surface549:$_{\varepsilon 560}$ = 150,000 M/cm. VopL and VopF were flash-frozen in liquid nitrogen and stored at −80 °C. Actin was purified from chicken skeletal muscle acetone powder by a cycle of polymerization and depolymerization and gel filtration (Spudich & Watt 1971). Gel-filtered actin was labeled on Cys374 with Oregon Green iodoacetamide (Life Technologies, Carlsbad, CA) , or on random surface lysines with Alexa488 or Alexa647-succinimidylester (Life Technologies, Carlsbad, CA) (McCullough et al. 2011), (Kang et al. 2012). Mouse capping protein was expressed in bacteria and purified as described (Palmgren et al. 2001). The formin mDia2 was purified and labeled as described by (Suarez et al. 2015).

Glass Preparation. Microscope slides and coverslips (#1.5; Fisher Scientific) were washed for 10 min with acetone, then 10 min with isopropanol, then 10 min with MilliQ H_2O, then 10 min

with isopropanol. They were sonicated for 30 min with isopropanol, incubated for 1 h with piranha solution (80% H_2SO_4, 20% H_2O_2), washed with deionized water, then washed with isopropanol and dried. Glass then was incubated for 18 h with 1 mg/mL mPeg-Silane (5,000 MW) in 95% ethanol, pH 2.0. Slides were washed once with 95% ethanol then 5 times with MilliQ H_20, air dried and stored in petri dishes at 4 °C. Parallel strips of double-sided tape were placed on the coverslip to create multiple flow chambers.

Photobleaching and Analysis of Fluorescence Intensity. For photobleaching experiments to determine the oligomerization state of VopL and VopF, 549-SNAP-VopL or 549-SNAP-VopF were imaged continuously, whereas actin filaments were imaged intermittently. The observed distribution of photobleaching steps was compared with the number of steps predicted by a binomial distribution model where s = 0.50 (Breitsprecher et al. 2012). When spots did not bleach completely, the number of fluorescent subunits present was inferred by intensity and step size. Background fluorescence was subtracted with ImageJ using a rolling ball radius of 30 pixels, and the integrated fluorescence signals of 549-SNAP-VopL and 549-SNAP-VopF spots associated with the end of actin filaments were manually tracked and measured using ImageJ software.

Calculation of Residence Time. To calculate residence times on actin filament ends in all conditions, 549-SNAP-VopL and 549-SNAP-VopF spots associated with filament ends were tracked manually in ImageJ software. Residence times for single 549-SNAP-VopL or 549-SNAP-VopF dimers in spontaneous TIRF assays were determined by back-calculating from the length of the actin filament immediately before the 549-SNAP-VopL and 549-SNAP-VopF dissociated. Barbed-end elongation rates were calculated by measuring filament lengths over time with ImageJ software.

Quantification of partially bleached filaments

Partially bleached actin filaments were quantified by using the line-scan function in ImageJ. A line was drawn down the length of the filament at the last frame a 549-SNAP-VopL, 549-SNAP-VopF, or 549-SNAP-mDia2 were associated in the RGB merged image and saved as an ROI. These ROIs were imported into the 488-channel timelapse (with background subtracted) and a line-scan was taken at this point. The raw values were normalized from 0 to 1 for each individual filament. The three normalized values proximal or distal to the 549-SNAP-VopL, 549-SNAP-VopF, or 549-SNAP-mDia2 were averaged to account for noise. If the average of the normalized values was below 0.2 it was considered to be in the dimmest 20% of the filament, and if the value was above 0.8 it was considered to be in the brightest 20%. All 549-SNAP-VopL and 549-SNAP-VopF events were bound to the dimmest 20%, while all 549-SNAP-mDia2 events were bound to the brightest 20%.

Fluorescence Spectroscopy. Bulk actin assembly was measured from the fluorescence of pyrene-actin with a Safire2 (Tecan) fluorescent plate reader (Neidt and Kovar 2008). Briefly, the assembly of 10% pyrene-labeled Mg-ATP-actin monomers was initiated by the addition of 50 mM KCl, 1 mM MgCl2, 1 mM EGTA, 10 mM imidazole, pH 7.0, and other proteins to be assayed. Final protein concentrations are indicated in the figure legends.

CHAPTER 4 CONCLUSIONS, IMPLICATIONS AND FUTURE DIRECTIONS

SECTION 4.1 AIMS OF THE WORK:

The aim of this work was two-fold. First, to investigate the regulation of the actin cytoskeleton by homeostasis-driven internetwork competition for actin monomers and second to determine the biochemical molecular mechanism of actin filament assembly by the *Vibrio* virulence and WH2-domain assembly factors VopL and VopF. Since each aim required its own approach I utilized two different systems to address these two questions.

In the first part of my thesis my goal was to understand how actin assembly factors compete for a shared pool of actin monomer within single cells. I utilized the fission yeast *S. pombe* and a combination of pharmacological inhibitors and genetic depletion to systematically remove actin assembly factors or modify the cellular concentration of actin. Quantitative confocal fluorescence microscopy of manipulated cells revealed new findings pertaining to this regulatory mechanism. Although our findings were the result of a study in a relatively basic model organism, other groups have published studies reporting the same phenomenon in multicellular organisms thus extending the impact and applicability of our own findings.

For the second part of my thesis my goal was to understand the mechanism of actin filament assembly by the WH2-domain assembly factors VopL and VopF at the single filament and single molecule level. I utilized *in vitro* biochemical techniques including purifying and fluorescently labeling VopL, VopF, and actin monomers coupled with TIRF-M to visualize single actin filaments and the effects VopL and VopF had on actin dynamics. My results are important given the field is still studying how the ever-growing collection of WH2-domain assembly factors facilitate actin filament assembly.

Overall my findings contribute to the knowledge of how actin cytoskeletal networks are regulated *in vivo* as well as how the pathogen secreted actin assembly factors VopL and VopF disrupt G-to F-actin homeostasis.

SECTION 4.2 ACTIN ASSEMBLY FACTORS COMPETE FOR A LIMITED POOL OF ACTIN MONOMERS

I aimed to study if and how actin assembly factors and their respective networks are regulated by competition for a common pool of actin monomers. To control F-actin network density, actin polymerization is tightly regulated through the activation of assembly factors by upstream GTPase signaling cascades, the rate at which F-actin barbed ends are capped, the rate at which assembly factors are turned off, and F-actin disassembly factors (Campellone & Welch 2010; Chesarone & Goode 2009; Michelot & Drubin 2011). The supply of unassembled G-actin was not generally considered to be limiting (Mullins, Kelleher, et al. 1998; Zigmond et al. 1998). We proposed an alternative regulatory mechanism, wherein the actin cytoskeleton is homeostatic with a limited concentration of G-actin, which is competed for by assembly factors to help regulate its incorporation into diverse F-actin networks (Gao & Bretscher 2008; Nakano & Mabuchi 2006b; Chesarone & Goode 2009; Kovar et al. 2011). Using a combination of pharmacological inhibition and genetic depletion, I found that depletion of one actin network led to ectopic assembly by the remaining networks. Specifically I showed that inhibition of Arp2/3 complex in the fission yeast *S. pombe* not only eliminates Arp2/3 complex-mediated endocytic actin patches, but also induces a dramatic excess of formin-assembled F-actin. Conversely, disruption of the formins increases the density of Arp2/3 complex-mediated patches. Furthermore, modifying actin levels significantly perturbs the fission yeast actin cytoskeleton. Increasing actin favors Arp2/3 complex-mediated actin assembly, whereas decreasing actin

favors formin-mediated contractile rings. Therefore, the specific actin concentration in a cell is critical, and competition for G-actin helps regulate the proper amount of F-actin assembly for diverse processes.

SECTION 4.3 MECHANISM OF ACTIN FILAMENT ASSEMBLY BY VopL and VopF

I aimed to study the molecular mechanism of actin filament assembly by the WH2-domain assembly factors VopL and VopF. More specifically I attempted to determine whether previous studies that were in conflict over two different mechanisms, pointed versus barbed end binding of the actin filament, could be reconciled (Pernier et al. 2013; Namgoong et al. 2011). Utilizing multi-color TIRF-M I examined the dynamics and localization of recombinantly purified fluorescently labeled VopL and VopF on single actin filaments *in vitro*. Contrary to previous reports I found that VopL and VopF share an actin assembly mechanism. It was essential to compare VopL and VopF's *in vitro* affects on actin assembly in side-by-side experiments rather than the previous efforts of different labs that utilize different assays. I found VopL and VopF share the same multi-functional actin assembly properties and vary in their capabilities depending on the experimental conditions. In conditions dominated by free G-actin both VopL and VopF nucleate filaments and remain bound to the pointed end for approximately 76 seconds followed by filament release. In these conditions VopL and VopF do not bind pre-existing filaments and only nucleate filaments from the pool of actin monomers. In the presence of pre-assembled filaments but in the absence of actin monomers VopL and VopF bind both the barbed and pointed ends of pre-assembled filaments for approximately 30 seconds. In the presence of actin monomers and saturating profilin VopL and VopF nucleate filaments a majority of the time

(90%) while a small subset of VopL and VopF molecules bind briefly to the barbed ends of pre-assembled filaments. When bound to the barbed end VopL and VopF act as capping proteins, halting actin filament elongation.

SECTION 4.4 FUTURE DIRECTIONS FOR ACTIN ASSEMBLY FACTOR COMPETITION FOR MONOMERS

Although we have revealed that F-actin cytoskeletal networks are subject to the additional form of regulation wherein actin assembly factors are competing for the same common pool of actin monomers, many questions remain and more were discovered by our results. One major question that arrises from our results is why do fission yeast make more patches of the same size when formins are depleted or the actin levels are modified? More generally, why do fission yeast make more patches versus increasing their average size? Additionally, we know that the actin binding proteins Adf1p/cofilin and capping protein can drastically affect all three F-actin networks if their levels are modulated. However their contributions to actin assembly factor competition for monomers and the F- to G-actin homeostasis in cells has yet to be rigorously tested. Therefore I will propose multiple experiments to address the questions raised.

Initiation or maintenance that dictates network size and density?

The data from my study on actin assembly factor competition and F to G-actin homeostasis left many open questions. One in particular relates to changes or the lack thereof in patch dynamics in different experimental backgrounds. Specifically I want to know: (1) Why do fission yeast make fewer patches that are approximately the same "size" (i.e. the amount of Lifeact-GFP incorporated) when treated with CK-666 and not the same quantity of smaller and smaller

patches, (2) Why does the quantity of patches increase in the double formin mutant (*cdc12-112 for3Δ*) while their dynamics stay relatively the same as wildtype, and (3) Why do fission yeast cells make fewer patches of the same size in the actin under-expression cells and profilin over-expression cells? All of these questions relate to a central question of what determines the "size" of an actin patch in fission yeast. This can be treated as a microcosm of the self-organization of the entire actin cytoskeleton. There are factors that are intrinsically limiting that influence the quantity and extent of F-actin assembly. All three questions can be investigated by researching the contributions of factors that control initiation of actin polymerization at the endocytic patches like the NPFs Wsp1p, Myo1p or Vrp1p or factors that influence the maintenance of the patch after it is assembled like Adf1/cofilin and capping protein.

To investigate question (1) "Why do fission yeast make fewer patches that are the same size when treated with CK-666 and not smaller patches?" I would quantify the localization and density of the NPFs on the cell wall in cells that are treated with the Arp2/3 complex inhibitor CK-666 as changes in the localization of NPFs may influence Arp2/3 complex mediated actin polymerization. Initial data acquired by our lab indicates that in cells treated with CK-666 the NPF Wsp1p localizes into condensed areas at the cell tips compared to a more distributed, punctate localization in control cells. This implies a yet uninvestigated phenomenon where actin polymerization by the Arp2/3 complex somehow feeds back into the localization of its upstream activators. However this localization could also be due to the increased formin activity that could alter the overall polarization of the cell. By increasing the polymerization of the formin For3p in CK-666 treated cells I could be hyper-polarizing cells and not allowing factors to diffuse to the extent they would in WT cells. In order to determine if the same amount of Wsp1p was present on the cortex in WT and CK-666 treated cells I would need to do whole cell quantitative

fluorescence microscopy to compare total Wsp1p fluorescence levels on the cortex in treated and untreated cells. I would compare the distribution the other NPFs (Vrp1p and Myo1p) to determine if they too exhibited this hyper-polarized behavior as this might why fission yeast cells treated with CK-666 do not make multiple smaller patches.

Quantitative microscopy could also be used to determine how the accumulation of Arp2/3 complex subunits compares to CK-666 and untreated cells. If CK-666 treated cells accumulated fewer Arp2/3 complexes per patch than untreated cells, this would indicate that the overall architecture of the F-actin at the patches would be significantly different. If it is true that the same amount of actin is incorporated into patches whether or not cells are treated with CK-666, this means there must be defects in the F-actin organization at the patches in CK-666 treated cells. We would hypothesize that the actin filaments in the patches of CK-666 treated cells would be longer than normal because of an increased G-actin concentration available for consumption by a potentially unchanged quantity of F-actin barbed ends. This could be verified with electron microscopy analysis of the cortical actin organization in CK-666 treated and untreated cells. Analyzing how much capping protein is present in the patches could provide valuable insight. If there are fewer, longer filaments there should be a lower ratio of capping protein:LifeAct per patch since each actin filament can only bind one capping protein at its barbed end.

To investigate question (2) “Why does the quantity of patches increase in the double formin mutant while the dynamics stay relatively the same as wildtype?” I would investigate the distribution of the Arp2/3 complex NPFs as mentioned above. Utilizing quantitative fluorescence microscopy I would determine whether all sites of NPF accumulation became sites of actin polymerization, or in other words what percent of “pre-patches” actually become endocytic actin patches? A simple comparison of sites of NPF localization versus Lifeact, Arp2/3 complex,

fimbrin and capping protein fluorescence would elucidate whether all or a subset of pre-patches become actual endocytic actin patches. I would hypothesize that most if not all pre-patches would become true patches. I obtained data that implicates competition between patches for actin in the single and double formin mutants. Analyzing patch dynamics and polymerization kinetics shows that the double formin mutant endocytic actin patches have approximately 60% of the maximum Lifeact-GFP fluorescence than WT patches do, yet they still have the same average Lifeact-GFP fluorescence indicating the increased quantity and density of patches is sharing the modest increase in G-actin due to the lack of formin-mediated actin networks.

I would use a similar approach to investigate question (3) "Why do fission yeast cells make fewer patches of the same size in the actin under-expression cells and the profilin over-expression cells?" Utilizing quantitative microscopy to analyze NPF, Arp2/3 complex, and actin patch specific ABPs (see: (Kovar et al. 2011), I could determine what differed and/or remained the same in patch dynamics for the actin under-expression and profilin over-expression cells. I could also determine what compensatory mutations or treatments would rescue the actin over-expression cells. I hypothesize either over-expressing capping protein or adding low concentrations of CK-666 could ameliorate the dense swaths of Arp2/3 complex mediated actin in the actin over-expression cells much like over-expressing profilin does (Suarez et al. 2015). Understanding the localization of Adf1p/cofilin in the actin under and over-expression backgrounds could provide valuable insight as well. It is assumed that cofilin is responsible for the "maintenance" phase of actin polymerization at endocytic patches by preventing over-assembly of F-actin. Therefore tracking cofilin's localization in WT and the actin under and over-expression backgrounds could help determine whether the differences in patch size are due to initiation or maintenance.

Contributions of Capping protein and ADf1/Cofilin to F-actin network size

Related to (1-3), the specific contributions of capping protein and cofilin to F-actin homeostasis and assembly factor competition for monomers in fission yeast cells remains unstudied. It is known that depletion of cofilin and modulation of capping protein levels in fission yeast affects the F-actin endocytic patches and the contractile ring (Nakano & Mabuchi 2006a; Nakano & Mabuchi 2006b; Kovar et al. 2005). However it is still undetermined how small, non-lethal modulations of either protein affects the amount of actin incorporated into each one of the three F-actin networks in fission yeast. Since both are directly implicated in actin polymerization and turnover in vivo, mild manipulations of either capping protein or cofilin individually or together could provide insight into whether the amount of actin in a particular network is dictated by maintenance rather than initiation. As an example I would hypothesize that increasing concentrations of capping protein would lead to fewer, smaller patches since capping protein can only localize to F-actin, not sites of future polymerization. The opposite could be true as well. By increasing capping protein in fission yeast cells the amount of G-actin incorporated into a single filament would decrease, thereby increasing the pool of G-actin for other nucleation factors to consume. This may lead to more patches and potentially larger formin-mediated actin cables. Over and under-expression of Adf1p/cofilin would be a useful tool to determine if modulating the cofilin concentration has any effect on the average patch size and quantity much like the proposed experiments about capping protein above. If the size and density of F-actin networks is relatively unchanged at low-level manipulations of capping protein and cofilin, one could study the endocytic patch dynamics and timing of the contractile ring formation and constriction to determine if the F-actin network architectures are disrupted. The experiments proposed above comparing the contributions of the NPFs of the Arp2/3 complex and the maintenance factors

Adf1p/cofilin and capping protein could determine whether the size of an actin network is modulated by "active" processes that solely rely on signaling and/or modulated by a "passive", constitutive control where the size of any given network results from the balance of continuous assembly and disassembly.

SECTION 4.5 FUTURE DIRECTIONS FOR VopL and VopF

Although we have provided insight into how VopL and VopF assemble actin under various conditions, many questions remain to be answered about further molecular details of actin filament assembly as well as the relatively unstudied aspect of the *in vivo* biology of how VopL and VopF affect the host cell's F-actin cytoskeleton. The main topics of further work that I will propose here address: What the biochemical and molecular details are of pointed end binding during nucleation versus binding the ends of preassembled filaments, if and how VopF uncaps actin filaments, and how the host cell's actin cytoskeleton is re-arranged upon addition of VopL and VopF?

Additionally I tested how VopL and VopF's actin assembly capabilities were affected in the presence of covalently cross-linked actin oligomers. *V. cholerae* possess many actin modulating proteins besides VopF, one of them being the MARTX toxin. The actin cross-linking domain (ACD) of the MARTX toxin acts on actin monomers and covalently binds them into unusable actin oligomers (Kudryashov et al. 2008). I found that not only do the oligomers affect formin mediated assembly, but VopL and VopF mediated assembly as well. Further investigation is needed to determine the potency of the actin oligomers for various actin assembly factors.

Molecular mechanism of pointed versus barbed end binding of VopL and VopF.

We have shown that VopL and VopF possess multiple functions depending on the availability of actin monomer. When added to pure G-actin monomer both VopL and VopF promote rapid cycles of nucleation and remain bound to the pointed end of the nucleated filament for approximately 76 seconds and do not associate with pre-assembled filaments. In the absence of monomer both VopL and VopF are competent to bind both the barbed and pointed ends of actin filaments for approximately 27 seconds. In the presence of actin monomer and saturating profilin VopL and VopF are predominantly actin nucleators bound to the barbed end like with actin alone, but a small percentage of events (10%) are now bound to the barbed end of pre-assembled filaments for approximately 25 seconds. We have verified and investigated the reports of VopL and VopF's modes of actin assembly, however the molecular details of these mechanisms are still unclear. The main questions that are raised from our new results are aimed at what domains and residues of VopL and VopF mediate each mode of actin binding and assembly.

To determine the molecular mechanism mediating the 76-second association time with nucleated filaments I would create SNAP-tagged constructs of the VopL VCD mutants generated by Zahm et al. Residues E251, Y275, V405, E408, N397, Y425, and R428 within the VCD were all implicated in binding and organizing actin monomers for VopL nucleated actin filaments (Zahm et al. 2013). Mutating groups of residues to alanines (E251, Y275, V405, and E408) and (N397, Y425, and R428) was shown to decrease the nucleation efficiency of full-length VopL constructs. I would start by mutating the full groups of residues followed by smaller groups and then individual residues to determine which had the greatest effect on time to half-max pyrene fluorescence in bulk actin polymerization assays. I would then utilize the mutants in spontaneous

two-color TIRF-M to determine if the decrease in nucleation efficiency and lifetime on the pointed end of filaments was correlated. I would hypothesize that if the VCD is mediating the binding between VopL and the newly nucleated actin filament that mutating the residues within the VCD would shorten the lifetime of VopL on filaments. Any difference observed could be translated to VopF by performing the same mutagenesis on homologous residues. There is the possibility that mutating the above residues would just decrease the nucleation efficiency and not change the lifetime of VopL on nucleated filaments. It was inferred from X-ray crystallography results that the actin monomers organized by the VCD form a "filament-like" configuration that has a slightly different twist and spacing between monomers compared to an unbound control filament, and that after the filament polymerizes to a certain length the true actin filament twist and conformation propagates down from the free barbed end to the bound pointed end (Zahm et al. 2013). This change in conformation is what causes VopL to release the filament and become available for the next round of nucleation. This could be tested by either increasing or decreasing the concentration of actin in the two-color spontaneous TIRF-M assays. If VopL releases the nucleated actin filament at a certain length, then the lifetime of VopL on an actin filament should be inversely correlative to the G-actin concentration in the assay. Increasing the actin concentration will decrease the lifetime of VopL on nucleated actin filaments and decreasing the actin concentration should increase the lifetime.

To deduce what domains of VopL and VopF bind to pre-assembled filaments in the absence of monomer I would utilize either SNAP-VCD or SNAP-3xWH2 (WH2 domains only) truncations. As mentioned above, the VCD is implicated in binding the pointed end of actin filaments, and prior structural results on isolated WH2 domains show that the WH2 domain binds to the barbed end of a G-actin monomer (Chereau et al. 2005; Dominguez 2010). Although

it is difficult to determine the barbed from the pointed end in the absence of actin monomers, I would hypothesize that unlike the full-length SNAP-VopL and SNAP-VopF that can bind both ends of the actin filament, that the SNAP-VCD and SNAP-3xWH2 would only bind one end of the filament, predictably the pointed end and barbed end, respectively. I would predict that the SNAP-3xWH2 truncation would bind the barbed end given that is the only region on the filament that has the necessary residues available on the actin monomer for WH2 domain binding. Truncating the WH2 domains (SNAP-2xWH2, SNAP-WH2) should decrease the frequency of events and the lifetime of the VopL truncation on the barbed end. If the SNAP-VCD construct did only bind one end of the filament I could use the alanine mutations mentioned from Zahm et al. in other SNAP-VCD constructs to verify that it was indeed the pointed end as those residues were implicated in mediating the pointed end contacts by the VCD. I would predict the SNAP-VCD alanine mutants would bind for a decreased amount of time to the end of the filament if those residues were mediating the pointed end binding. Finally, if the SNAP-VCD and SNAP-3xWH2 truncations do only bind to one end of the filament, I would do three color TIRF-M with SNAP-VCD and SNAP-3xWH2 labeled with different fluorophores. If they do bind to opposite ends, I would expect to see a dumbbell like pattern on the pre-assembled actin filaments and no change in the frequency of binding nor the lifetime of either construct for ends since they would not be competing for binding spots.

Finally I would utilize the SNAP-VCD and SNAP-3xWH2 constructs with pre-assembled filaments and saturating profilin to determine what domains of VopL and VopF are mediating barbed-end binding. I would hypothesize that only the SNAP-3xWH2 construct would bind the barbed end given the residues necessary for WH2-domain binding to G-actin are exposed. If the SNAP-3xWH2 domain construct did bind the barbed end I would truncate WH2 domains from

the full-length protein (SNAP-2W-VCD, SNAP-1W-VCD). I hypothesize that SNAP-2W-VCD and SNAP-1W-VCD of both VopL and VopF would bind barbed ends less frequently and for a decreased amount of time.

Do VopL and VopF uncap actin filaments?

To address the claim of VopF uncapping actin filaments bound by capping protein I would take two approaches. First, I would do co-immunoprecipitation assays to determine if VopL or VopF interact with capping protein directly. Second, I would do three color flow-in TIRF-M. Briefly, actin filaments would be polymerized in the presence of fluorescently labeled SNAP-capping protein. I would then flow in fluorescently labeled SNAP-VopL or SNAP-VopF in the absence of actin monomers since we know that VopL and VopF only bind the ends of filaments in that condition. I would quantify how often, if at all, that a SNAP-VopL or SNAP-VopF replaced a SNAP-capping protein from the barbed end of the actin filament. SNAP-VopL or SNAP-VopF may co-localize with SNAP-capping protein before uncapping, as it was recently shown that formins and capping protein can form a "decision complex" at the barbed end before one displaces the other (Bombardier et al. 2015; Shekhar et al. 2015). By comparing SNAP-capping protein lifetimes on filaments with and without SNAP-VopL or SNAP-VopF I will determine if VopL and VopF modify capping protein's lifetime on actin filaments.

How do VopL and VopF rearrange the host cell's actin cytoskeleton?

Aside from the biochemical characterization of the molecular mechanism of actin filament assembly by VopL and VopF very little is known about how VopL and VopF affect the cytoskeleton of the host cell in real time. Static assays have been done with mammalian cells expressing plasmids with VopL or VopF which are then fixed and stained for actin and actin-binding proteins(Tam et al. 2007; Liverman et al. 2007). However that approach only shows an

end-point of a highly rearranged cytoskeleton. We do not know what individual actin networks are affected, how they are affected, and in what order. We also do not know how many molecules of VopL or VopF *Vibrio parahaemolyticus* and *Vibrio cholerae* secrete into host cells. I propose to use live-cell confocal imaging coupled with a flow chamber to address the *in vivo* questions.

The experimental setup would be as such: 1) Mammalian cells expressing the general actin marker LifeAct-mCherry would be loaded into a flow chamber. 2) After initial imaging to determine the dynamics of the endogenous actin networks, a solution containing a known density of *Vibrio parahaemolyticus* or *Vibrio cholerae* expressing GFP-VopL or GFP-VopF would be introduced to the chamber with the LifeAct-mCherry expressing mammalian cells. 3) Image the cells over time to visualize the actin re-arrangements of the host cells. This experimental setup would allow for visualization of the actin cytoskeleton undergoing VopL or VopF mediated re-arrangements as well as transfer of GFP-VopL and GFP-VopF from the bacteria into the host cell and could be quantified through a change in GFP fluorescence within the host cells. Quantitative microscopy coupled with Western Blotting of the input solution the bacteria could roughly calculate how many GFP-VopL or GFP-VopF molecules could be transferred through the type-III secretion machinery. Further analysis would include discerning if any specific actin networks were targeted by VopL or VopF, if any endogenous actin assembly factors or actin binding proteins were displaced from actin filaments, and if, much like *in vitro*, VopL and VopF eventually bind to actin filaments after a certain period of time when the actin monomer pool is exhausted.

SECTION 4.6 FUTURE DIRECTIONS FOR ACD DERIVED ACTIN OLIGOMERS

Determining the relative efficacy of ACD-mediated actin oligomers on formin, Arp2/3 complex, VopL and VopF mediated actin assembly.

Vibrio bacteria contain a suite of virulence factors that are actin cytoskeleton modulating proteins that they export into host cells. Besides the actin assembly factors VopL and VopF, species of *Vibrio* can secrete the actin bundler VopV, the RhoGTPase effector VopO, and the MARTX toxin that contains an actin cross-linking domain (ACD) that locks actin monomers into an unpolymerizable oligomers (Hiyoshi et al. 2011; Hiyoshi et al. 2015; Kudryashov et al. 2008). The ACD cross-links two actin monomers together by creating an iso-peptide bond between E270 on one monomer and K50 on another. This dimer of cross-linked actin can then be cross-linked to another dimer and so on, forming higher order actin oligomers (Kudryashov et al. 2008). The ACD causes actin cross-linking *in vivo* as well causing intestinal inflammation in mice that are infected with MARTX-ACD containing *Vibrio* bacteria (Ma & Mekalanos 2010; Dolores et al. 2015). Recently, in a collaboration with our lab, Heisler et al. demonstrated that actin oligomers made from the ACD of a related bacterial species *A. hydrophila* "poison" formin mediated actin assembly in vitro (Heisler et al. 2015). Utilizing pyrene bulk polymerization assays and single molecule two-color TIRF-M our collaboration determined the formins mDia1 and mDia2 were sensitive to actin oligomers. If an actin oligomer bound to a mDia1 or mDia2 that was processively elongating an actin filament, the formin was turned into a capping protein and remained stationary on the barbed end of the actin filament. This processive-to-capper transition was mapped to the FH1 domains of the formin as the FH2-only truncations were barely affected. It is still unknown if and how these ACD-mediated actin oligomers affect other actin assembly factors including VopL and VopF. We hypothesized that VopL and VopF would

be immune to actin oligomers for two reasons. First, both proteins come from the same organism, so why would two known virulence factors evolved for the same purpose be detrimental to the other? Second, we know that the oligomers affect formin-mediated processive elongation at the barbed end and VopL and VopF nucleate filaments from the opposite, pointed end.

To investigate whether actin oligomers affect VopL and VopF mediated actin assembly I purified the ACD domain (residues 1925-2391) of the MARTX toxin from *A. hydrophila* that was used in Heisler et al. by attaching at 6xHIS tag to the C-terminus and following the standard purification protocol. Following and modifying the protocols from Kudryashov et al., Heisler et al., and Kudryashova et al. (Kudryashov et al. 2008; Heisler et al. 2015; Kudryashova et al. 2014) I successfully made actin oligomers (Fig 4.1).

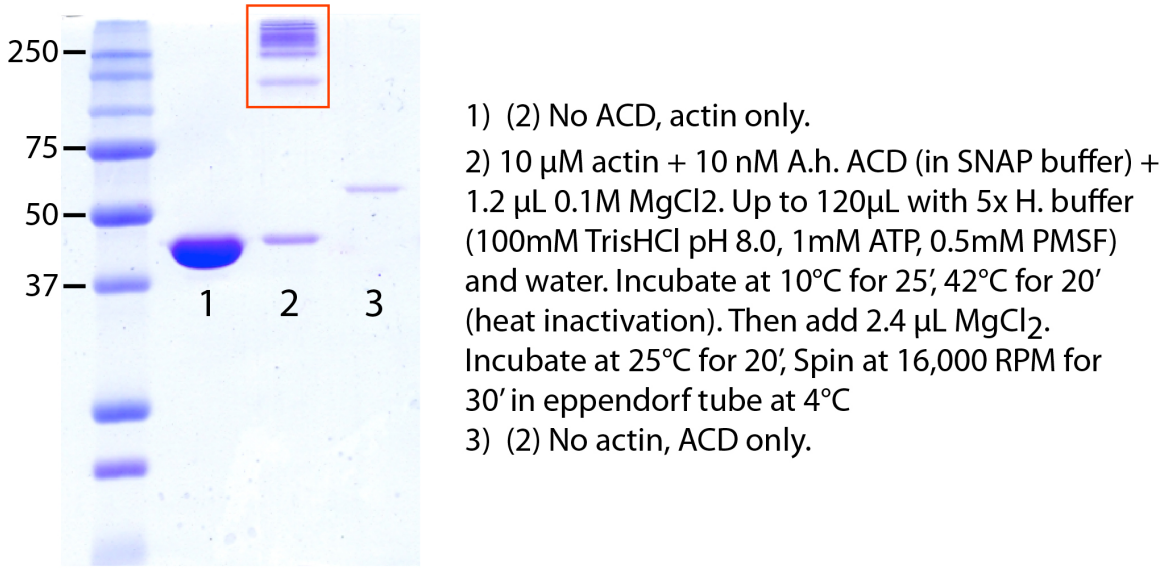

Figure 4-1: The ACD of *A. hydrophila* makes actin oligomers
Representative Coomasie-blue stained SDS-PAGE gel of (1) actin alone (2) actin + ACD and (3) ACD alone. Red box indicates actin oligomers. Conditions for formation of oligomers are in the figure. Protocol assembled and modified from (Kudryashova et al. 2014; Heisler et al. 2015)

I utilized pyrene bulk polymerization assays to determine if actin oligomers affected the nucleation capabilities of VopL and VopF in comparison to the formin mDia2. Surprisingly the actin oligomers did affect the nucleation capabilities of VopL and VopF as well as mDia2 (Fig 4-2). However the most drastic decrease seen in VopL and VopF's nucleation capabilties came at a ratio of VopL/F:oligomer of 10:1 versus the same effect for formin was seen at a ratio of 2:1. This could mean that there is an inherent difference in efficacy of actin oligomer "poisoning" of actin assembly factors. At first the results were unexpected, but given VopL and VopF both have a total of six WH2 actin monomer binding sites it was unreasonable to believe VopL and VopF would be totally immune to the effect of actin oligomers.

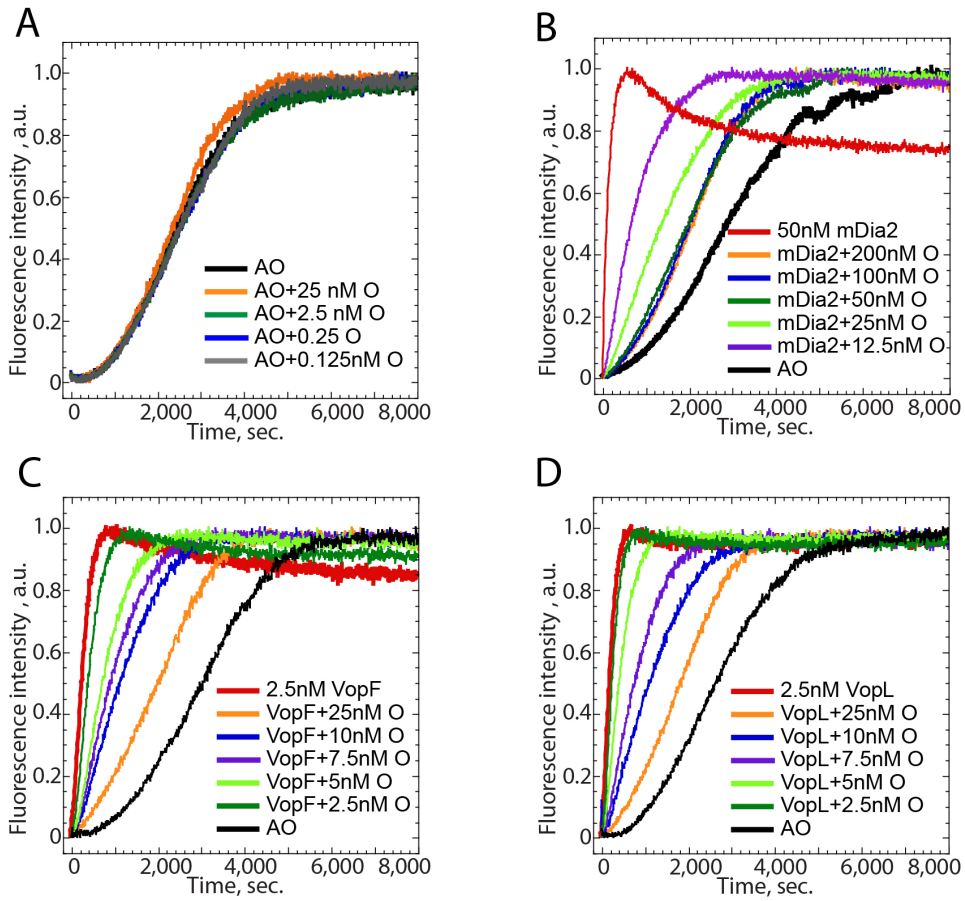

Figure 4-2: Actin oligomers decrease bulk polymerization kinetics of the formin mDia2, VopL and VopF.

(A-D) Spontaneous assembly of 1.0 μM Mg-ATP actin monomers (10% pyrene-labeled). (A) Time course of actin assembly in the absence (black) or presence of increasing concentrations of *A. hydrophila* ACD mediated actin oligomers. (B) Time course of actin assembly in the presence of 50 nM mDia2 (red) with increasing amounts of actin oligomers. (C) Time course of actin assembly in presence of 2.5 nM SNAP-VopF (red) with increasing amounts of actin oligomers. (D) Time course of actin assembly in presence of 2.5 nM SNAP-VopL (red) with increasing amounts of actin oligomers.

Although I have shown that VopL and VopF are sensitive to actin oligomers, additional questions remain. The pyrene assays shown in (Figure 4-2) were done with actin only and no profilin which may be a confounding factor given the greatest actin oligomer mediated decrease in mDia2 assembly came in assays with profilin (Heisler et al. 2015). Profilin should be added to the pyrene assays to ensure the mechanism of inhibition is conserved from previous reports. Also the same concentration of VopL, VopF and mDia2 should be used in the bulk pyrene experiments to ensure comparable data. Once a consistent system is in place to test the efficacy of actin oligomers, many other actin assembly factors such as the Arp2/3 complex could be tested for susceptibility. If VopL and VopF are less susceptible to actin oligomers than formins or the Arp2/3 complex, one could attempt to reconstitute multiple aspects of *Vibrio* mediated virulence in one TIRF-M assay. With four colors to use, I would create actin oligomers from Alexa-405 labeled actin and add those to TIRF reactions with Alexa-488 labeled actin filaments, 549-SNAP-VopL and 647-SNAP-mDia2 to determine if the threshold for actin oligomer mediated formin inhibition is low enough for VopL to continue to nucleate filaments. If it were, I would predict to see red VopL dots continuously nucleating actin filaments while cyan mDia2 dots co-localized with the tips of the green actin filaments and a blue actin oligomer(s).

SECTION 4.7 CONCLUSIONS

In conclusion, I studied a new aspect of regulation for the actin cytoskeleton wherein actin networks are in homeostasis and actin assembly factors are in competition for a shared pool of actin monomers in the fission yeast *S. pombe*. I also studied the molecular mechanism of actin filament assembly by the WH2-domain actin assembly factors VopL and VopF utilizing *in vitro* TIRF-M and unlike previous studies with conflicting results, I found VopL and VopF share the same multi-functional mechanism of actin filament nucleation and actin filament binding. Although the specific methods and approaches used in my two projects vary greatly, together the results from both studies reinforce the importance of G- to F-actin homeostasis in cells. Each F-actin network in cells is tailored for a specific process and utilizes a given amount of G-actin. When the monomer pool is modified by depleting an actin network artificially, raising or lowering the G-actin concentration, or by introducing virulence factors that are actin assembly factors the normal G- to F-actin homeostasis is disrupted causing many, if not all actin networks to suffer.

REFERENCES

ABMM, J.M.J.P.D., MPH, A.E.N. & MS, C.A.B., 2015. Vibriosis. *Clinics in Laboratory Medicine*, 35(2), pp.273–288.

Ahuja, R. et al., 2007. Cordon-bleu is an actin nucleation factor and controls neuronal morphology. *Cell*, 131(2), pp.337–350.

Aktories, K. & Barbieri, J.T., 2005. Bacterial cytotoxins: targeting eukaryotic switches. *Nature Reviews Microbiology*, 3(5), pp.397–410.

Almonacid, M. et al., 2011. Temporal Control of Contractile Ring Assembly by Plo1 Regulation of Myosin II Recruitment by Mid1/Anillin. *Current Biology*, 21(6), pp.473–479.

Amann, K.J. & Pollard, T.D., 2000. Cellular regulation of actin network assembly. *Current biology : CB*, 10(20), pp.R728–30.

Amann, K.J. & Pollard, T.D., 2001a. Direct real-time observation of actin filament branching mediated by Arp2/3 complex using total internal reflection fluorescence microscopy. *Proceedings of the National Academy of Sciences of the United States of America*, 98(26), pp.15009–15013.

Amann, K.J. & Pollard, T.D., 2001b. The Arp2/3 complex nucleates actin filament branches from the sides of pre-existing filaments. *Nature cell biology*, 3(3), pp.306–310.

Avvaru, B.S., Pernier, J. & Carlier, M.-F., 2015. Dimeric WH2 repeats of VopF sequester actin monomers into non-nucleating linear string conformations: An X-ray Scattering Study. *Journal of structural biology*.

Balasubramanian, M.K. et al., 1996. Fission yeast Sop2p: a novel and evolutionarily conserved protein that interacts with Arp3p and modulates profilin function. *The EMBO Journal*, 15(23), pp.6426–6437.

Balasubramanian, M.K. et al., 1994. The *Schizosaccharomyces pombe cdc3*+Gene Encodes a Profilin Essential for Cytokinesis. *Journal of cell science*, 125, pp.1289–1301.

Balasubramanian, M.K., Helfman, D.M. & Hemmingsen, S.M., 1992. A new tropomyosin essential for cytokinesis in the fission yeast S. pombe. *Nature*, 360(6399), pp.84–87.

Basu, R. & Chang, F., 2011. Characterization of dip1p reveals a switch in Arp2/3-dependent actin assembly for fission yeast endocytosis. *Current biology : CB*, 21(11), pp.905–916.

Bear, J.E. & Gertler, F.B., 2009. Ena/VASP: towards resolving a pointed controversy at the barbed end. *Journal of cell science*, 122(12), pp.1947–1953.

Berro, J., Sirotkin, V. & Pollard, T.D., 2010. Mathematical modeling of endocytic actin patch kinetics in fission yeast: disassembly requires release of actin filament fragments. *Molecular Biology of the Cell*, 21(16), pp.2905–2915.

Bilancia, C.G. et al., 2014. Enabled negatively regulates diaphanous-driven actin dynamics in vitro and in vivo. *Developmental cell*, 28(4), pp.394–408.

Blanchoin, L. et al., 2014. Actin Dynamics, Architecture, and Mechanics in Cell Motility. *Physiological Reviews*, 94(1), pp.235–263.

Bohnert, K.A. et al., 2013. SIN-dependent phosphoinhibition of formin multimerization controls fission yeast cytokinesis. *Genes & development*, 27(19), pp.2164–2177.

Bombardier, J.P. et al., 2015. Single-molecule visualization of a formin-capping protein "decision complex" at the actin filament barbed end. *Nature Communications*, 6, p.8707.

Breitsprecher, D. & Goode, B.L., 2013. Formins at a glance. *Journal of cell science*, 126(Pt 1), pp.1–7.

Breitsprecher, D. et al., 2008. Clustering of VASP actively drives processive, WH2 domain-mediated actin filament elongation. *The EMBO Journal*, 27(22), pp.2943–2954.

Breitsprecher, D. et al., 2012. Rocket launcher mechanism of collaborative actin assembly defined by single-molecule imaging. *Science*, 336(6085), pp.1164–1168.

Burke, T.A. et al., 2014. Homeostatic Actin Cytoskeleton Networks Are Regulated by Assembly Factor Competition for Monomers. *Current Biology*, 24(5), pp.1–7.

Campellone, K.G. & Welch, M.D., 2010. A nucleator arms race: cellular control of actin assembly. *Nature Reviews Molecular Cell Biology*, 11(4), pp.237–251.

Carlier, M.-F. et al., 2011. *Control of Actin Assembly by the WH2 Domains and Their Multifunctional Tandem Repeats in Spire and Cordon-—Bleu* 1st ed., Elsevier Inc.

Carlier, M.F. et al., 1993. Modulation of the interaction between G-actin and thymosin beta 4 by the ATP/ADP ratio: possible implication in the regulation of actin dynamics. *Proceedings of the National Academy of Sciences of the United States of America*, 90(11), pp.5034–5038.

Chang, F., Drubin, D. & Nurse, P., 1997. cdc12p, a protein required for cytokinesis in fission yeast, is a component of the cell division ring and interacts with profilin. *JCB*, 137(1), pp.169–182.

Chang, F., Woollard, A. & Nurse, P., 1996. Isolation and characterization of fission yeast mutants defective in the assembly and placement of the contractile actin ring. *Journal of cell science*, 109 (Pt 1), pp.131–142.

Chen, H., Bernstein, B.W. & Bamburg, J.R., 2000. Regulating actin-filament dynamics in vivo. *Trends in biochemical sciences*, 25(1), pp.19–23.

Chen, Q. & Pollard, T.D., 2013. Actin Filament Severing by Cofilin Dismantles Actin Patches and Produces Mother Filaments for New Patches. *Current biology : CB*, 23(13), pp.1–9.

Chen, Q. & Pollard, T.D., 2011. Actin filament severing by cofilin is more important for assembly than constriction of the cytokinetic contractile ring. *The Journal of Cell Biology*, 195(3), pp.485–498.

Chereau, D. et al., 2005. Actin-bound structures of Wiskott-Aldrich syndrome protein (WASP)-homology domain 2 and the implications for filament assembly. *Proceedings of the National Academy of Sciences of the United States of America*, 102(46), pp.16644–16649.

Chesarone, M.A. & Goode, B.L., 2009. Actin nucleation and elongation factors: mechanisms and interplay. *Current opinion in cell biology*, 21(1), pp.28–37.

Chhabra, E.S. & Higgs, H.N., 2006. INF2 Is a WASP Homology 2 Motif-containing Formin That Severs Actin Filaments and Accelerates Both Polymerization and Depolymerization. *The Journal of Biological Chemistry*, 281(36), pp.26754–26767.

Cossart, P., 2000. Actin-based motility of pathogens: the Arp2/3 complex is a central player. *Cellular microbiology*, 2(3), pp.195–205.

Decker, M. et al., 2011. Limiting amounts of centrosome material set centrosome size in C. elegans embryos. *Current biology : CB*, 21(15), pp.1259–1267.

Dolores, J.S. et al., 2015. Vibrio cholerae MARTX toxin heterologous translocation of beta-lactamase and roles of individual effector domains on cytoskeleton dynamics. *Molecular microbiology*, 95(4), pp.590–604.

Dominguez, R., 2010. Structural insights into de novo actin polymerization. *Current Opinion in Structural Biology*, 20(2), pp.217–225.

Dominguez, R., 2007. The beta-thymosin/WH2 fold: multifunctionality and structure. *Annals of the New York Academy of Sciences*, 1112, pp.86–94.

Dominguez, R., 2016. The WH2 Domain and Actin Nucleation: Necessary but Insufficient. *Trends in biochemical sciences*, pp.1–13.

Engel, B.D., Ludington, W.B. & Marshall, W.F., 2009. Intraflagellar transport particle size scales inversely with flagellar length: revisiting the balance-point length control model. *JCB*, 187(1), pp.81–89.

Faruque, S.M., Albert, M.J. & Mekalanos, J.J., 1998. Epidemiology, genetics, and ecology of toxigenic Vibrio cholerae. *Microbiology and Molecular Biology Reviews*, 62(4), pp.1301–1314.

Feierbach, B. & Chang, F., 2001. Roles of the fission yeast formin for3p in cell polarity, actin cable formation and symmetric cell division. *Current biology : CB*, 11(21), pp.1656–1665.

Firat-Karalar, E.N. & Welch, M.D., 2011. New mechanisms and functions of actin nucleation. *Current opinion in cell biology*, 23(1), pp.4–13.

Franco, I.S., Shohdy, N. & Shuman, H.A., 2012. The Legionella pneumophila Effector VipA Is an Actin Nucleator That Alters Host Cell Organelle Trafficking C. E. Stebbins, ed. *PLoS Pathogens*, 8(2), p.e1002546.

Galán, J.E. & Wolf-Watz, H., 2006. Protein delivery into eukaryotic cells by type III secretion machines. *Nature*, 444(7119), pp.567–573.

Gao, L. & Bretscher, A., 2008. Analysis of unregulated formin activity reveals how yeast can balance F-actin assembly between different microfilament-based organizations. *Molecular Biology of the Cell*, 19(4), pp.1474–1484.

Glynn, J.M. et al., 2001. Role of bud6p and tea1p in the interaction between actin and microtubules for the establishment of cell polarity in fission yeast. *Current Biology*, 11(11), pp.836–845.

Goehring, N.W. & Hyman, A.A., 2012. Organelle growth control through limiting pools of cytoplasmic components. *Current biology : CB*, 22(9), pp.R330–R339.

Goley, E.D. & Welch, M.D., 2006. The ARP2/3 complex: an actin nucleator comes of age. *Nature Reviews Molecular Cell Biology*, 7(10), pp.713–726.

Good, M.C. et al., 2013. Cytoplasmic volume modulates spindle size during embryogenesis. *Science*, 342(6160), pp.856–860.

Goode, B.L. & Eck, M.J., 2007. Mechanism and function of formins in the control of actin assembly. *Annual review of biochemistry*, 76, pp.593–627.

Greenan, G. et al., 2010. Centrosome Size Sets Mitotic Spindle Length in Caenorhabditis elegans Embryos. *Current Biology*, 20(4), pp.353–358.

Haag, N. et al., 2012. The actin nucleator Cobl is crucial for Purkinje cell development and works in close conjunction with the F-actin binding protein Abp1. *The Journal of neuroscience : the official journal of the Society for Neuroscience*, 32(49), pp.17842–17856.

Haglund, C.M. et al., 2010. Rickettsia Sca2 is a bacterial formin-like mediator of actin-based motility. *Nature cell biology*, 12(11), pp.1057–1063.

Hansen, S.D. & Mullins, R.D., 2010. VASP is a processive actin polymerase that requires monomeric actin for barbed end association. *The Journal of Cell Biology*, 191(3), pp.571–584.

Heisler, D.B. et al., 2015. ACTIN-DIRECTED TOXIN. ACD toxin-produced actin oligomers poison formin-controlled actin polymerization. *Science*, 349(6247), pp.535–539.

Helgeson, L.A. et al., 2014. Interactions with Actin Monomers, Actin Filaments and Arp2/3 Complex Define the Roles of WASP Family Proteins and Cortactin in Coordinately Regulating Branched Actin Networks. *Journal of Biological Chemistry*.

Hetrick, B. et al., 2013. Small Molecules CK-666 and CK-869 Inhibit Actin-Related Protein 2/3 Complex by Blocking an Activating Conformational Change. *Chemistry & biology*.

Higashida, C. et al., 2008. G-actin regulates rapid induction of actin nucleation by mDia1 to restore cellular actin polymers. *Journal of cell science*, 121(Pt 20), pp.3403–3412.

Higgs, H.N. & Pollard, T.D., 2000. Activation by Cdc42 and PIP(2) of Wiskott-Aldrich syndrome protein (WASp) stimulates actin nucleation by Arp2/3 complex. *JCB*, 150(6), pp.1311–1320.

Higgs, H.N. & Pollard, T.D., 2001. Regulation of actin filament network formation through ARP2/3 complex: activation by a diverse array of proteins. *Annual review of biochemistry*, 70, pp.649–676.

Hiyoshi, H. et al., 2015. Interaction between the type III effector VopO and GEF-H1 activates the RhoA-ROCK pathway. *PLoS Pathogens*, 11(3), p.e1004694.

Hiyoshi, H. et al., 2011. VopV, an F-actin-binding type III secretion effector, is required for Vibrio parahaemolyticus-induced enterotoxicity. *Cell Host and Microbe*, 10(4), pp.401–409.

Hotulainen, P. & Lappalainen, P., 2006. Stress fibers are generated by two distinct actin assembly mechanisms in motile cells. *JCB*, 173(3), pp.383–394.

Huang, J. et al., 2012. Nonmedially assembled F-actin cables incorporate into the actomyosin ring in fission yeast. *The Journal of Cell Biology*, 199(5), pp.831–847.

Huang, Y., Yan, H. & Balasubramanian, M.K., 2008. Assembly of normal actomyosin rings in the absence of Mid1p and cortical nodes in fission yeast. *The Journal of Cell Biology*, 183(6), pp.979–988.

Husson, C. et al., 2011. Cordon-Bleu uses WH2 domains as multifunctional dynamizers of actin filament assembly. *Molecular Cell*, 43(3), pp.464–477.

Jewett, T.J. et al., 2006. Chlamydial TARP is a bacterial nucleator of actin. *Proceedings of the National Academy of Sciences of the United States of America*, 103(42), pp.15599–15604.

Kamasaki, T., Osumi, M. & Mabuchi, I., 2007. Three-dimensional arrangement of F-actin in the contractile ring of fission yeast. *The Journal of Cell Biology*, 178(5), pp.765–771.

Kang, H. et al., 2012. Identification of cation-binding sites on actin that drive polymerization and modulate bending stiffness. *PNAS*, 109(42), pp.16923–16927.

Khanduja, N. & Kuhn, J.R., 2013. Processive acceleration of actin barbed-end assembly by N-WASP. *MBoC*, 25(1), pp.55–65.

Kovar, D.R., 2006. Molecular details of formin-mediated actin assembly. *Current opinion in cell biology*, 18(1), pp.11–17.

Kovar, D.R., 2003. The fission yeast cytokinesis formin Cdc12p is a barbed end actin filament capping protein gated by profilin. *The Journal of Cell Biology*, 161(5), pp.875–887.

Kovar, D.R. et al., 2006. Control of the assembly of ATP- and ADP-actin by formins and profilin. *Cell*, 124(2), pp.423–435.

Kovar, D.R., Sirotkin, V. & Lord, M., 2011. Three's company: the fission yeast actin cytoskeleton. *Trends in Cell Biology*, 21(3), pp.177–187.

Kovar, D.R., Wu, J.-Q. & Pollard, T.D., 2005. Profilin-mediated Competition between Capping Protein and Formin Cdc12p during Cytokinesis in Fission Yeast. pp.1–12.

Krause, M. et al., 2003. Ena/VASP Proteins: Regulators of the Actin Cytoskeleton and Cell Migration. *Annual review of cell and developmental biology*, 19(1), pp.541–564.

Kudryashov, D.S. et al., 2008. Connecting actin monomers by iso-peptide bond is a toxicity mechanism of the Vibrio cholerae MARTX toxin. *PNAS*, 105(47), pp.18537–18542.

Kudryashova, E. et al., 2014. Thermodynamic properties of the effector domains of MARTX toxins suggest their unfolding for translocation across the host membrane. *Molecular microbiology*, 92(5), pp.1056–1071.

Kwiatkowski, A.V., Gertler, F.B. & Loureiro, J.J., 2003. Function and regulation of Ena/VASP proteins. *Trends in Cell Biology*, 13(7), pp.386–392.

Laporte, D. et al., 2011. Assembly and architecture of precursor nodes during fission yeast cytokinesis. *The Journal of Cell Biology*, 192(6), pp.1005–1021.

Laporte, D., Zhao, R. & Wu, J.-Q., 2010. Mechanisms of contractile-ring assembly in fission yeast and beyond. *Seminars in Cell & Developmental Biology*, 21(9), pp.892–898.

Leavitt, J. et al., 1987. Expression of transfected mutant beta-actin genes: alterations of cell morphology and evidence for autoregulation in actin pools. *Molecular and Cellular Biology*, 7(7), pp.2457–2466.

Lee, I.-J., Coffman, V.C. & Wu, J.-Q., 2012. Contractile-ring assembly in fission yeast cytokinesis: Recent advances and new perspectives. *Cytoskeleton (Hoboken, N.J.)*, 69(10), pp.751–763.

Lee, S.H. & Dominguez, R., 2010. Regulation of actin cytoskeleton dynamics in cells. *Molecules and Cells*, 29(4), pp.311–325.

Lee, W.L., Bezanilla, M. & Pollard, T.D., 2000. Fission yeast myosin-I, Myo1p, stimulates actin assembly by Arp2/3 complex and shares functions with WASp. *JCB*, 151(4), pp.789–800.

Liverman, A.D.B. et al., 2007. Arp2/3-independent assembly of actin by Vibrio type III effector VopL. *Proceedings of the National Academy of Sciences of the United States of America*, 104(43), pp.17117–17122.

Lomakin, A.J. et al., 2015. Competition for actin between two distinct F-actin networks defines a bistable switch for cell polarization. *Nature cell biology*.

Lu, J. & Pollard, T.D., 2001. Profilin Binding to Poly-L-Proline and Actin Monomers along with Ability to Catalyze Actin Nucleotide Exchange Is Required for Viability of Fission Yeast. *Molecular Biology of the Cell*, pp.1161–1175.

Ludington, W.B. et al., 2012. Organelle Size Equalization by a Constitutive Process. *Current Biology*, 22(22), pp.2173–2179.

Ma, A.T. & Mekalanos, J.J., 2010. In vivo actin cross-linking induced by Vibrio cholerae type VI secretion system is associated with intestinal inflammation. *PNAS*, 107(9), pp.4365–4370.

Madasu, Y. et al., 2013. Rickettsia Sca2 has evolved formin-like activity through a different molecular mechanism. *PNAS*, 110(29), pp.E2677–86.

Marchand, J.B. et al., 2001. Interaction of WASP/Scar proteins with actin and vertebrate Arp2/3 complex. *Nature cell biology*, 3(1), pp.76–82.

Martin, S.G. & Chang, F., 2006. Dynamics of the formin for3p in actin cable assembly. *Current biology : CB*, 16(12), pp.1161–1170.

Martin, S.G. et al., 2007. Regulation of the formin for3p by cdc42p and bud6p. *MBoC*, 18(10), pp.4155–4167.

Mattila, P.K. & Lappalainen, P., 2008. Filopodia: molecular architecture and cellular functions. *Nature Reviews Molecular Cell Biology*, 9(6), pp.446–454.

McCollum, D. et al., 1996. The Schizosaccharomyces pombe actin-related protein, Arp3, is a component of the cortical actin cytoskeleton and interacts with profilin. *The EMBO Journal*, 15(23), pp.6438–6446.

McCullough, B.R. et al., 2011. Cofilin-linked changes in actin filament flexibility promote severing. *Biophysical Journal*, 101(1), pp.151–159.

McGhie, E.J., Hayward, R.D. & Koronakis, V., 2001. Cooperation between actin-binding proteins of invasive Salmonella: SipA potentiates SipC nucleation and bundling of actin. *The EMBO Journal*, 20(9), pp.2131–2139.

Michelot, A. & Drubin, D.G., 2011. Building Distinct Actin Filament Networks in a Common Cytoplasm. *Current Biology*, 21(14), pp.R560–R569.

Montaville, P. et al., 2014. Spire and Formin 2 synergize and antagonize in regulating actin assembly in meiosis by a ping-pong mechanism. *PLoS Biology*, 12(2), p.e1001795.

Morrell, J.L., Morphew, M. & Gould, K.L., 1999. A mutant of Arp2p causes partial disassembly of the Arp2/3 complex and loss of cortical actin function in fission yeast. *MBoC*, 10(12), pp.4201–4215.

Mullins, R.D. & Pollard, T.D., 1999. Rho-family GTPases require the Arp2/3 complex to stimulate actin polymerization in Acanthamoeba extracts. *Current Biology*, 9(8), pp.405–415.

Mullins, R.D., Heuser, J.A. & Pollard, T.D., 1998. The interaction of Arp2/3 complex with actin: nucleation, high affinity pointed end capping, and formation of branching networks of filaments. *Proceedings of the National Academy of Sciences of the United States of America*, 95(11), pp.6181–6186.

Mullins, R.D., Kelleher, J.F., et al., 1998. Arp2/3 complex from Acanthamoeba binds profilin and cross-links actin filaments. *MBoC*, 9(4), pp.841–852.

Nakano, K. & Mabuchi, I., 2006a. Actin-capping protein is involved in controlling organization of actin cytoskeleton together with ADF/cofilin, profilin and F-actin crosslinking proteins in fission yeast. *Genes to Cells*, 11(8), pp.893–905.

Nakano, K. & Mabuchi, I., 2006b. Actin-depolymerizing protein Adf1 is required for formation and maintenance of the contractile ring during cytokinesis in fission yeast. *MBoC*, 17(4), pp.1933–1945.

Nakano, K. et al., 2010. GMF is an evolutionarily developed Adf/cofilin-super family protein involved in the Arp2/3 complex-mediated organization of the actin cytoskeleton. *Cytoskeleton (Hoboken, N.J.)*, 67(6), pp.373–382.

Nakano, K. et al., 2001. Interactions among a Fimbrin, a Capping Protein, and an Actin-depolymerizing Factor in Organization of the Fission Yeast Actin Cytoskeleton. pp.1–12.

Namgoong, S. et al., 2011. Mechanism of actin filament nucleation by Vibrio VopL and implications for tandem W domain nucleation. *Nature Structural & Molecular Biology*, 18(9), pp.1060–1067.

Neidt, E.M., Scott, B.J. & Kovar, D.R., 2008. Formin Differentially Utilizes Profilin Isoforms to Rapidly Assemble Actin Filaments. *Journal of Biological Chemistry*, 284(1), pp.673–684.

Nolen, B.J. et al., 2009. Characterization of two classes of small molecule inhibitors of Arp2/3 complex. *Nature*, 460(7258), pp.1031–1034.

Ohkura, H., Hagan, I.M. & Glover, D.M., 1995. The conserved Schizosaccharomyces pombe kinase plo1, required to form a bipolar spindle, the actin ring, and septum, can drive septum formation in G1 and G2 cells. *Genes & development*, 9(9), pp.1059–1073.

Padrick, S.B. et al., 2011. Arp2/3 complex is bound and activated by two WASP proteins. pp.1–8.

Palmgren, S. et al., 2001. Interactions with PIP2, ADP-actin monomers, and capping protein regulate the activity and localization of yeast twinfilin. *JCB*, 155(2), pp.251–260.

Paul, A. & Pollard, T., 2008. The Role of the FH1 Domain and Profilin in Formin-Mediated Actin-Filament Elongation and Nucleation. *Current Biology*, 18(1), pp.9–19.

Paunola, E., Mattila, P.K. & Lappalainen, P., 2002. WH2 domain: a small, versatile adapter for actin monomers. *FEBS letters*, 513(1), pp.92–97.

Pelham, R.J. & Chang, F., 2002. Actin dynamics in the contractile ring during cytokinesis in fission yeast. *Nature*, 419(6902), pp.82–86.

Pelham, R.J. & Chang, F., 2001. Role of actin polymerization and actin cables in actin-patch movement in Schizosaccharomyces pombe. *Nature cell biology*, 3(3), pp.235–244.

Pernier, J. et al., 2013. Dimeric WH2 domains in Vibrio VopF promote actin filament barbed-end uncapping and assisted elongation. *Nature Structural & Molecular Biology*, 20(9), pp.1069–1076.

Pernier, J. et al., 2016. Profilin Interaction with Actin Filament Barbed End Controls Dynamic Instability, Capping, Branching, and Motility. *Developmental cell*, 36(2), pp.201–214.

Pfender, S. et al., 2011. Spire-type actin nucleators cooperate with Formin-2 to drive asymmetric oocyte division. *Current biology : CB*, 21(11), pp.955–960.

Pollard, T.D., 2007. Regulation of Actin Filament Assembly by Arp2/3 Complex and Formins. *Annual Review of Biophysics and Biomolecular Structure*, 36(1), pp.451–477.

Pollard, T.D. & Borisy, G.G., 2003. Cellular motility driven by assembly and disassembly of actin filaments. *Cell*, 112(4), pp.453–465.

Pollard, T.D. & Cooper, J.A., 2009. Actin, a Central Player in Cell Shape and Movement. *Science*, 326(5957), pp.1208–1212.

Pollard, T.D., Blanchoin, L. & Mullins, R.D., 2000. Molecular mechanisms controlling actin filament dynamics in nonmuscle cells. *Annual Review of Biophysics and Biomolecular Structure*, 29, pp.545–576.

Pring, M. et al., 2003. Mechanism of Formin-Induced Nucleation of Actin Filaments. *Biochemistry*, 42(2), pp.486–496.

Qualmann, B. & Kessels, M.M., 2009. New players in actin polymerization--WH2-domain-containing actin nucleators. *Trends in Cell Biology*, 19(6), pp.276–285.

Quinlan, M.E., 2013. Direct interaction between two actin nucleators is required in Drosophila oogenesis. *Development (Cambridge, England)*, 140(21), pp.4417–4425.

Quinlan, M.E. et al., 2005. Drosophila Spire is an actin nucleation factor. *Nature*, 433(7024), pp.382–388.

Quinlan, M.E. et al., 2007. Regulatory interactions between two actin nucleators, Spire and Cappuccino. *JCB*, 179(1), pp.117–128.

Ramabhadran, V., Hatch, A.L. & Higgs, H.N., 2013. Actin monomers activate Inverted Formin 2

by competing with its auto-inhibitory interaction. *Journal of Biological Chemistry*.

Rasson, A.S. et al., 2015. Filament assembly by spire: key residues and concerted actin binding. *Journal of molecular biology*, 427(4), pp.824–839.

Reidl, J. & Klose, K.E., 2002. Vibrio cholerae and cholera: out of the water and into the host. *FEMS Microbiology Reviews*, 26(2), pp.125–139.

Rizvi, S.A. et al., 2009. Identification and characterization of a small molecule inhibitor of formin-mediated actin assembly. *Chemistry & biology*, 16(11), pp.1158–1168.

Rogers, S.L. et al., 2003. Molecular requirements for actin-based lamella formation in Drosophila S2 cells. *JCB*, 162(6), pp.1079–1088.

Rotty, J.D. et al., 2015. Profilin-1 serves as a gatekeeper for actin assembly by arp2/3-dependent and -independent pathways. *Developmental cell*, 32(1), pp.54–67.

Rotty, J.D., Wu, C. & Bear, J.E., 2013. New insights into the regulation and cellular functions of the ARP2/3 complex. *Nature Reviews Molecular Cell Biology*, 14(1), pp.7–12.

Safer, D., Elzinga, M. & Nachmias, V.T., 1991. Thymosin beta 4 and Fx, an actin-sequestering peptide, are indistinguishable. *The Journal of Biological Chemistry*, 266(7), pp.4029–4032.

Sarmiento, C. et al., 2008. WASP family members and formin proteins coordinate regulation of cell protrusions in carcinoma cells. *The Journal of Cell Biology*, 180(6), pp.1245–1260.

Scott, B.J., Neidt, E.M. & Kovar, D.R., 2011. The functionally distinct fission yeast formins have specific actin-assembly properties. *Molecular Biology of the Cell*, 22(20), pp.3826–3839.

Shekhar, S. et al., 2015. Formin and capping protein together embrace the actin filament in a ménage à trois. *Nature Communications*, 6, p.8730.

Sirotkin, Vladimir et al., 2010. Quantitative analysis of the mechanism of endocytic actin patch assembly and disassembly in fission yeast. *Molecular Biology of the Cell*, 21(16), pp.2894–2904.

Sirotkin, Vladmir et al., 2008. Interactions of WASp, myosin-1, and verprolin with Arp2/3 complex during actin patch assembly in fission yeast. *JCB*, pp.1–13.

Skau, C.T. & Kovar, D.R., 2010. Fimbrin and Tropomyosin Competition Regulates Endocytosis and Cytokinesis Kinetics in Fission Yeast. *Current Biology*, 20(16), pp.1415–1422.

Skoumpla, K. et al., 2007. Acetylation regulates tropomyosin function in the fission yeast Schizosaccharomyces pombe. *Journal of cell science*, 120(9), pp.1635–1645.

Spudich, J.A. & Watt, S., 1971. The regulation of rabbit skeletal muscle contraction. I. Biochemical studies of the interaction of the tropomyosin-troponin complex with actin and

the proteolytic fragments of myosin. *The Journal of Biological Chemistry*, 246(15), pp.4866–4871.

Steffen, A. et al., 2006. Filopodia formation in the absence of functional WAVE- and Arp2/3-complexes. *MBoC*, 17(6), pp.2581–2591.

Suarez, C. et al., 2015. Profilin Regulates F-Actin Network Homeostasis by Favoring Formin over Arp2/3 Complex. *Developmental cell*, pp.1–11.

Suraneni, P. et al., 2015. A mechanism of leading-edge protrusion in the absence of Arp2/3 complex. *Molecular Biology of the Cell*, 26(5), pp.901–912.

Suraneni, P. et al., 2012. The Arp2/3 complex is required for lamellipodia extension and directional fibroblast cell migration. *The Journal of Cell Biology*, 197(2), pp.239–251.

Svitkina, T.M. et al., 2003. Mechanism of filopodia initiation by reorganization of a dendritic network. *JCB*, 160(3), pp.409–421.

Tam, V.C. et al., 2007. A type III secretion system in Vibrio cholerae translocates a formin/spire hybrid-like actin nucleator to promote intestinal colonization. *Cell Host and Microbe*, 1(2), pp.95–107.

Tam, V.C. et al., 2010. Functional analysis of VopF activity required for colonization in Vibrio cholerae. *mBio*, 1(5).

Ti, S.-C. & Pollard, T.D., 2011. Purification of Actin from Fission Yeast Schizosaccharomyces pombe and Characterization of Functional Differences from

Muscle Actin. *Journal of Biological Chemistry*, pp.1–9.

Vitriol, E.A. et al., 2015. Two functionally distinct sources of actin monomers supply the leading edge of lamellipodia. *Cell reports*, 11(3), pp.433–445.

Wang, H. & Vavylonis, D., 2008. Model of For3p-mediated actin cable assembly in fission yeast. *PloS one*, 3(12), p.e4078.

Welch, M.D. et al., 1998. Interaction of human Arp2/3 complex and the Listeria monocytogenes ActA protein in actin filament nucleation. *Science*, 281(5373), pp.105–108.

Winkelman, J.D. et al., 2014. Ena/VASP Enabled is a highly processive actin polymerase tailored to self-assemble parallel-bundled F-actin networks with Fascin. *PNAS*, 111(11), pp.4121–4126.

Winter, D.C. et al., 1997. The complex containing actin-related proteins Arp2 and Arp3 is required for the motility and integrity of yeast actin patches. *Current Biology*, pp.1–11.

Wu, C. et al., 2012. Arp2/3 is critical for lamellipodia and response to extracellular matrix cues but is dispensable for chemotaxis. *Cell*, 148(5), pp.973–987.

Wu, J.-Q. et al., 2006. Assembly of the cytokinetic contractile ring from a broad band of nodes in fission yeast. *The Journal of Cell Biology*, 174(3), pp.391–402.

Wu, J.-Q. et al., 2003. Spatial and temporal pathway for assembly and constriction of the contractile ring in fission yeast cytokinesis. *Developmental cell*, 5(5), pp.723–734.

Wu, J.Q., 2005. Counting Cytokinesis Proteins Globally and Locally in Fission Yeast. *Science*, 310(5746), pp.310–314.

Xu, P. et al., 2012. Spire, an actin nucleation factor, regulates cell division during Drosophila heart development. *PloS one*, 7(1), p.e30565.

Yang, C. et al., 2007. Novel roles of formin mDia2 in lamellipodia and filopodia formation in motile cells. *PLoS Biology*, 5(11), p.e317.

Yang, Q. et al., 2012. Arp2/3 complex-dependent actin networks constrain myosin II function in driving retrograde actin flow. *The Journal of Cell Biology*, 197(7), pp.939–956.

Yonetani, A. & Chang, F., 2010. Regulation of cytokinesis by the formin cdc12p. *Current biology : CB*, 20(6), pp.561–566.

Yonetani, A. et al., 2008. Regulation and targeting of the fission yeast formin cdc12p in cytokinesis. *Molecular Biology of the Cell*, 19(5), pp.2208–2219.

Young, L.E., Heimsath, E.G. & Higgs, H.N., 2015. Cell type-dependent mechanisms for formin-mediated assembly of filopodia. *Molecular Biology of the Cell*, 26(25), pp.4646–4659.

Yu, B. et al., 2011. Mechanism of actin filament nucleation by the bacterial effector VopL. *Nature Structural & Molecular Biology*, 18(9), pp.1068–1074.

Zahm, J.A. et al., 2013. The Bacterial Effector VopL Organizes Actin into Filament-like Structures. *Cell*, 155(2), pp.423–434.

Zigmond, S.H. et al., 1998. Mechanism of Cdc42-induced Actin Polymerization

in Neutrophil Extracts. *The Journal of Cell Biology*, pp.1–12.

Zuchero, J.B. et al., 2009. p53-cofactor JMY is a multifunctional actin nucleation factor. *Nature cell biology*, 11(4), pp.451–459.